Technische Universität München

Fakultät für Medizin

Institut für Klinische Chemie und Pathobiochemie

Analysis of the transcription factor Foxp1 in T cell differentiation and function

Frank Oliver Gorka

Vollständiger Abdruck der von der Fakultät für Medizin der Technischen Universität München zur Erlangung des akademischen Grades eines

Doktors der Naturwissenschaften (Dr. rer. nat.)

genehmigten Dissertation.

Vorsitzender: Univ.-Prof. Dr. Dirk Busch

Prüfer der Dissertation:

1. Univ.-Prof. Dr. Jürgen Ruland
2. Univ.-Prof. Dr. Bernhard Küster

Die Dissertation wurde am 12.02.2015 bei der Technischen Universität München eingereicht und durch die Fakultät für Medizin am 13.05.2015 angenommen.

Table of contents

Summary **8**

Zusammenfassung **10**

1 Introduction **12**

1.1 The immune system *12*

1.1.1 Features of the immune system 12

1.1.2 Lymphocytes 12

1.2 T cells *13*

1.2.1 T cell development in the thymus 13

1.2.2 T cells in the periphery – homing and homeostasis 15

1.2.3 T cell activation and differentiation 16

1.2.4 Memory T cells 19

1.2.5 Regulatory T cells 22

1.3 The transcription factor Foxp1 *23*

1.3.1 The fork-head box protein family 23

1.3.2 Foxp1 in non-hematopoietic tissues 27

1.3.3 Foxp1 in cancer 28

1.3.4 Foxp1 in cells of the immune system 29

2 Research objective **33**

3 Materials **34**

3.1 Reagents *34*

3.2 Genotyping primers *34*

3.3 Real time PCR Primer *34*

3.4 Pull-down oligonucleotides *35*

3.5 Western blotting antibodies *35*

3.6 Flow cytometry antibodies *35*

3.7 Reagents used for T cell stimulations *36*

4 Methods **37**

4.1 Work with nucleic acids *37*

4.1.1 Isolation of DNA 37

4.1.2 Genotyping PCRs 37

4.1.3 Agarose gel electrophoresis 38

4.1.4 Isolation of RNA 38

4.1.5 Reverse transcription 39

4.1.6 Quantitative Real time PCRs 39
4.2 Work with proteins *39*
4.2.1 Western blotting 39
4.2.2 Enzyme-linked immunosorbent assays (ELISAs) 40
4.2.3 Detection of auto-antibodies 41
4.2.4 Cytokine bead arrays 41
4.2.5 Oligonucleotide pull-down assay 42
4.3 Work with cells *42*
4.3.1 Flow cytometry 42
4.3.2 Purification of CD4+ T cells 43
4.3.3 FACS sorting of primary cells 43
4.3.4 Isolation of CNS-infiltrating lymphocytes 44
4.3.5 In vitro culture and stimulation of T cells 44
4.3.6 CFSE proliferation assay 45
4.3.7 In vitro survival assay 45
4.4 Work with animals *46*
4.4.1 Mouse strains 46
4.4.2 Ataxia scoring 46
4.5 Sequence alignment and phylogeny *47*
4.6 Statistical analysis *47*

5 Results **48**
5.1 Expression of Foxp1 in cells of the immune system *48*
5.2 T cell-specific Foxp1 knock-out *52*
5.2.1 Generation of a T cell-specific conditional Foxp1 CD4 Cre knock-out mouse 52
5.2.2 Immunophenotypical characterization of Foxp1^{cKO} CD4 Cre mice 54
5.2.3 Detailed analysis of altered T cell compartment in Foxp1^{cKO} CD4 Cre mice 57
5.2.4 Altered lifespan of Foxp1^{cKO} CD4 Cre mice and absence of auto-antibodies in sera of aged mice 63
5.2.5 Enhanced cytokine production of CD4+ T cell from Foxp1^{cKO} CD4 Cre 65
5.2.6 Analysis of Foxp1-binding to IL-2 promoter region 67
5.2.7 Proliferation of CD4+ T cells from Foxp1^{cKO} CD4 Cre mice 70
5.2.8 Survival assay and *in vitro* culture of Foxp1-deficient CD4+ T cells 70
5.3 Analysis of Foxp1^{cKO} CD4 Cre vav-Bcl2 tg mice *73*
5.3.1 Characterization of Foxp1^{cKO} CD4 Cre vav-Bcl2 tg mice 73
5.3.2 Survival of Foxp1^{cKO} CD4 Cre and Foxp1^{cKO} CD4 Cre vav-Bcl2 tg mice 76
5.4 Analysis of Foxp1^{cKO} Foxp3 Cre mice *78*
5.4.1 Immunophenotypical characterization of Foxp1^{cKO} Foxp3 Cre mice 78

5.5 Analysis of 2D2 MOG-specific Foxp1^{cKO} CD4 Cre mice *81*

5.5.1 Characterization of 2D2 MOG$_{(35-55)}$-specific Foxp1^{cKO} CD4 Cre mice 81

6 Discussion **85**

6.1 Reduced Foxp1 expression in memory T cells *85*

6.2 Foxp1-deficiency in T cells *86*

6.3 Foxp1-deficient T cells exert memory cells functions *91*

6.4 T cell apoptosis or T cell migration? *94*

6.5 Foxp1 in Foxp3+ regulatory T cells *95*

6.6 Foxp1-deficient T cells in a encephalitogenic mouse model *96*

7 Summary and Outlook **99**

8 Acknowledgements **100**

9 Publications **101**

10 Abbreviations **102**

11 Figure index **106**

12 Bibliography **108**

Summary

Immunological memory is an essential feature of the adaptive immune system, which ensures rapid clearance of pathogens upon their reencounter. However, the molecular basis that underlies the transition of naïve to memory T cells is still not completely understood. Forkhead-box (Fox) proteins, like Foxp3, have been demonstrated to play major roles in the immune system and are promising candidates in the regulation of terminal differentiation events. One of them, Foxp1, is a transcription factor that has initially been described as a tumour-suppressor, potential oncogen and critical player during early stages of B cell development. Yet, the specific function of Foxp1 in T cells and memory T cell differentiation has not been explored.

First evidence for a potential role of FoxP1 in T-cell differentiation was obtained from the expression pattern in wildtype mice: FoxP1 expression levels declined during the transition of naive to memory T-cells. In order to characterize the molecular function of Foxp1 in T cells, T cell-specific knock-out mice were generated by breeding a conditional knock-out mouse model for Foxp1 to a mouse strain expressing Cre recombinase under the CD4 promoter. Strikingly, all Foxp1-deficient T cells in these mice phenotypically resembled effector/memory T cells already after leaving the double-positive thymocyte stage showing high levels of CD44 expression. Additionally, T cells were easily activated by subtle T cell receptor stimulation to secrete large amounts of IL-2 and inflammatory cytokines. But surprisingly, no overt autoimmunity was detected in animals with Foxp1-deficient T cells. While numbers of regulatory T cells were increased, no obvious immune phenotype was observed when Foxp1 was specifically deleted in regulatory T cells using a Foxp3 Cre recombinase strain, arguing against a prominent intrinsic function of Foxp1 in regulatory T cells.

Given the prominent shift of Foxp1-deficient T cells to the memory compartment, the question arose whether these animals might be more vulnerable to autoimmune challenges. To test this hypothesis, animals with Foxp1-deficient T cells were bred to an autoimmune-prone genetic background of mice carrying an encephalitogenic MOG-specific 2D2 T cell receptor. Indeed, mice with Foxp1-deficient T cells in a 2D2 background developed spontaneously neurological symptoms resembling an atypical autoimmune encephalomyelitis.

Taken together, these observations reveal a memory function of Foxp1-deficient T cells and provide first evidence for a role of Foxp1 in autoimmune diseases. In conclusion, the

transcription factor Foxp1 is critical in maintaining naïve T cell identity and acts as a master regulator of memory T cell differentiation.

Zusammenfassung

Das immunologische Gedächtnis ist eine essentielle Eigenschaft des adaptiven Immunsystems und sorgt für eine schnelle Bekämpfung bereits bekannter Pathogene. Die molekularen Grundlagen des hierfür notwendigen Übergangs von naiven zu Gedächtnis-T-Zellen sind jedoch nur ansatzweise verstanden. Forkhead-box (Fox) Proteine, wie beispielsweise Foxp3, wurden bereits als wichtige Bestandteile des Immunsystems identifiziert und sind vielversprechende Kandidaten für die Regulation von terminalen Differenzierungsschritten. Der Transkriptionsfaktor Foxp1 wurde initial als Tumorsuppressor, potentielles Onkogen und essentieller Faktor für die frühe B Zellentwicklung beschrieben. Die spezifische Funktion von Foxp1 in T-Zellen wurde jedoch bisher nicht entschlüsselt.

Erste Hinweise auf eine potentielle Rolle von Foxp1 in der T-Zelldifferenzierung kamen von Expressionsstudien in Wildtyp-Mäusen, in denen die Expression von Foxp1 ausgehend von naiven T-Zellen hin zu Gedächtnis-T-Zellen abnahm. Zur Charakterisierung der molekularen Funktionsweise von Foxp1 in T-Zellen wurde ein konditionales Knock-out Mausmodel für Foxp1 generiert und zur Erzeugung eines T-Zell-spezifischen Knock-outs mit einer Mauslinie verpaart die Cre-Rekombinase unter Kontrolle des CD4 Promoters exprimiert. Überraschenderweise zeigte sich bei der Analyse der Tiere ein stark verändertes T-Zell-Kompartiment, das phenotypisch ausschließlich Effektor-/Gedächtnis-T-Zellen mit einem CD44+ Expressionsprofil aufwies. Foxp1-defiziente T-Zellen konnten bereits durch schwache, suboptimale Stimulation des T-Zell-Rezeptors aktiviert und zur Ausschüttung großer Mengen IL-2 und inflammatorischer Zytokine gebracht werden. Trotz dieser drastischen Veränderungen der T-Zellbiologie zeigen Tiere mit Foxp1-defizienten T-Zellen keine Anzeichen einer Autoimmunerkrankung. Obwohl zusätzlich größere Mengen an regulatorischen T-Zellen in diesen Tieren gefunden wurden, wies die spezifische Deletion von Foxp1 in regulatorischen T-Zellen keine Veränderung des Immunphänotyps auf, wodurch eine prominente Rolle von Foxp1 in diesem Zelltyp ausgeschlossen werden kann.

Die Verschiebung des T-Zellkompartiments hin zu Gedächtnis-T-Zellen in Mäusen mit Foxp1-defizienten T-Zellen lies die Frage nach einer möglichen Empfänglichkeit der Tiere gegenüber Autoimmunerkrankungen aufkommen. Zur Überprüfung dieser Hypothese wurden Tiere mit Foxp1-defizienten T-Zellen in eine zur Autoimmunität neigenden Mauslinie mit transgen exprimierten MOG-spezifischen 2D2 T-Zell-Rezeptor gekreuzt. Tatsächlich entwickelten Tiere mit Foxp1-defizienten T-Zellen im 2D2 Hintergrund spontan neurologische Symptome einer atypischen autoimmunen Enzephalomyelitis.

Diese Beobachtungen bestätigen die Konversion Foxp1-defizienter T-Zellen hin zu Gedächtnis-T-Zellen und zeigen zum ersten Mal eine Rolle von Foxp1 im Kontext von Autoimmunerkrankungen auf. Anhand der vorliegenden Ergebnisse kann daher geschlussfolgert werden, dass der Transkriptionsfaktor Foxp1 eine zentrale Rolle bei der Aufrechterhaltung der Identität von naiven T-Zellen spielt und als ein Schlüsselregulator der Gedächtnis-T-Zelldifferenzierung angesehen werden kann.

1 Introduction

1.1 The immune system

1.1.1 Features of the immune system

Every living organism needs to interact with its environment and is thereby threatened by confrontation with numerous microbial organisms, parasites and viruses. Through evolutionary processes over millions of years, sophisticated mechanisms have evolved that enable organisms not only to detect pathogens, but also to fight intruders effectively. Mechanisms of detecting danger signals developed since the dawn of the animal evolution as a central element of innate immunity. Recognition of molecular patterns associated with pathogens and fast responses upon encountering danger signals are hallmarks of innate immunity (Leulier and Lemaitre, 2008; Medzhitov, 2007). In contrast, adaptive immunity has developed more recently on an evolutionary time scale, as its origin can be dated back to the evolutionary break point of agnathans (jawed fish) and gnathostomes (jawed vertebrates) (Pancer and Cooper, 2006). The main characteristic of adaptive immunity is its antigen-specificity accomplished by rearrangement of variable gene regions. Importantly, cells of the adaptive immune system can turn into memory cells, which keep their specificity towards antigens they encountered once and are able to elicit fast responses upon reencounter. Thus, the adaptive immunity strongly depends on innate features such as antigen-presentation on major-histocompatibility complexes (MHCs) of antigen-presenting cells, like dendritic cells and macrophages, as well as their co-activatory signals.

1.1.2 Lymphocytes

Evolution of the adaptive immune system is strongly connected with the development of the lymphocyte cell lineage. In general, mesodermic pluripotent hematopoietic stem cells give rise to common myeloid and lymphocytic progenitors, the latter being the source of lymphocytes. In modern vertebrates, the two major subsets of lymphocytes are B and T cells.

B cells develop in the bone marrow and can become either immunoglobulin secreting plasma cells or memory B cells upon encountering their specific antigen. In addition, B cells function as antigen-presenting cells. In contrast, T cells undergo their central maturation steps in the thymus and circulate through the body after their maturation to T helper cells or cytotoxic T

cells. Both B and T cells transit though several stages of maturation, undergo gene-recombination, and are selected for functional antigen-receptors (Murphy et al., 2008).

In addition to B and T cells, several different cell-types derive from hematopoietic precursors, including natural killer (NK) cells or natural killer T cells (NKT). NK cells are seen as part of the innate immune system and express invariant receptors that can recognize the absence of MHC-class I molecules on infected or malignant cells. Using this mechanism, NK cells play an important role in tumour-immunity and anti-viral responses. In contrast, NKT cells have some common characteristics with T cells: they also mature in the thymus, express semi-invariant T cell receptors (TCRs), and produce great amounts of cytokines upon stimulation. A role for NKT cell has been implicated in autoimmunity and immune-responses to bacteria, viruses, and cancer cells. Also intraepithelial lymphocytes and different subsets of innate lymphoid cells derive from hematopoietic precursors and have been found both in mice and men (Murphy et al., 2008). As this work mainly focuses on T lymphocytes the following paragraphs will introduce their development and function in the immune system in greater detail.

1.2 T cells

1.2.1 T cell development in the thymus

T cells undergo their central maturation steps in the thymus, a highly specialised organ originating from the third pharyngeal pouch. Committed lymphoid progenitors leave the bone marrow and migrate to the thymus where they undergo various stages of development. The thymus can be anatomically subdivided into capsule, cortex and medulla. Thymocyte maturation mainly takes place in the cortex, medulla, and at the cortico-medullary junction (Germain, 2002).

According to their expression of the co-receptors CD4 and CD8, T cells can be divided into CD4+ T helper and CD8+ cytotoxic T cells. These markers help to differentiate four distinct stages of maturation, as thymocytes develop following a strict sequence from double-negative (CD4- CD8-) over double-positive (CD4+ CD8+) to single-positive (CD4+ CD8- or CD4- CD8+) cells. The double-negative thymocytes stage can be further subdivided in four separate maturation steps, according to the expression of CD44 and CD25. Double-negative thymocytes in the outer thymic cortex are initially CD44+ CD25- (DN1), and advance to

CD44+ CD25+ (DN2), CD44- CD25+ (DN3), and finally to CD44- CD25- (DN4) (Ceredig and Rolink, 2002; Germain, 2002).

During early thymocyte stages, gene segment rearrangements take place, first starting with the Dβ-Jβ rearrangement of the TCRβ locus in the transition of DN1 to DN2. Subsequently, the Vβ-DJβ rearrangement occurs during the transition from DN2 to DN3. In DN3 thymocytes, the rearranged TCRβ chain is expressed together with a pre-TCR receptor. An incorrect TCRβ rearrangement inhibits the progression of thymocytes to the double-positive stage (Robey and Fowlkes, 1994). This first step of thymocyte selection is therefore termed β-selection (Ceredig and Rolink, 2002). All rearrangement processes depend on the molecular machinery involving recombination-activating genes 1 and 2 (Rag1/Rag2). Deficiency of either of those proteins leads to a stagnation of thymocyte maturation in DN3. Similarly, the absence of Rag genes also prevents gene segment recombination of the B cell receptor and leads to an arrest in early B cell development (Mombaerts et al., 1992; Shinkai et al., 1992).

A second process of genetic alterations marks the transition of DN4 to double-positive thymocytes. Here, the TCRα locus is diversified by the Vα-Jα rearrangement, leading to the expression of a complete TCRα/β receptor on the surface of double-positive thymocytes. The expression of a functional TCRα/β receptor goes along with further selection processes. Firstly, the newly generated TCRs are tested for their recognition of MHC-proteins during positive selection. Failure in recognition of MHC proteins on thymic antigen-presenting cells by the TCR receptor of a given thymocyte will eventually lead to its apoptosis due to the lack of tonic survival signals. This process is often termed as ‘death by neglect’ (Germain, 2002; Murphy et al., 2008). Secondly, lineage commitment is taking place at this stage of maturation, restricting the selected thymocytes to either CD4 or CD8 lineage. In general, CD4+ T cells are restricted to recognition of antigen in the context of MHC-class II molecules, whereas CD8+ T cells are confined to MHC-class I complexes. After becoming single-positive thymocytes, the cells exit the cortex and enter the thymic medulla. Finally, thymocytes are negatively selected in the medulla by eliminating self-reactive T cells. This last mechanism of selection is of critical importance in order to generate T cells which correctly distinguish between self and non-self, thereby preventing autoimmunity (Murphy et al., 2008).

Medullary thymic epithelial cells (mTECs) play a fundamental role in the process of negative selection. This non-hematopoietic subset of cells promiscuously presents tissue-specific self-antigens, such as insulin, whose production is normally restricted to pancreatic β cells, or

salivary proteins, expressed only in salivary glands. The expression of peripheral tissue-specific antigens in mTECs is regulated by the protein autoimmune regulator (Aire) (Anderson et al., 2002; Mathis and Benoist, 2007). Aire is thought to bind to inactivating histone modifications and thereby activate transcription of tissue-specific antigens (Tykocinski et al., 2010). Interestingly, individual mTECs differ in their expression patterns of tissue-specific self-antigens, suggesting a stochastic regulation of transcription (Derbinski et al., 2008).

After T cell selection in the thymus, central tolerance has been established and CD4+ and CD8+ single-positive thymocytes are migrating to the periphery to circulate through lymphatic organs in order to find their cognate antigen. Both T cell subsets play distinct roles in the immune system: CD4+ T helper cells are crucial players of the adaptive immune system and regulate both cellular and humoral immune responses. They are essential for regulating isotype-class-switching in B cells and contribute to germinal centre reactions and affinity-maturation of immunoglobulins. Additionally, CD4+ T cells provide activating signals to macrophages and support CD8+ T cell responses. In contrast, cytotoxic CD8+ T cells are mainly responsible for the recognition and elimination of virus-infected or cancerous cells (Murphy et al., 2008).

1.2.2 T cells in the periphery – homing and homeostasis

A predominant fraction of all CD4+ and CD8+ T lymphocytes in the periphery of wildtype mice are naïve, meaning that they have not yet encountered their specific antigen and are maintained in a state of quiescence. Naïve T cells migrate through the secondary lymphatic organs of the body, including spleen, lymph nodes and gut-associated lymphoid tissue, and scan for their cognate antigen presented in the context of a MHC protein on antigen-presenting cells. A key feature of naïve T cells is the expression of CD62L (L-selectin) and low abundance of CD44 ($CD62L^{high}$ $CD44^{low}$), which together enable homing of the cells to secondary lymphoid organs. Additionally, naïve T cells are characterized by expression of IL-7 receptor α chain CD127, which is important for T cell homeostasis, as well as low levels of IL-2 receptor CD25 and C-type lectin protein CD69 (Schluns et al., 2000); (Murphy et al., 2008).

Homing capacities of naïve T cells are mainly regulated by their expression of CD62L and C-C chemokine receptor 7 (CCR7). The entrance of naïve T cells into lymphoid organs is initiated by binding of CD62L to CD34 and GlyCAM-1, two mucin-like vascular addressins

bearing sulphated sialyl-Lewis^x carbohydrate moieties, which are expressed on high endothelial venules (HEV). After initial adhesion to the endothelium, migration is promoted by CCR7, a chemokine receptor for the chemokines CCL19 and CCL21. Both chemokines are produced in lymphoid organs by stromal cells, cells in HEVs, and dendritic cells. Upon detection of the chemokines, naïve T cells enter the lymphoid organ and migrate to specific T cell zones, where they scan the available dendritic cells presenting peptide-loaded MHC molecules (Murphy et al., 2008).

Homeostasis of naïve T cells is maintained by TCR engagement via self-peptide-MHC ligands and IL-7 stimulation (Schluns et al., 2000). Recognition of self-peptide-MHC molecules in antigen-presenting cells of the periphery resembles the events of positive selection in the thymus, providing the naïve T cells with tonic survival signals necessary to prevent cell death. The cytokine IL-7 is produced by non-hematopoietic stromal and epithelial cells of the bone marrow and the thymus, as well as by fibroblastic reticular cells in lymphoid organs (Surh and Sprent, 2008). Binding of IL-7 to the heterodimeric IL-7 receptor on T cells (consisting of CD127 and the common cytokine-receptor γ chain, CD132) engages Janus kinases (Jak) 1 and 3, and is followed by the activation of Stat5, which in turn leads to increased expression of the anti-apoptotic factors Bcl2 and Mcl1. The availability of both self-peptide-MHC ligands and IL-7 limits the size of the naïve T cell pool in CD4 and CD8 T cell subsets (Surh and Sprent, 2008).

1.2.3 T cell activation and differentiation

Antigen-presenting cells like dendritic cells present peptides, which they have taken up in the periphery, on MHC proteins. Additionally, dendritic cells become activated by engagement of pathogen-associated molecular pattern receptors at the site of infection. The activation not only results in up-regulation of MHC molecules and co-stimulatory molecules such as CD80 and CD86, but also in migration of the dendritic cell to the T cell zone of a draining lymph node in proximity to the site of infection (Murphy et al., 2008).

Inside the T cell zone, naïve T cells sample the surrounding dendritic cells and their peptide-MHC complexes. Once a naïve T cell has encountered its cognate antigen in the context of a MHC molecule on an activated dendritic cell, a structure called ‘immunological synapse’ is formed to induce more stable protein-protein interactions between the two cells and activate the T cell. Engagement of the co-stimulatory receptor CD28 by CD80 and CD86 on activated dendritic cells provides a secondary signal, which is necessary for T cell activation. TCR

stimulation alone, in absence of a co-stimulatory signals would render naïve T cells anergic (Macián et al., 2004).

Activation of the TCR first leads to phosphorylation of Src-family kinases associated with the co-receptor and phosphorylation of the cytoplasmic motifs of the TCR complex. The TCR complex is formed not only by TCR α and β chains, but also consists of CD3 γ, δ, and ε proteins which bear cytoplasmic immunoreceptor tyrosine-based activation motifs (ITAMs) (Love and Hayes, 2010). Additionally, ζ chain proteins containing multiple ITAMs are part of the complex. After TCR engagement, Src-family kinases like Lck become activated and phosphorylate the cytoplasmic CD3 ITAMs and zeta-chain-associated protein kinase of 70 kDa (ZAP70) (Chan et al., 1995; 1991). ZAP70 in turn localizes to the modified ITAMs, becomes activated and phosphorylates linker of activated T cells (LAT) and the signal transduction adapter SH2 domain containing leukocyte protein of 76kDa (SLP76) (Chan et al., 1992; Zhang et al., 1998). The latter binds and thereby activates phospholipase C γ (PLCγ), Tec kinases and guanine-nucleotide exchange factors (GEFs) (Smith-Garvin et al., 2009). Activated PLCγ cleaves phosphatidylinositol bisphosphate (PIP_2) and generates diacylglycerol (DAG) and inositol trisphosphate (IP_3). On one hand, IP_3 induces intracellular calcium release by binding and opening IP_3-sensitive Ca^{2+} channels at the endoplasmic reticulum, which in turn leads to activation of calcium-release activated Ca^{2+} channels in the plasma membrane. Ca^{2+} itself acts as a second messenger that eventually provokes a nuclear translocation of the transcription factor 'nuclear factor of activated T cells' (NFAT) (Smith-Garvin et al., 2009). On the other hand, DAG induces the activation of protein kinase C (PKC), resulting in the assembly of the Carma-Bcl10-Malt1 complex and the activation and translocation of 'nuclear factor kappa-light-chain-enhancer of activated B cells' (NFκB) subunits to the nucleus (Thome, 2004). In a third branch of activation, GEFs (like Sos and RasGRP) trigger the MAP kinase cascade and hence induce the nuclear translocation of Jun and Fos forming the heterodimeric transcription factor AP-1 (Genot and Cantrell, 2000; Jain et al., 1992). Together, NFAT, NFκB, and AP-1 drive the transcription of a variety of genes critically involved in proliferation, cell survival, cytokine production (especially IL-2), and differentiation, thereby orchestrating T cell activation (Figure 1) (Smith-Garvin et al., 2009). This response upon encounter of a specific ligand leads to a propagation of antigen-specific effector T cells during the expansion phase of a T cell-dependent immune response.

Following activation, T helper cells can differentiate further to become specialized cytokine-producer effector T cells. Depending on the specific cytokine milieu a CD4+ T cell encounters during activation with its cognate antigen, the T cell initializes intrinsic

mechanisms that lead to the expression of distinct lineage-specific transcription factors controlling its prospective cytokine profile. Besides of regulatory T cells, which are discussed in a separate chapter, T helper cells can become Th1, Th2, or Th17 cells.

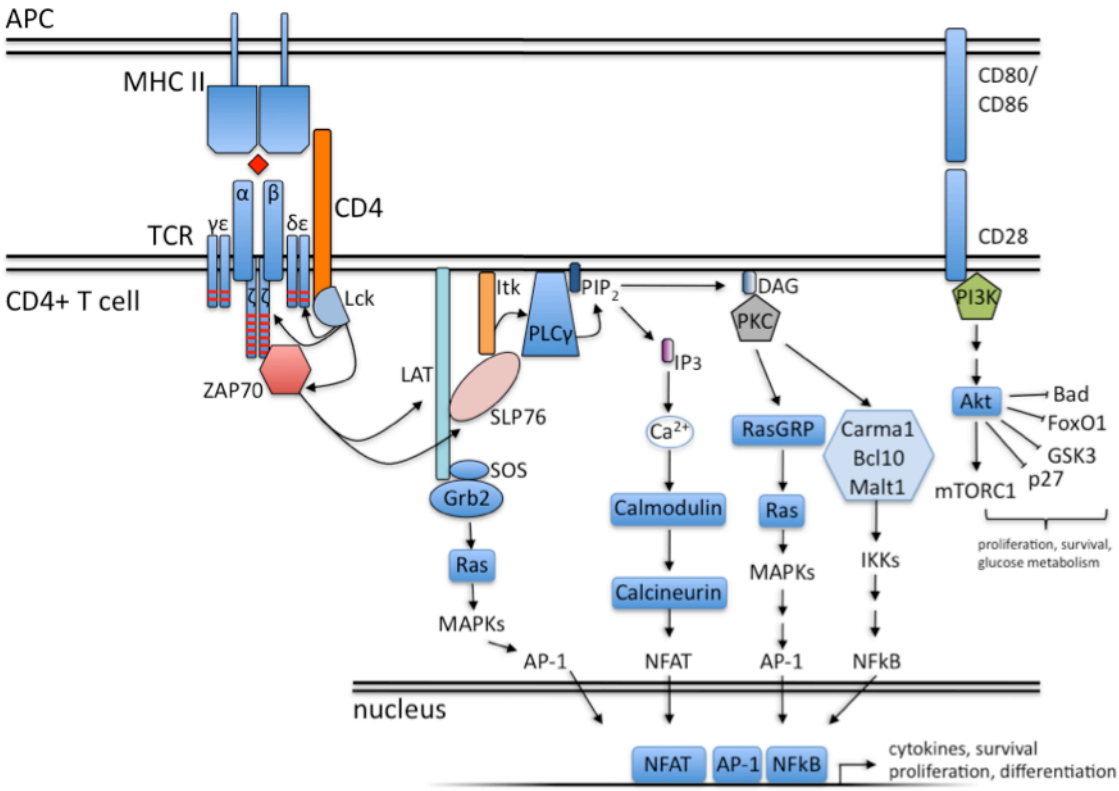

Figure 1 Simplified overview of T cell receptor signalling pathways. When T cells encounter their cognate antigen presented on MHC molecules of an antigen-presenting cell, a complex signalling cascade is induced. Briefly, ITAM-motifs (red lines) become phosphorylated by Lck and provide a docking site for ZAP70, which in turn phosphorylates SLP76 and LAT. Eventually, PLCγ becomes engaged and cleaves PIP_2 into DAG and IP_3. DAG induces activation of PKCs and the CBM-complex resulting in nuclear translocation of NFkB subunits. Additionally, MAP kinase signalling is initiated leading to AP-1 activation. In contrast, IP_3 induces Ca^{2+} influx and promotes activation of NFAT. However, a full-blown T cell activation also depends on CD28 co-stimulation mainly leading to activation of Akt, which plays a major role survival and proliferation of activated T cells. Together NFkB, AP-1, NFAT, and downstream targets of Akt drive transcriptional programs, which are of critical importance for a functional immune system.

Th1 cells are marked by the expression of T-box transcription factor T-bet and are mainly producing IFNγ as a hallmark cytokine, but also TNF and IL-2. Th1 cytokines are crucial for macrophage activation and expansion of cytotoxic T cells. Also, class-switch recombination

towards opsonizing immunogobulins is driven by IFNγ. Epigenetic remodelling and increased accessibility of specific genetic loci can be observed in all T cell differentiation lineages. For the Th1 lineage, a remodelling of the *Ifng* locus has been described, whereas other loci, such as *Il4/Il13* of *Il17a/f* are conversely kept in a closed heterochromatic state. Differentiation of Th1 cells is driven by IL-12 via STAT4 and IL-2 cytokines (Wan and Flavell, 2009).

In contrast, Th2 cells are controlled by the transcription factor Gata-3 and express IL-4 as a signature cytokine as well as IL-5 and IL-13. Th2 cells are critical for host immunity to extracellular parasites like helminths and are drivers of class-switch recombination towards neutralizing antibodies including IgE. Th2 differentiation is promoted by IL-4 and inhibited by the presence of IFNγ (Zhu et al., 2010).

Finally, Th17 cells are the major producers of IL-17A/F, potent pro-inflammatory cytokines, but also IL-22 and IL-21. Th17 cell express the transcription factors retinoic-acid-receptor-related orphan receptor alpha (RORα) and gamma (RORγt) and are critical players during fungal infections and immune response against extracellular bacteria. Differentiation of Th17 cells strongly depends on TGF-beta and IL-6 (Weaver et al., 2006; Zhu et al., 2010).

A further lineage, named T follicular helper cells (Tfh), resides within germinal centres and is characterized by the expression of CXCR5, PD-1, Icos and Bcl-6. Tfh cells are critical players in the development of antigen-specific B cell immunity and contribute to the generation of antibody-producing plasma cells and memory B cells. Whether Tfh cells are a lineage on their own or resemble a phenotypic copy of the other lineages in a distinct location is subject of an ongoing debate (Ma et al., 2012; Tangye et al., 2013).

1.2.4 Memory T cells

Upon activation by their specific antigen in the context of an MHC molecule presented by an activated antigen-presenting cell, naïve CD4+ and CD8+ T cells exit their quiescent state to become effector T cells and undergo a phase of extensive expansion. In the course of weeks after the initial infection, the pathogen-specific T cell pool declines in a contraction phase and only a few antigen-specific T cells remain over a longer period of time. These cells are marked by longevity and constitute the pool of memory T cells. Upon re-encounter of antigen, the specific memory T cells can expand rapidly and generate an effector response which is faster and more sensitive to low antigen doses than during the first encounter of the antigen (Jameson and Masopust, 2009).

The memory T cell pool consists of heterogeneous cell populations that differ according to how they were initially stimulated. Depending on whether they were induced by infectious pathogens, self antigens, commensals, or protein antigens in addition to adjuvants, CD4 and CD8 T cells exhibit different phenotypes in terms of turn-over rates and expression of CD127 and CD122, one protein of the heterotrimeric IL-2 receptor (Surh and Sprent, 2008; Surh et al., 2006). Furthermore, memory T cell subsets can greatly differ in their proliferation potential and longevity (Jameson and Masopust, 2009). The majority of memory T cells depend on IL-7 and IL-15 for survival and homeostatic proliferation, while they are - in contrast to naïve T cells - largely independent of self-peptide-MHC contact (Schluns et al., 2000).

In a simplified model, memory T cells can be subdivided into central-memory and effector-memory T cells by their homing and effector characteristics. This distinction is valid for both CD4 and CD8 T cell lineages. Central-memory T cells are characterized as $CD62L^{high}$ $CD44^{high}$ $CCR7^{high}$, whereas effector-memory T cells are identified as $CD62L^{low}$ $CD44^{high}$ $CCR7^{low}$ T cells (Sallusto et al., 1999). Along with the differential expression of CD62L and CD44, both cell types show distinct homing properties and cytokine profiles. Central-memory T cells are primarily found in lymphoid tissue and lack immediate effector function, while they are robust producers of IL-2. In contrast, effector-memory T cells can also be detected in non-lymphoid tissues and produce effector cytokines including IFNγ and IL-4 (Pepper and Jenkins, 2011).

Upon re-stimulation with antigen, central-memory T cells can acquire effector-memory phenotype and function. However, it is a matter of debate whether the differentiation pathway from naïve T cells via effector T cells to effector-memory and central-memory T cells follows linear or dynamic principles. The linear model suggests both memory T cells to be distinct lineages, whereas the dynamic model proposes interactions between the two memory T cell subtypes (Ahmed et al., 2009; Seder and Ahmed, 2003; Seder et al., 2008).

Effector and memory T cells show a partial phenotypic overlap as both effector and effector-memory T cell population express a similar molecular pattern being CD44+ CD62L-. This effector cell population also shares functional characteristics with memory T cells and therefore cannot be clearly distinguished from them (Kaech et al., 2002). In the following I will refer to both T helper and cytotoxic T cell lineages expressing CD62L+ CD44- as naive T cells, whereas CD62L+ CD44+ T cells are identified as central-memory T cells.

Furthermore, T cell expressing CD62L- CD44+ will be termed effector/memory T cells, as they comprise both effector and effector-memory T cells.

Even though memory T cells exhibit very different characteristics when compared to naïve T cells, microarray analysis revealed over 95% similarity in gene expression profiles between the two stages of differentiation (Weng et al., 2012). The changes in expression profiles are partially caused by changes in chromatin structure such as histone modifications and DNA methylation, which memory T cells acquire during differentiation. For instance, CD8+ memory T cells display hypomethylated (and therefore open) *Il2* and *Ifng* DNA loci which are a prerequisite for high expression of effector cytokines (Kersh et al., 2006). In human memory T cells, the expression of a variety of genes associated with adhesion (e.g. *CCR5* and *CCR6*), signalling (e.g. *MAP3K5*), and effector molecules (e.g. *GZMB*) is correlated with opening of the chromatin state (Weng et al., 2012). Analysis of the CD8+ T cell transcriptome during induction of a memory T cell response has further revealed key molecular activators and repressors: Notably, transcriptional regulators such as Tbx21, Prdm1, Bcl6, Foxo1, Foxo3, and Id2 play a major role in modulating the transition from naïve to memory CD8+ T cells (Best et al., 2013).

The transition from naïve to effector T cells, and subsequently to memory T cells, is of great importance for a functioning immune system as it is key in providing long lasting immunity. However, little is known about the molecular regulators of quiescence that maintain the naïve state. Kuo et al. reported a zinc finger transcription factor 'lung Kruppel-like factor' (Lklf) as a regulator of quiescence and survival (Kuo, 1997). Lklf knock-out T cells show a spontaneously activated phenotype reminiscent of effector T cells as well as reduced cell survival mediated by Fas:Fas-ligand interaction. Conversely, forced expression of Lklf in Jurkat T cells is sufficient to induce a state of quiescence, marked by reduced proliferation and activation upon stimulation (Buckley et al., 2001). Furthermore, it was observed that Lklf modulates T cell function by acting as a negative regulator of c-Myc.

Also involved in the maintenance of quiescence in T cells is Tob (transducer of ErbB), a member of the Tob and BTG-family of anti-proliferative proteins (Tzachanis et al., 2001). Tob is normally down-regulated upon T cell activation and overexpression of the protein results in impaired proliferation and cytokine production. In contrast, silencing of Tob leads to increased responses upon TCR-ligation and abrogates the necessity of co-stimulation. Further analysis showed that Tob interacts with Smad-proteins and promotes their binding to

Smad-consensus sites in the IL-2 promoter and thereby inhibition of IL-2 transcription (Tzachanis et al., 2001).

1.2.5 Regulatory T cells

Peripheral T cell tolerance is mainly maintained by the presence and actions of regulatory T cells. This subset of T cells was initially described as CD4+ T cells with suppressive characteristics, combined with high expression levels of CD25, one part of the trimeric high affinity IL-2 receptor (Sakaguchi et al., 1995; 1982). A second hallmark of regulatory T cells is the expression of Foxp3, a forkhead-box transcription factor that acts as a master-regulator of regulatory T cell function and differentiation (Hori et al., 2003). Deletion or loss-of-function mutations of Foxp3 lead to a lack of regulatory T cells and results in severe autoimmunity, as seen in *scurfy* mice and patients with 'immune dysregulation, polyendocrinopathy, enteropathy X-linked' (IPEX) syndrome (Bennett et al., 2001; Brunkow et al., 2001).

Regulatory T cells developing in the periphery are termed 'induced regulatory T cells' (iTregs) and strongly depend on TGFbeta and IL-2 signals during differentiation (Chen et al., 2003). Another subset of regulatory T cells develops in the thymus during T cell maturation. These thymus-derived 'natural' regulatory T cells (nTregs) are originating from thymocytes which received intermediate to strong TCR signals during negative selection (Josefowicz et al., 2012). Instead of undergoing apoptosis, this species of thymocytes turns into a regulatory subset of T cells, which exits the thymus and contributes to peripheral tolerance.

Regulatory T cells act as suppressors of effector T cell proliferation and function, thereby preventing exaggerated T cell responses. This suppression is supposedly achieved by the competition for IL-2, antigen, and co-stimulation. Additionally, regulatory T cells produce suppressive cytokines such as IL-10, IL-35 and TGF-β which are critically involved in the regulation of inflammatory disease and can affect other types of immune cells such as B cells and dendritic cells (Collison et al., 2007; Li et al., 2007; Rubtsov et al., 2010).

The Treg-specific transcription profile is in part regulated by Foxp3 itself and by changes in the chromatin modification landscape silencing genetic loci, which are otherwise accessible in effector T cells. At the same time, access is granted to other loci supporting the inhibitory function of regulatory T cells, like 'conserved non-coding sequences' in the *Foxp3* promoter region (Josefowicz et al., 2012). Furthermore, Foxp3 has been described to interact with

transcriptional activators like NFAT, NFκB, and AML1/Runx1, to negatively regulate effector gene transcription in regulatory T cells (Bettelli et al., 2005; Ono et al., 2007; Wu et al., 2006).

In summary, regulatory T cells are irreplaceable for maintaining peripheral tolerance of the adaptive immune system and their loss leads to fatal autoimmunity.

1.3 The transcription factor Foxp1

1.3.1 The fork-head box protein family

Proteins of the fork-head box (Fox) family are transcription factors, which share a common DNA-binding domain, consisting of two loops flanking three α helices. The domain is often referred to as 'winged-helix' domain due to its three-dimensional structure (Figure 2) (Benayoun et al., 2011).

Originally, the name 'fork head' was derived from a Drosophila loss-of-function mutant which resulted in a double-spiked-head structure during larval stage (Weigel et al., 1989). The Fox family comprises about 2000 known genes from more than 100 different species (Benayoun et al., 2011). In mice and men, 50 known Fox proteins can be divided in 19 subclasses, indicated in nomenclature by an additional letter (A-S) (Benayoun et al., 2011; Hannenhalli and Kaestner, 2009). Related Fox genes can be found in all opisthokonts (i.e.

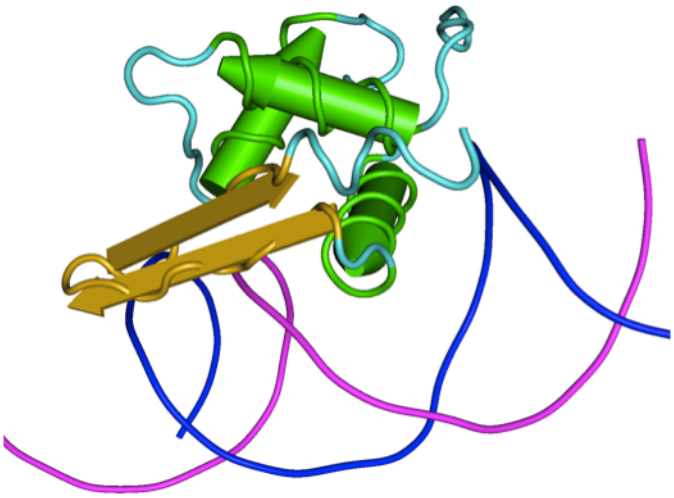

Figure 2 Crystal structure of Foxp2 fork-head domain bound to DNA. Partial view of a Foxp2 fork-head domain monomer binding to the antigen receptor response element in the IL-2 enhancer (ARRE2) according to Wu et al. (Wu et al., 2006). Alpha helix three is binding to the major DNA groove in the centre of the picture. Structure 2AS5 from NCBI Entrez Structure database was drawn with Cn3D 4.3 in worm display and domain colouring without depicting the co-crystallized NFAT structure (Y. Wang et al. 2000).

eukaryotes, including animals, fungi with rear flagellum and protozoa). Interestingly, the number of Fox genes found in an organism increases with its complexity (Carlsson and Mahlapuu, 2002). Consistent with this observation, the majority of Fox genes are involved in developmental or differentiation processes, and most murine null mutants of Fox genes show pre- or perinatal lethality (Benayoun et al., 2011; Carlsson and Mahlapuu, 2002).

Figure 3 Multiple sequence alignments of Foxp subfamily members. Sequence alignment for human (hs) and murine (mm) Foxp members performed with ClustalOmega (Sievers et al. 2011). Boxes indicate conserved zinc-finger motifs (red), leucine-zipper (green), and fork-head domain (black). Grade of full conservation is given below each line of sequence alignment.

Fox family proteins have been found to act in concert with other proteins, such as transcription factors (also of the Fox family), co-activators and co-repressors (Benayoun et al., 2011). Most Fox proteins bind DNA as monomers (e.g. FoxA), whereas others have been shown to interact with DNA as homo- or heterodimers (e.g. FoxP2) (Clark et al., 1993; Stroud et al., 2006).

Several Fox transcription factors have been attributed to important functions in the immune system. Foxn1 was one of the first Fox genes related to an immunological phenotype. *Nude* mice, in which Foxn1 is disrupted, suffer from complete alopecia and athymia, due to defective differentiation of epithelial progenitor cells in the thymus (Nehls et al., 1994). Thymic malformation eventually leads to impaired T cell development and severe immunodeficiency, similarly observed in a human nonsense mutation of FoxN1 (Frank et al., 1999).

The Foxo subfamily has been found to play a major role in T cell trafficking, survival, and homeostasis, as well as in induction of peripheral tolerance (Ouyang and Li, 2011). Foxo1-deficent T cells show reduced expression of sphingosine-1-phosphate-receptor 1 (S1P1), CD62L, and CCR7 (Kerdiles et al., 2009). Furthermore, lack of Foxo1 in T cells results in loss of IL-7R expression and thereby impaired homeostasis of naïve T cells (Ouyang et al., 2009). Foxo3-deficient mice show aberrant regulation of NFκB, leading to T cell activation and moderate autoimmunity (Lin et al., 2004a). Due to a defect in regulatory T cell differentiation, a double-knock out of Foxo1 and Foxo3 results in massive expansion of activated effector T cells and lethal autoimmunity (Ouyang et al., 2010).

T cell hyper-responsiveness is also observed in foetal-liver chimeras of Foxj1-deficient mice which develop systemic inflammation and multi-organ infiltration of spontaneously activated T cells (Lin et al., 2004b). In contrast, Foxj1 full knock-out animals exhibit impaired development of cilia in ciliated epithelium and die perinatally (Chen et al., 1998).

The Foxp subfamily includes four different proteins, Foxp1 – 4, which share a highly conserved DNA-binding domain as well a leucine zipper and a N-terminal zinc-finger domain (Figure 3). In addition, Foxp1 and Foxp2 proteins have poly-glutamine (poly-Q) stretches, which presumably mediate protein-protein interactions. Interestingly, the murine Foxp1 protein bears an additional stretch of 30 poly-Q of yet unknown function. Moreover, proteins of this subfamily show highly conserved sequences in mice and men. Especially the forkhead domain is almost fully conserved in all four proteins. Notably, Foxp1 and Foxp2 show the highest degree of identity according to phylogenetic analysis of protein sequences (Figure 4).

The most studied member of the Foxp family by far is Foxp3, which has been described as master-regulator of regulatory T cell differentiation and function. Importantly, FOXP3 was described to interact with FOXP1 through its leucine zipper domain and form heterodimers (Song et al., 2012). This heterodimerization is likely to be a mechanism of regulation, as it is competing with FOXP3 homodimerization and therefore presumably function.

FoxP2 has been found to be mutated in a family with 15 affected individuals with congenital speech and language disorders (Lai et al., 2001). Disruption of the *Foxp2* gene in mice leads to impaired ultrasonic vocalization and cerebellar abnormalities, especially affecting Purkinje cells (French et al., 2007; Shu et al., 2005).

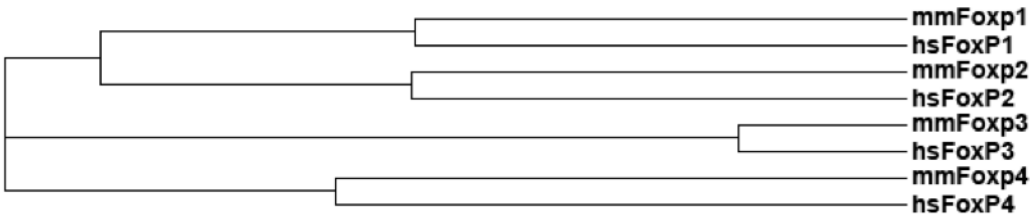

Figure 4 Phylogeny of Foxp subfamily members. Phylogenetic distance between protein sequences calculated with ClustalOmega (Sievers et al. 2011) and depicted in a cladogram neighbour-joining tree without distance corrections.

Foxp4 is expressed in various tissue, such as lung, gut and brain (Lu et al., 2002); (Takahashi et al., 2008). In epithelial cells, Foxp4 was found to act in concert with Foxp1 to control cell fate during lung development and regeneration (Li et al., 2012). In the developing brain, Foxp2 and Foxp4 also regulate the maintenance of neuroepithelial progenitors by suppression of N-Cadherin expression (Rousso et al., 2012).

The last transcription factor of the murine Foxp subfamily, Foxp1, is expressed in alternatively spliced isoforms, which define the regulatory properties of the protein by selection of different exons (Wang, 2003). Wang et al. described four different isoforms Foxp1 A-D and defined a DNA consensus binding sequence for Foxp1 (T A T T T G/A T) (Wang, 2003). The role of Foxp1 in non-hematopoietic tissues, in cells of the immune system and in malignancies is discussed in the subsequent sections.

1.3.2 Foxp1 in non-hematopoietic tissues

In 2001, Shu et al. first described Foxp1 and Foxp2 as two novel transcription factors expressed in the developing and adult lung. Here, both proteins act as transcriptional repressors of surfactant protein SP-C and secretoglobin CC10. Moreover, expression of Foxp1 and Foxp2 is observed during development in neural, intestinal and cardiovascular cell types (Shu et al., 2001). In addition to its expression in the developing nervous system, Foxp1 was identified in various regions of the mature central nervous system and in projection neurons of the striatum (Tamura et al., 2004; 2003). In the context of human neurological disorders, FOXP1 was also found to interact with polyglutamine-expanded mutant huntingtin protein (Tang et al., 2012). Microarray and ChIP-seq analysis revealed a role for the transcription factor in regulation of inflammatory responses in immortalized striatal neurons. Thus, the authors hypothesized a critical role for FOXP1 in the immune response to Huntington's disease (Tang et al., 2012).

Most notably, a full knock-out model of Foxp1 showed embryonic lethality around E14.5 (Wang, 2004). Specifically, knock-out embryos suffered from defects in cardiac morphogenesis, outflow tract septation and endocardial cushion malformation. The defects were based on altered proliferation and maturation of Foxp1-deficient myocytes. Together, these aberrations resulted in perivascular hemorrhage and edema leading to premature death of the embryo.

Another critical function for Foxp1 and Foxp2 has been described during development of lung and esophageal tissue (Shu et al., 2007). Here, both transcription factors cooperatively control the expression of crucial regulators of lung development, such as N-myc and Hop. Whereas Foxp1 Foxp2 double knock-out mice succumb prior to E11.5, an allelic combination of $Foxp1^{+/-}$ $Foxp2^{-/-}$ led to severe defects of lung airways, resulting in perinatal death (Shu et al., 2007).

After previous studies had implicated expression of Foxp1 in cells of the nervous system, two independent studies described the importance of Foxp1 during formation of motor neurons in the spinal cord (Dasen et al., 2008; Rousso et al., 2008). The authors report Foxp1 to function as an essential accessory factor to a network of transcription factors of the Hox family, which have been known to direct motor innervation patterns. Lack of Foxp1 function resulted in the loss of motor neuron specification and produced a spinal cord resembling that of primitive vertebrates, which lack segmentation of the spine into brachial, thoracic, and lumbar parts.

From this it became clear, that Foxp1 is critically involved in a variety of developmental processes and might act as a key regulator of differentiation. Consistent with that, Gabut et al. showed in an elegant study that alternative splicing of FOXP1 regulates embryonic stem cell (ESC) pluripotency (Gabut et al., 2011). Here, an alternative selection of exon 18 and exon 18b results in two different Foxp1 isoforms, which show distinct DNA-binding properties. FOXP1-ES, the alternate from of the transcription factor present in ESCs, activates the expression of several pluripotency genes, including *NANOG*, *OCT4*, *GDF3*, and *NR5A2*. At the same time, FOXP1-ES suppresses gene transcription associated with differentiation of ESCs (Gabut et al., 2011).

Taken together, Foxp1 plays a fundamental role in several non-hematopoietic tissues regulating differentiation, maturation and proliferation of various cell types. The importance of Foxp1 is further underlined by the early death and the multitude of developmental defects observed in Foxp1 knock-out embryos.

1.3.3 Foxp1 in cancer

In 2001, the full-length cDNA and polypeptide sequences for FoxP1 were described and suggested to be a tumour-suppressor gene candidate. Furthermore, the gene was mapped to human chromosomal region 3p14.1, a locus recurrently disrupted in solid tumours (Banham et al., 2001). Comparative analysis of tumour samples revealed differential expression and cellular localization of FoxP1 in a variety of tumours. A majority of colon cancers showed loss of Foxp1 expression, while most of the studied gastric tumours exhibited strong overexpression of the protein (Banham et al., 2001). Additionally, this study first described high Foxp1 expression in diffuse large B cell lymphoma (DLBCL) samples.

DLBCL is a common subgroup of non-Hogkin lymphomas (NHL) and can be subcategorized further into activated-B cell (ABC) and germinal centre (GC) types, according to gene expression pattern obtained in microarray analysis (Shaffer et al., 2002). Further examination of FoxP1 expression in the context of DLBCLs showed that high Foxp1 expression is largely restricted to activated B cells and ABC-DLBCLs (Shaffer et al., 2002). In addition, strong FoxP1 expression is correlated with poor outcome in cases of non-GC DLBCL and is proposed as a prognostic marker for clinical classification of the disease (Banham et al., 2005; Barrans et al., 2004).

A study by Wlodarska et al. suggested, based on fluorescent *in situ* hybridisation (FISH) and cytogenetic data, that the FOXP1 gene is a recurrent site of chromosomal aberration, resulting in t(3;14)(p13;q32) translocations. These translocations bring FOXP1 under the control of IGH enhancers and thereby lead to overexpression of the protein (Wlodarska et al., 2005). Comparable translocations of t(3;14)(p14;q32) were observed in cases of DLBCL, also leading to aberrant expression of FOXP1 (Fenton et al., 2006; Haralambieva et al., 2006). Additional studies also reported a different t(3;14)(p14.1;q32) genetic translocation of the FOXP1 locus in MALT lymphomas commonly occurring in the stomach (Streubel et al., 2005). Interestingly, ABC-type DLBCL also expressed smaller isoforms of FOXP1, which are normally found in B cells after activation. These isoforms are N-terminally truncated and are suspected to be of oncogenic nature (Brown et al., 2008).

In contrast to DLBCLs, high expression of Foxp1 in non-hematopoietic cancers was correlated with variable outcomes. In patients suffering from primary breast carcinoma, strong Foxp1 expression was associated with improved survival rates (Fox et al., 2004). In a rat model of lung adenocarcinoma induced by N-nitroso-bis(2-hydroxypropyl)-amine treatment, Foxp1 expression was reduced in cancerous compared to healthy lung tissue (Shimizu et al., 2006). Also, the localization of Foxp1 was reported to be of critical importance: in endometrial cancers, a cytoplasmic Foxp1 expression pattern resulted in enhanced myometrial invasion of the tumour and was associated with HIF-1α overexpression (Giatromanolaki et al., 2006).

Taken together, the transcription factor Foxp1 is differentially expressed in several forms of hematopoietic and non-hematopoietic cancers. Depending on the cell type and the state of differentiation, Foxp1 was either found to be up- or downregulated suggesting indeed a potential role as tumour-suppressor and oncogen, respectively. Finally, translocations and overexpression of Foxp1 in ABC-type DLBCLs indicate a critical role of the protein in B cell activation and differentiation.

1.3.4 Foxp1 in cells of the immune system

Several transcription factors of the Fox-family are critically involved in development and function of the immune system. Namely, the most striking phenotypes were observed in mice lacking Foxn1 or Foxp3 (Brunkow et al., 2001; Nehls et al., 1994). Similarly, the function of Foxp1 seems to be crucial for the development and proper function of the immune system.

The first implication for Foxp1 in the immune system was given by Shi et al., who reported the importance of the transcription factor in regulation of monocyte differentiation (Shi et al., 2004). The authors described Foxp1 as a direct repressor of the *c-fms* gene, which encodes for the M-CSF receptor and is critical for proliferation and survival of monocytic phagocytes. Upon clustering of integrin receptors by fibrinogen or stimulation of THP-1 monocytes with PMA, Foxp1 expression declined. Concurrently, overexpression of Foxp1 lead to impaired maturation of monocytes upon PMA stimulation. Finally, the authors showed that Foxp1 directly regulates *c-fms* transcription by binding to a DNA consensus site in the gene promoter. In a second publication, the same authors reported a mouse model of Foxp1 overexpression under control of the CD68 promoter (Shi et al., 2008). The transgenic mouse exhibited reduced expression of M-CSF receptor on monocytes and impaired macrophages functions *in vivo*. Additionally, intraperitoneal challenge with *S. aureus* resulted in reduced survival in Foxp1 transgenic mice supporting the notion for a critical role of Foxp1 in differentiation and function of myeloid cells.

Also in B cell development, Foxp1 acts as a critical regulator (Hu et al., 2006). Since Foxp1-deficienct mice are not viable, Hu et al. took advantage of foetal-liver chimeric mice and reported a block during pro-B to pre-B cell transition in the bone marrow. The authors provided evidence that Foxp1 binds directly to the Erag enhancer and acts as an activator of gene transcription. Loss of Foxp1 thereby results in diminished expression of Rag1 and Rag2 leading to reduced V(D)J recombination and a block during early B cell development (Hu et al., 2006). In a different study, binding of Foxp1 to the Erag enhancer was reproduced in different cancer cell lines (Chen et al., 2011). Together with Foxo1 and E2A, the transcription factor Foxp1 binds to the gene locus, and overexpression of Foxp1 resulted in increased Rag expression. Therefore, Foxp1 is another key player in the regulatory transcription network controlling early B lymphocyte development in the bone marrow, together with others such as Pax5, Ikaros, E2A, Foxo1, NFATc1, and NFκB (Kuo and Schlissel, 2009).

Early B cell maturation is in part dependent on p53, which regulates pro-B cell apoptosis (Lu and Osmond, 2000). p53 is involved in transactivation of the microRNA (miRNA) family 34, which includes miRNA-34a (Chang et al., 2007). To investigate the role of this miRNA, Rao et al. generated chimeric mice, which were reconstituted with miRNA-34a transduced bone marrow (Ackermann et al., 2010). A block in pro- to pre-B cell transition was found, comparable to the one observed in Foxp1-deficient B cells. Furthermore, in an elegant series of experiments, the authors showed that Foxp1 is a direct target of miRNA-34a, and is therefore strongly reduced in chimeric cells. Concordantly, bone-marrow co-transduction with

a Foxp1 overexpressing construct compensated for the observed phenotype. These results pointed out the regulatory function of Foxp1 in early B cell maturation.

Investigation of Foxp1 expression in later stages of B cell development revealed a distinct role for the transcription factor in the transition of naïve to germinal centre B cells (Sagardoy et al., 2013). Foxp1 is down-regulated in germinal centres, conversely to the high expression of Bcl-6, a master regulator of germinal centre reactions and well-studied oncogene in B cell lymphomagenesis (Basso and Dalla-Favera, 2010). Additionally, Foxp1 and Bcl6 targets are partially overlapping, suggesting differential engagement of the two transcription factors during germinal centre formation. Sagardoy et al. also generated a transgenic mouse strain expressing human FOXP1 under the control of Eμ-enhancer and SR-α promoter. Aberrant FOXP1 expression resulted in minor changes in the B cell compartment *in vivo*, but abnormal class-switch recombination *in vitro,* indicated by reduced switching to IgG1 and diminished presence of γ1 germline transcripts (Sagardoy et al., 2013).

Even though Foxp1 has not yet been implicated in autoimmunity in a mouse model, a genome-wide association study in humans found a connection: In search of genetic loci linked to generalized vitiligo in humans (a progressive autoimmune disease, resulting in the loss of melanocytes), single-nucleotide polymorphisms in chromosome 3p13 were found to be correlated with susceptibility to the disease (Jin et al., 2010). The most significant polymorphisms were mapped to the *FOXP1* locus, suggesting allelic variations of this transcription factor to be associated with the autoimmune disease.

Until 2008, when the work presented here was started, Foxp1 had been only investigated in monocytes and B lymphocytes, but no study had addressed its relevance in T cells. The striking importance of Foxp1 for early development of B cells in the bone marrow and its regulation of *Rag* genes pointed out that the transcription factor could play a critical role in CD4+ and CD8+ T lymphocytes as well. If Foxp1 would act as an important factor in T cell development, one would expect a prominent phenotype by ablating the transcription factor from T lymphocytes. To test this hypothesis, we took advantage of a conditional knock-out mouse model for the transcription factor Foxp1 that was previously generated in our laboratory as the full knock-out was reported to succumb at day E14.5 (Patzelt, 2010). In his work, the author described the generation and specific ablation of Foxp1 in B cells and presented preliminary data on the loss of Foxp1 in T cells. However, the main questions concerning the role of Foxp1 in T cell differentiation and function were still open.

While this work was in preparation, two studies addressing the role of Foxp1 in T cells were published, which paralleled and posthoc confirmed part of the independently acquired results which are presented here (Feng et al., 2010; 2011). In the first publication, Feng et al. described the transcription factor Foxp1 as a critical regulator of naïve T cell quiescence (Feng et al., 2010). In a second work, Feng et al. characterized the role of Foxp1 in the cell-intrinsic regulation of quiescence (Feng et al., 2011). In the discussion section of this work, these studies will be reviewed in detail and critically compared to the data presented here.

2 Research objective

Fox proteins play an essential role during development and differentiation of many cell types and tissues. Indeed, Foxp1 has been shown to be crucial during early B cell maturation and the activation of Rag genes (Hu et al., 2006). Also in monocytes and macrophages, a role for the transcription factor has been implicated (Shi et al., 2004; 2008). However, until the start of this project, the role of Foxp1 in the T cell lineage had not been investigated. Therefore, this thesis aimed at analyzing the role of the transcription factor Foxp1 in T cell differentiation and function. In addition to an in depth phenotypic and functional characterization of Foxp1-deficient T cells, the work presented here also set out to dissect the role of Foxp1 in peripheral tolerance and in a context of autoimmunity.

In order to determine the expression profile of the transcription factor Foxp1, expression levels in different lymphocyte lineages and T cell subpopulations of wildtype mice were investigated. Motivated by the observation that Foxp1 expression is tightly regulated during T cell maturation, the impact of a T cell-specific ablation of Foxp1 was investigated. To this end, a previously established Foxp1 conditional knock-out mouse model was bred to a CD4 Cre background and the T cell compartment of the resulting Foxp1 conditional knock-out CD4 Cre mice was immunophenotypically characterized in detail. Subsequently, Foxp1-deficient CD4+ T cells were functionally tested in multiple *in vitro* assays for proliferation, survival, and cytokine production. Moreover, to genetically rescue a survival defect observed in Foxp1-deficient T cells, a Bcl2 transgenic mouse strain was employed and analyzed. In an additional transgenic approach the immunphenotype of a specific ablation of Foxp1 in regulatory T cells was studied by breeding conditional knock-out animal to a Foxp3 Cre line. Finally, to gain new insights into the importance of Foxp1 in autoimmunity and its regulation of inflammatory T cell responses, the loss of Foxp1 was studied in an autoimmune-prone background. Therefore, the encephalitogenic 2D2 mouse strain, carrying a transgenic MOG-specific T-cell receptor, was bred to Foxp1 conditional knock-out mice in a CD4 Cre background and phenotypically analyzed.

In summary, the work presented here aimed at investigating the general role of the transcription factor Foxp1 in T cell differentiation and function, its relevance in regulatory T cells and its importance for T cells in an autoimmune disease model for multiple sclerosis.

3 Materials

3.1 Reagents

All chemical reagents were purchased by Sigma-Aldrich, if not stated otherwise.

3.2 Genotyping primers

All genotyping primers were obtained from Sigma Aldrich.

Foxp1 common fwd	5'-CTG CAC AGC AGG GTA GTT AGT G-3'
Foxp1 wt rev	5'-CTG CTC TAC TGC GTT CTT CCT C-3'
Foxp1 flox rev	5'-GCT CTA CTG CGT TCT TTG TAC ATT T-3'
Foxp1 del rev	5'-ATG CTA GGC GGT ACT AAA TAG AAC-3'
CD4 Cre fwd	5'-ACC AGC CAG CTA TCA ACT CG-3'
CD4 Cre rev	5'-TTA CAT TGG TCC AGC CAC C-3'
Vav-Bcl2 fwd	5'-GCC GCA GAC ATG ATA AGA TAC ATT GAT G-3'
Vav-Bcl2 rev	5'-AAA ACC TCC CAC ACC TCC CCC TGA A-3'
Foxp3 GFP fwd	5'-AAG TTC ATC TGC ACC ACC G-3'
Foxp3 GFP rev	5'-TCC TTG AAG AAG ATG GTG CG-3'
2D2 fwd	5'-CCC GGG CAA GGC TCA GCC ATG CTC CTG-3'
2D2 rev	5'-GCG GCC GCA ATT CCC AGA GAC ATC CCT CC-3'

3.3 Real time PCR Primer

All real time PCR primers were obtained from Sigma Aldrich.

Foxp1 RT fwd	5'-CAT GCT TCA ACA GCA GCT TCA A-3'
Foxp1 RT rev	5'- GGT AGC CAC CTG CTG CTC TTT C-3'
Tbp RT fwd	5'-CCA CCA GCA GTT CAG TAG CTA TGA-3'
Tbp RT rev	5'-TGC TCT AAC TTT AGC ACC TGT TAA TAC AAC-3'

3.4 Pull-down oligonucleotides

All pull-down oligonucleotides were obtained from Eurofins MWG Operon. Forward oligonucleotides were synthesized with biotin modifications at the 5' end.

IL-2 oligo fwd	biot-5'-AAG AGG AAA ATT TGT TTC ATA CAG AAG G-3'
IL-2 oligo rev	5'-CCT TCT GTA TGA AAC AAA TTT TCC TCT T-3'
mut IL-2 oligo fwd	biot-5'-AAG AGG AAA ATT **A**GT T**A**C ATA CAG AAG G-3'
mut IL-2 oligo rev	5'-CCT TCT GTA TGT AAC TAA TTT TCC TCT T-3'

3.5 Western blotting antibodies

Rabbit anti-Foxp1 (#2005, Cell Signaling Technology)

Rabbit anti-β-actin (Sigma)

Anti-Rabbit-HRP (Cell Signaling Technology)

3.6 Flow cytometry antibodies

Fluorescently labelled antibodies used for extracellular staining in flow cytometry:

Anti-CD4 (GK1.5), anti-CD8a (53-6.7), anti-B220 (RA3-6B2), anti-CD19 (eBio1D3), anti-TCRβ (H57-597), anti-NK1.1 (PK136), anti-TCRα/β (eBioGL3), anti-CD25 (PC61.5), anti-CD62L (MEL-14), anti-CD44 (IM7), anti-CD69 (H1.2F3), anti-GR-1 (RB6-8C5), anti-CD11b (M1/70), anti-CD127 (A7R34), anti-CD122 (TM-b1), anti-KLRG1 (2F1), anti-CD28 (37.51), anti-CD27 (LG.7F9), anti-CD95 (Jo2), anti-CCR7 (4B12), anti-Vα3.2 (RR3-16), anti-Vβ11 (RR3-15), and anti-CD16/CD32 (Clone 93) all obtained from eBioscience.

Fluorescently labelled antibodies used for intracellular staining in flow cytometry:

Anti-IL-17 (eBio17B7), anti-IL-4 (11B11), anti-IL-2 (JES6-5H4), anti-Foxp3 (FJK-16s) all obtained from eBioscience, Rabbit anti-Foxp1 (#2005, Cell Signalling), Alexa Fluor 488 Goat Anti-Rabbit (H+L) and Alexa Fluor 647 Goat Anti-Rabbit (H+L) (both Molecular Probes), anti-TNF-α (MP6-XT22), and anti-IFNγ (XMG1.2) purchased from BD Biosciences.

Antibodies were labelled with Fluorescein isothiocyanate (FITC), Phycoerythrin (PE), Phycoerythrin-Cyanine5 (PE-Cy5), Peridinin Chlorophyll (PerCP), Phycoerythrin-Cyanine7 (PE-Cy7), Allophycocyanin (APC), Allophycocyanin-Cyanine7 (APC-Cy7), and Pacific blue.

3.7 Reagents used for T cell stimulations

Reagents used for T cell receptor stimulations:

AffiniPure Rabbit Anti-Syrian Hamster IgG (2,4 mg/ml, H+L, Jackson Immuno Research)

Anti-CD3e antibody (1mg/ml, Clone 145-2C11, eBioscience)

Anti-CD28 (1mg/ml, Clone 37.51, eBioscience)

Reagents used for T cell receptor-independent stimulations:

PMA (1mM stock in DMSO, Sigma-Aldrich)

Ionomycin (1mM stock in DMSO, Sigma-Aldrich)

Cytokines used in survival and proliferation assays:

Mouse recombinant IL-2 (10 µg/ml stock, R&D Systems)

4 Methods

4.1 Work with nucleic acids

4.1.1 Isolation of DNA

Isolation of genomic DNA from mouse tail tips was performed with Wizard SV Genomic DNA Purification System (Promega). Briefly, the extracted tissue was incubated with digestion solution (nucleic lysis solution, 0.5M EDTA (pH 8.0), Proteinase K and RNase A solution) and incubated for 16 h at 56°C heat block shaker. After addition of Wizard SV lysis buffer, the solution was transferred to a mini-column and washed according to manufacturer's recommendation. Purified DNA was eluted with nuclease-free H_2O and stored at 4°C.

4.1.2 Genotyping PCRs

Mouse genotypes were identified by genotyping polymerase chain reactions (PCRs) using purified DNA samples of housed animals. PCR amplifications were performed with primers specific for genetically modified alleles (described in Materials section 3.2). A typical PCR reaction contained template DNA (approx. 50ng), dNTP mix (200µM each), 2.5 µl 10x Taq reaction buffer, forward and reverse primers (200nM each) and 0,2 µl of Illustra Taq DNA Polymerase (GE Healthcare) added up to a total volume of 25 µl with nuclease-free H_2O.

Foxp1 genotyping PCRs were performed with a common forward primer (Foxp1 common fwd) and three distinct reverse primer identifying either wildtype (Foxp1 wt rev), flox (Foxp1 flox rev), or del (Foxp1 del rev) alleles (Patzelt, 2010). For all three Foxp1 PCRs, amplification cycles were 1. 95°C, 5min, 2. 95°C, 30 sec, 3. 63°C, 30sec, 4. 72°C, 1min, 5. 72°C, 10min, 6. 4°C until stopping. Steps 2 – 4 were repeated 38 times. Amplicon sizes were 342 bp for Foxp1 wt and 478 bp for Foxp1 flox, whereas the Foxp1 del PCR yielded a fragment of 623 bp if the respective allele was present.

CD4 Cre PCR amplification cycles: 1. 95°C, 2min, 2. 95°C, 45 sec, 3. 57°C, 45sec, 4. 72°C, 50sec, 5. 72°C, 10min, 6. 4°C until stopping. Steps 2 – 4 were repeated 30 times. DNA containing a CD4 Cre allele yielded a specific band at 200 bp when analysed by agarose gel electrophoresis.

For PCR genotyping of vav-Bcl2 transgenic alleles, the following amplification cycles were used: 1. 92°C, 2min, 2. 92°C, 1min, 3. 68°C, 1min, 4. 72°C, 1min, 5. 72°C, 10min, 6. 4°C

until stopping. Steps 2 – 4 were repeated 35 times. A vav-Bcl2 positive samples showed an amplicon size of 200 bp.

Foxp3 Cre mice were genotyped by GFP-specific PCR analysis, as mice carry an Enhanced Green Fluorescent Protein (*EGFP*) fused to a Cre recombinase coding sequence under the control of the endogenous Foxp3 promoter (Zhou et al., 2008). Amplification cycles were performed like the following: 1. 92°C, 2min, 2. 92°C, 1min, 3. 68°C, 1min, 4. 72°C, 1min, 5. 72°C, 10min, 6. 4°C until stopping. Steps 2 – 4 were repeated 35 times. A Foxp3 EGFP Cre positive samples showed an amplicon size of 200 bp.

2D2 mice carrying a transgenic allele encoding for MOG-specific TCR were analysed by PCR using Phire Polymerase (Thermo Scientific) with the following amplification cycles: 1. 98°C, 30sec, 2. 98°C, 5sec, 3. 56°C, 5sec, 4. 72°C, 15sec, 5. 72°C, 1min, 6. 4°C until stopping. Steps 2 – 4 were repeated 35 times. DNA from 2D2 transgenic mice showed an amplicon size of 675 bp.

4.1.3 Agarose gel electrophoresis

Amplicons generated in the above-mentioned genotyping PCRs were separated by gel electrophoresis according to their size by migration through an agarose gel in an electrical field. Agarose gels were prepared by dissolving 1-2% agarose (w/v) in TAE buffer (400 mM Tris base, 500mM EDTA, 1.1% (v/v) acetic acid). Briefly before gels were poured, a solution of intercalating ethidium bromide (Eurobio) was added. PCR samples were supplemented with 10x loading-dye (50% glycerol (v/v), 0.05% bromophenol blue (w/v), 1mM EDTA, pH 8.0) and loaded to agarose gels. Runs were performed inside of a gel electrophoresis chamber (Biorad) in TAE buffer at 100-140 V for 30-60min. Intercalated ethidium bromide was visualized by ultraviolet light of 320 nm on a GelDoc 2000 (Biorad). Amplicon sizes were determined by comparison to DNA standard ladders (Peqlab).

4.1.4 Isolation of RNA

RNA extraction was performed using Trizol Reagent (Sigma). 1-3x10^6 FACS-sorted thymocytes were washed with ice-cold PBS, resuspended in 1ml Trizol and incubated for 5 min before storage at -20°C. After thawing, 200 µl Chloroform were added to each sample. Samples were mixed by inversion of the tubes and centrifuged (14000g, 10min, 4°C) before

the upper aqueous phase was transferred to fresh tubes and supplemented with 1 volume 100% ethanol. Samples were mixed and transferred to RNeasy spin columns (Qiagen). Washing procedures were performed according to manufacturer's instructions. Finally, purified RNA was eluted in RNase-free H_2O and stored at -80°C.

4.1.5 Reverse transcription

First strand cDNA synthesis was performed using SuperScript II system (Invitrogen) according to the manufacturer's instructions. Briefly, purity and concentration of RNA samples was determined using a Nanodrop spectrophotometer (Thermo Scientific) and 500ng – 1 µg RNA were used for reverse transcription. RNA was supplemented with 250ng random primers, 0.5mM dNTPs each, 5mM DTT, 5x reaction buffer, RNase-free H_2O and 10U/µl SuperScript II enzyme to a total volume of 20µl. Reverse transcription was carried out in a PCR Thermocyler (Biorad). After synthesis of cDNA, samples were diluted in H_2O and stored at -20°C

4.1.6 Quantitative Real time PCRs

For quantitative Real time PCR analysis, specific primer pairs were designed spanning exon-exon boundaries and are given in Materials section 3.3. For analysis of cDNA, qPCR Core kit for SYBR Green (Eurogentec) and ABI PRISM 7700 Sequence Detection System were used according to manufacturer's protocols. All samples were measured in triplicates and real-time PCR signals for Foxp1 were normalized to those of Tbp of the corresponding samples using ΔΔCt method (Pfaffl, 2001).

4.2 Work with proteins

4.2.1 Western blotting

For the analysis of protein expression, purified CD4+ T cells (isolation procedure described in chapter 4.3.2) were washed in ice-cold PBS and lysed in CHAPS lysis buffer (30 mM Tris/HCl (pH 7.5), 150 mM NaCl, 1% CHAPS (w/v), in deionized H_2O, 1 µM PMSF, 1 µM DTT, 1x Protease Inhibitor Cocktail) for 30 min on ice. Samples were spun down in a pre-cooled tabletop centrifuge (20817 g, 15 min, 4°C), before lysates were transferred to fresh 1.5

ml tubes and stored at -20°C. Protein concentration in lysates was determined by colorimetric BCA assay (Pierce). Lysates were spiked with 5x Laemmli buffer (250 mM Tris/HCl (pH 6.8), 25% Glycerol, 10% β-Mercaptoethanol, 5% SDS (v/v), 0.1% Bromphenol blue (w/v)) and boiled at 95°C for 10 min. Subsequently, 5-10µg of each lysate was loaded per lane on a 10% SDS-polyacrylamid gel (Volumes for 2 Minigels of 8.3 cm x 7.3 cm x 1 mm - Stacking gel: 3 ml deionized H_2O, 1.2 ml 0.5 M Tris/HCl (pH 6.6), 0.7 ml 30% Acrylamid/Bisacyrlamid solution, 25 µl 20% SDS solution, 25 µl 10% APS solution and 5 µl TEMED (N, N, N, N' tetramethyl-ethylenediamine); Running gel: 4.1 ml deionized H_2O, 2.5 ml 1.5 M Tris/HCl (pH 8.8), 3.3 ml 30% Acrylamid/ Bisacyrlamid solution, 50 µl 20% SDS solution, 50µl 10% APS solution and 5 µl TEMED) and run at 100 – 140 V in a western blotting chamber (Biorad) containing sufficient amounts of running buffer (10x running buffer: 250 mM Tris, 1.92 M Glycine, 1% SDS (v/v) in deionized H_2O). For semi-dry blotting, PVDF transfer membranes (Amersham Hybond-P, GE Healthcare) were activated with methanol and equilibrated in transfer buffer (10x transfer buffer: 480 mM Tris, 390 mM Glycine, 0.315% SDS (v/v) in deionized H_2O; 20% Methanol freshly added to 1x Transfer buffer) before blotting procedure. Blotting was performed between stacked Whatman papers (Biorad) in the presence of transfer buffer. Membranes were blocked with 5% Bovine serum albumin (w/v, Albumin Fraktion V, Roth) in 1x TBST (10x TBS buffer: 200 mM Tris, 1.37 M NaCl in deionized H_2O, adjust pH to 7,4; addition of 0.1% Tween-20 to 1x Transfer buffer), before incubation with specific antibodies. Antibodies used for Western blotting are given in Materials section 3.5. For chemiluminsecent detection of primary antibodies, HRP-conjugated secondary antibodies and Lumigen TMA-6, Solution A+B (GE Healthcare) substrate solution was used. Emitted light signals were collected by photosensitive films, which were subsequently developed.

4.2.2 Enzyme-linked immunosorbent assays (ELISAs)

Anti-CD3 titration experiments were carried out on isolated CD4+ T cells incubated with various amounts of soluble anti-CD3e antibody (5 µg/ml, Clone 145-2C11, eBioscience) in combination with anti-CD28 (2µg/ml, Clone 37.51, eBioscience). After 24 h of stimulation IL-2 levels in cell culture supernatants were harvested and stored at -80°C. Cytokine concentration were determined with OptEIA mouse IL-2 ELISA Set (BD Pharmingen) according to manufacturer's protocol. Briefly, Nunc Maxisorp 96 plates were coated with IL-2 capture antibody solution diluted in coating buffer (eBioscience) at 4°C over night. ELISA

plates were blocked for 1 h at room temperature using PBS + 10% FCS (v/v) solution. After blocking, plates were washed three times with washing buffer (PBS + 0.05% Tween-20), before samples and standards were applied and incubated over night at 4°C. The next day, plates were washed three times with washing buffer before incubation with working detector solution (containing biotinylated detection-antibodies and streptavidin-labelled horseradish peroxidase) for 2 h at room temperature. After five washing steps, substrate buffer (volumes for one 96 well plate: 2,5 ml Na_2HPO_4, 2,5 ml citric acid monohydrate, 5 ml H_2O, 1 reagent tablet 3, 3', 5, 5'-Tetramethylbenzidine (TMB) and 2µl 30% H_2O_2) was added and incubated until a change in colour became visible for half the standard dilutions. The reaction was stopped by addition of one volume 2N H_2SO_4. Finally, plates were read on a Magellan Sunrise plate reader (Tecan) by endpoint measurement at a wavelength of 450 nm. Sample concentrations were calculated in Microsoft Excel (2008 for Mac).

4.2.3 Detection of auto-antibodies

For detection of auto-antibodies in sera, blood was drawn from the superficial temporal vein of mice, collected in 1,5 ml tubes and subjected to coagulation on ice for 30 min. Subsequently, samples were centrifuged (14000g, 10min, 4°C), the serum phase was transferred in fresh tube and stored at -80°C. Auto-antibody detection was performed with ELISA kits specific for ssDNA, dsDNA, Histones, and ENA/ANA antibodies (Alpha Diagnostics Intl.) according to manufacturer's recommendation. Plates were read on a Magellan Sunrise plate reader (Tecan) by endpoint measurement at a wavelength of 450 nm.

4.2.4 Cytokine bead arrays

Cell culture supernatants from *in vitro* stimulations of MACS-purified CD4+ T cells with PMA (100nM) and Ionomycin (500nM) for the indicated time points were analyzed with mouse FlowCytomix Th1/Th2 10plex Kit (Bender MedSystems) according to manufacturer's protocol by flow cytometry. Briefly, cell culture supernatants and standards of the respective cytokines were incubated with beads specific for IL-2, IFNγ, TNF, IL-4, IL-17, and GM-CSF. After incubation, beads were washed and a biotin-conjugate mixture was added. After incubation and washing, streptavidin-PE solution was incubated with the beads. After thorough washing, beads were measured on a FACSCantoII flow cytometer (Becton Dickinson) and analyzed by FlowCytoMix Pro 2.3 software.

4.2.5 Oligonucleotide pull-down assay

Oligonucleotide pull-down assays were performed with biotinylated double-stranded DNA probes (Bürckstümmer et al., 2009). Probes were designed according to previously published Foxp1/2/3 DNA consensus sequences in the antigen receptor response element (ARRE2) in a distal IL-2 enhancer region (Wang, 2003; Wu et al., 2006). Biotinylated oligonucleotides were obtained from Eurofins MWG Operon and are given in Materials section 3.4.

Forward and reverse oligonucleotides were annealed by heating oligonucleotide solution to 85°C for 20 min and cooling down to RT. Strep-Tactin Superflow resins (IBA) were washed three times with PBS before addition 2 nmol dsDNA oligonucleotides and rotor incubation at 4 °C for 2h. MACS-purified CD4+ T cells from Foxp1^{cKO} control and Foxp1^{cKO} CD4 Cre mice were lysed in NP-40 lysis buffer (50 mM Tris, pH 7.5, 100 mM NaCl, 5% glycerol (v/v), 0.2% Nonidet-P40 (v/v), 1.5 mM $MgCl_2$, 25 mM NaF, 1 mM Na_3VO_4 and protease inhibitor cocktail (Roche)). Resins were washed in lysis buffer before incubation with equal amounts of cell lysates and rotor incubation at 4°C over night. Subsequently, resins were washed three times in NP-40 lysis buffer to remove unbound protein. Finally, resins were boiled in laemmli buffer to elute bound proteins before supernatant was separated by SDS-PAGE. Input samples were diluted 1/10 in lysis buffer. Antibodies used in Western blot are listed in Material section 3.5.

4.3 Work with cells

4.3.1 Flow cytometry

Single cell suspensions of thymi, spleens, and lymph nodes were prepared by meshing organs through 100µm strainer (BD Falcon). After red-blood cell lysis, cells were washed and counted. Every staining was carried out using $1x10^6$ cells in FACS buffer (PBS + 3% FCS). Fc-receptor blocking was performed by incubation with purified anti-mouse CD16/CD32 antibodies to block unspecific binding of antibodies to Fc receptors. Subsequently, cells were stained in a volume of 50 - 100 µl of FACS buffer with combinations of fluorescently labelled antibodies listed in Material section 3.6.

Intracellular staining was carried out with fixation/permeabilization reagents (eBioscience) according to the manufacturer's protocol. Antibodies used in intracellular stainings are listed in Material section 3.6. For intracellular stainings, LIVE/DEAD Fixable Near-IR amine-

reactive dyes (Invitrogen) were used before the extracellular staining procedure to exclude dead cells during analysis.

Stained samples were measured on a FACSCantoII flow cytometer (Becton Dickinson), and analyzed using FlowJo (Version 8 and 9, TreeStar). For analysis, cell doublets were omitted by a forward-scatter-area (FSC-A) versus forward-scatter-height (FSC-H) gating strategy. Furthermore living lymphocytes were distinguished by FSC and sideward-scatter (SSC).

4.3.2 Purification of CD4+ T cells

Cell suspensions of pooled spleens and lymph nodes of a respective genotype were treated with red blood cell lysis buffer (eBioscience) and living cells were counted in a Neubauer glass chamber after addition of Trypan-Blue solution (Gibco). Purification of CD4+ T cells was carried out using CD4+ T cells isolation Kit II (Miltenyi Biotech) according to manufacturer's recommendation. Briefly, cells were incubated with a ready-made cocktail of biotinylated antibodies specific for antigens not present on CD4+ T cells. In a second step, magnetic streptavidin-microbeads were added to the cell suspension. After incubation, cells were transferred to LS columns (Miltenyi Biotech) and placed in a magnetic stand. The columns were washed for three times and the flow-through containing purified CD4+ T cells was collected. Purity of CD4+ T cells was measured by flow cytometry after incubation of an aliquot of the flow-through with fluorochrome-labeled anti-CD4 antibodies. The purification procedure was carried out in a laminar flow hood when sterile conditions were required.

4.3.3 FACS sorting of primary cells

Single-cell suspensions of thymi, and spleens/lymph nodes were filtered and stained with fluorochrome-labelled antibodies specific for CD4, CD8, CD25, and CD19. Sorting was performed on a FACSAria III (Becton Dickinson) using a 70µm nozzle. Sorting gates for thymus cell suspensions were set on double-negative (CD4- CD8-), double-positive (CD4+ CD8+), and single-positive cells (CD4+ or CD8+), respectively. Sorting gates for spleen/ lymph node cells were set for B cells (CD19+), cytotoxic T cells (CD8+), T helper (CD4+ CD25-), and regulatory T cells (CD4+ CD25+). Cells were cooled pre- and post-sorting and subsequently used for RNA extraction or preparation of cell lysates for western blotting.

4.3.4 Isolation of CNS-infiltrating lymphocytes

For isolation of CNS-infiltrating lymphocytes, animals were sacrificed with isoflurane and immediately perfused through the left cardiac ventricle with ice-cold PBS. The complete brain was dissected and cut into cubes of 5 mm size in a 10 cm dish filled with cold PBS. The tissue was subjected to collagenase D (2.5 mg/ml, Roche Diagnostics) and DNAseI (100 µg/ml, Roche Diagnostics) digestion at 37°C for 45 min under constant agitation on a shaking platform. The digested solution was subsequently passed through a 70µm strainer and mononuclear cells were retrieved by percoll gradient centrifugation (37% over 70% percoll). Cells were harvested from the percoll interphase, washed in complete RPMI medium, and finally stained in FACS buffer for flow cytometric analysis.

4.3.5 In vitro culture and stimulation of T cells

For *in vitro* culture of purified CD4+ T lymphocytes, cells were kept in complete cell culture medium (RPMI 1640, 5% FCS, 1% penicillin/streptomycin, 1% L-glutamine, 0.1% β-mercaptoethanol) at 37°C, 5% CO_2. Cells were cultured in a density of $2x10^5$ cells/200µl medium in a 96 well up to $3x10^6$ cells/3ml medium in a 6 well plate.

For stimulation with plate-bound anti-CD3, wells were pre-coated over night at 4°C with AffiniPure Rabbit Anti-Syrian Hamster IgG in PBS. After washing, anti-CD3e antibodies (5µg/ml) were diluted in PBS, added to the wells and incubated for 1 hour at 37°C. Wells were washed again with PBS before addition of complete medium containing anti-CD28 antibodies (2µg/ml). CD4+ T cells were taken up in complete medium, added to the pre-coated wells and incubated at 37°C for the indicated time. Plate-bound stimulations were used for CFSE-proliferation assays and *in vitro* survival assays.

For stimulation of total splenocytes with plate-bound anti-CD3 ligation in order to perform intracellular flow cytometry, total splenocytes from control and $Foxp1^{cKO}$ CD4 Cre mice were incubated for 6 h with plate-bound anti-CD3e (5µg/ml) and anti-CD28 antibodies (2µg/ml) in the presence of Brefeldin A (10µg/ml; Sigma-Aldrich). Cytokine production of *ex vivo* stimulated splenic T cells was analyzed by intracellular flow cytometric analysis.

Stimulations of CD4+ T cells with soluble anti-CD3e antibodies were performed in 96 U-wells with different concentrations of anti-CD3e antibodies (0, 1, 10, 100, 1000, 10000 ng/ml) alone, or in the presence of soluble anti-CD28 antibodies (2µg/ml). Supernatants were harvested after 24 h and stored at -20°C before analysis by ELISA.

In time-course stimulation experiments, MACS-purified CD4+ T cells from Foxp1^{cKO} control and Foxp1^{cKO} CD4 Cre mice were stimulated with PMA (100nM) and Ionomycin (500 nM) in 96 U-well plates for 0, 4, 8, 16, and 24 h. Supernatants were collected at indicated time-points and stored at -20°C before analysis by cytokine bead array.

4.3.6 CFSE proliferation assay

Cell proliferation of purified CD4+ T cells was determined by carboxyfluorescein succinimidyl ester (CFSE) labelling of cells. In this assay, cell division is marked by the loss of fluorescence, as half the CFSE dye of a cell is passed on to its daughter cells. Proliferation therefore results in distinct peaks in a CFSE histogram. MACS-bead purified CD4+ T cells were washed and incubated with 2.5 µM CFSE in serum- and supplement-free RPMI 1640 medium for 10 min at 37°C at a concentration of 1x10^7 cells/ml. The reaction was stopped by addition of cold RPMI 1640 medium containing 10% FCS. After an additional washing step with complete cell culture medium, cells were cultured at 37°C under various conditions. Cell division was analysed by flow-cytometry on a FACSCantoII (BD) after indicated time-points.

4.3.7 In vitro survival assay

For *in vitro* culture of purified CD4+ T cells, cells were kept in complete cell culture medium (RPMI 1640, 5% FCS, 1% penicillin/streptomycin, 1% L-glutamine, 0.1% 2-mercaptoethanol, all by Gibco) at 37°C, 5% CO_2. Cells were maintained in a density of 2x10^5 cells/200µl medium in 96 flat-bottom wells.

For IL-2 treatment, recombinant murine IL-2 (5 or 10ng/ml) was added to the culture and double-concentrated cell suspensions were added to the wells. Finally, cell viability was quantified by flow cytometry by Annexin V and 7-AAD stainings (PE Annexin V Apoptosis Detection Kit I; BD Biosciences) at the start of the experiment and after indicated time-points. Percentage of living cells was calculated according to the percentage of Annexin V-, 7-AAD- CD4+ T cells at the start of the experiment.

4.4 Work with animals

4.4.1 Mouse strains

C57BL/6 at the age of 6 – 12 weeks were used in some experiments and are termed wildtype mice. Most experiments were carried out on Foxp1 conditional knock-out ($Foxp1^{cKO}$) mice that were generated in our lab and were described previously by Patzelt (Patzelt, 2010). In the present study, three different Foxp1 alleles were used: a floxed allele (flox), a deleted allele (del), and the wildtype allele (wt or +). T cell-specific $Foxp1^{cKO}$ mice were generated by breeding $Foxp1^{cKO}$ mice to a CD4 Cre strain, carrying a Cre recombinase in the context of a CD4 enhancer/promoter/silencer construct inside of the Lck promoter locus (Lee et al., 2001). Furthermore, $Foxp1^{cKO}$ CD4 Cre mice were bred to a vav-Bcl2 transgenic mouse strain to achieve overexpression of Bcl2 in all hematopoietic cells (Ogilvy et al., 1999). Additionally, $Foxp1^{cKO}$ mice were bred to a Foxp3 Cre mouse strain, enabling a specific deletion of Foxp1 in Foxp3-positive regulatory T cells (Zhou et al., 2008). To investigate the role of Foxp1 in an autoimmune-prone background, $Foxp1^{cKO}$ CD4 Cre mice were bred to 2D2 mice, carrying a transgenic TCR specific for myelin oligodendrocyte glycoprotein (MOG) peptides 35-55 (Bettelli et al., 2003). All mice were housed in a specific pathogen-free facility of the Technische Universität München Medical Faculty according to the FELASA recommendations (http://www.felasa.eu/recommendations).

4.4.2 Ataxia scoring

Neurological symptoms of $Foxp1^{cKO}$ CD4 Cre mice bred to 2D2 $MOG_{(35-55)}$-specific TCR mice were quantified by a composite phenotype scoring system, described by Guyenet et al. (Guyenet et al., 2010). Classical EAE scoring was not applicable, as affected mice did not develop typical signs of full-blown paralysis observed in EAE. Briefly, for ataxia scoring mice were tested for four different parameters, including ledge walk, hindlimb clasping, gait ataxia, and kyphosis. Each parameter was scored in a range between 0 and 3, whereas 0 indicated the absence and 3 the most severe manifestation of neurological symptoms. Finally, the total sum of all four parameter results was calculated (ranging between 0 and 12) and used as a quantification of neurological symptoms.

4.5 Sequence alignment and phylogeny

Sequence alignment and phylogenetic tree analysis was performed using ClustalOmega (Sievers et al., 2011). The following protein sequences were aligned: mmFoxp1 isoform 1 (NP_444432.1), hsFoxP1 isoform 1 (NP_001231743.1), mmFoxp2 (NP_444472.2), hsFoxP2 isoform II (NP_683696.2), mmFoxp3 (NP_001186276.1), hsFoxP3 isoform a (NP_054728.2), mmFoxp4 isoform 1 (NP_001104294.1), hsFoxP4 isoform 1 (NP_001012426.1). Corresponding NCBI accession numbers are given in brackets.

4.6 Statistical analysis

Values are given as mean ± standard error of the mean (SEM), if not indicated otherwise. Statistical analysis was performed using unpaired two-tailed Student's t-test function for unequal variances (Welch's correction). For statistical analysis of Kaplan-Meier survival curves, Logrank/Mantel-Cox tests were performed. Differences between groups were considered statistically significant at $p < 0.05$, indicated by an asterisk (*), while p-values < 0.01 are indicated by a double-asterisk (**). Statistical analysis was performed with Graphpad Prism 5 or Microsoft Excel 2008.

5 Results

5.1 Expression of Foxp1 in cells of the immune system

The transcription factor Foxp1 is widely expressed in various tissues and during different developmental stages. To investigate the expression level of Foxp1 in cells of the immune system, different lymphocyte subsets from spleen and lymph node cell suspensions of C57BL/6 wildtype mice were sorted by FACS according to their surface marker expression into B cells (CD19+), cytotoxic T cells (CD8+), T helper cells (CD4+ CD25-), and regulatory T cells (CD4+ CD25+). Next, cell lysates of all subsets were prepared and analysed by western blotting with Foxp1 and β-actin antibodies (Figure 5A). B cells as well as cytotoxic and T helper cells expressed similar amounts of the most prominent Foxp1 isoform 1A at a height of approximately 97 kDa, whereas regulatory T cells exhibited lower protein levels of this particular isoform. Lymphocytes additionally expressed different Foxp1 isoforms, such as Foxp1C (approx. 55 kDa) and Foxp1D (approx. 75 kDa). The latter was most prominently expressed in isolated CD19+ B cells, suggesting differential roles for Foxp1 isoforms in different cell types.

Next, effector/memory and naïve T cells from wildtype spleens were measured by flow cytometry and differentiated by their cell surface expression of CD4, CD44 and CD62L. Naïve T cells have a characteristic $CD62L^{high}$ $CD44^{low}$ pattern, whereas the most prominent effector and effector-memory T cell fraction shows a high expression of CD44 and concomitant low expression of CD62L (Mueller et al., 2013). Here, naïve T cells showed increased intracellular Foxp1 expression, when compared to effector/memory T cells. Dot plot representation of $CD44^{low}$ CD4+ T cells revealed higher expression of Foxp1, whereas $CD44^{high}$ CD4+ T cells showed lower abundance of the protein (Figure 5B, upper panel). Additionally, it was found that CD62L expression was associated with Foxp1 expression (Figure 5B, lower panel). Furthermore, a histogram overlay of both, naïve and memory CD4+ T cells showed down-regulation of Foxp1 in the memory T cell compartment in contrast to the naïve T cell fraction (Figure 5C).

The reduced expression of Foxp1 in regulatory T cells observed in Western blotting was confirmed by flow cytometry of regulatory T cells obtained from C57BL/6 wildtype mice after intracellular staining for Foxp1. Regulatory T cells were distinguished from conventional T helper cells by CD4+ CD25+ expression and further differentiated into CD62L (L-selectin)-positive and negative cells. CD62L-negative T helper cells and

regulatory T cells generally showed a lower expression of Foxp1 suggesting a concerted downregulation of both proteins (Figure 5D). Therefore, the reduced overall expression of Foxp1 in regulatory T cells observed by Western Blotting may be due to the larger fraction of CD62L negative cells in this particular T cell subset.

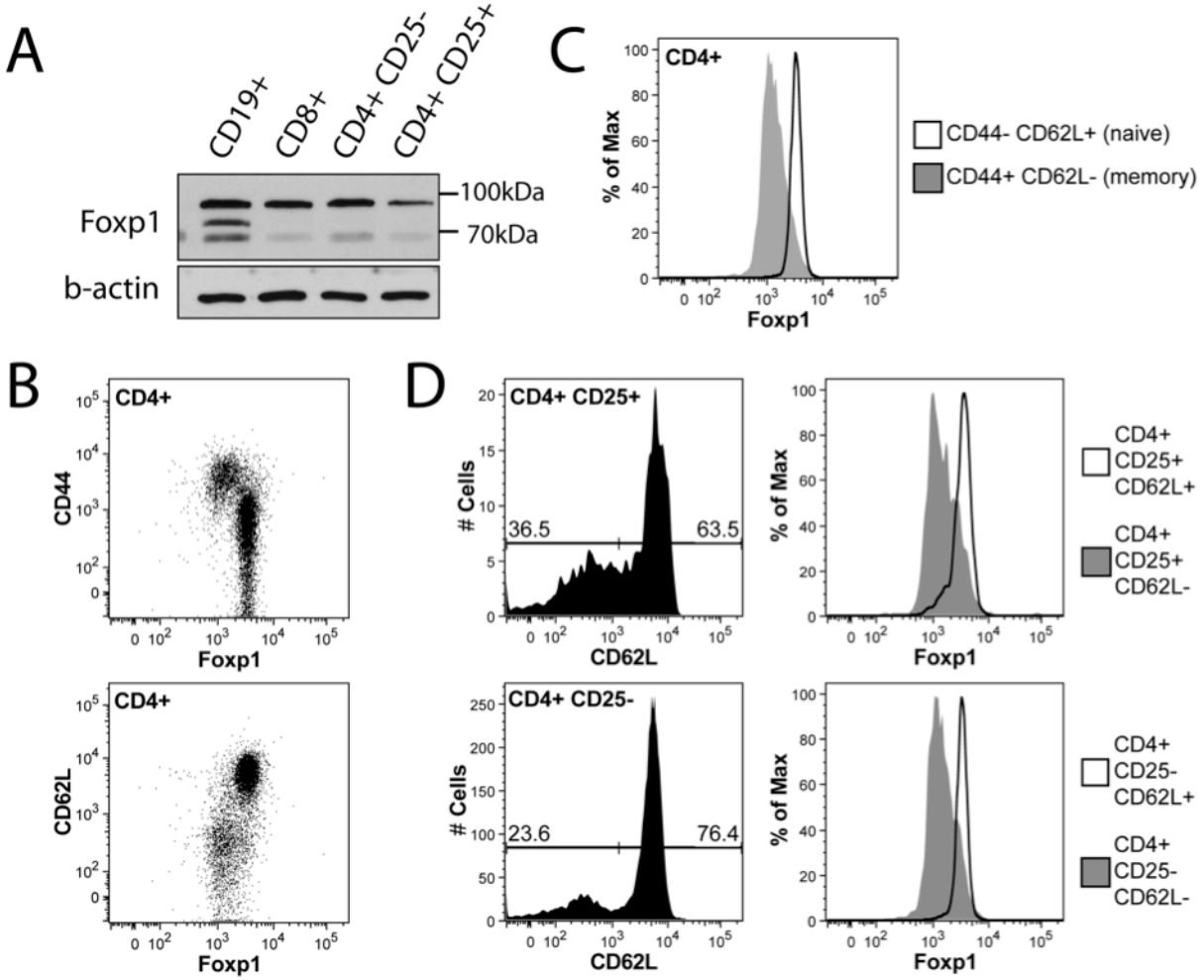

Figure 5 Reduced Foxp1 expression in memory T cells. (A) Western Blot analysis for Foxp1 of FACS-sorted lymphocytes, separated according to their expression of CD19+ (B cells), CD8+ (cytotoxic T cells), CD4+ CD25- (T helper cells) and CD4+ CD25+ (regulatory T cells). β-actin expression is shown as loading control. **(B)** Dot blots of CD44 and CD62L expression in CD4+ T cells compared to intracellular levels of Foxp1. Results show representative data of two independent experiments. **(C)** Comparison of Foxp1 expression in naïve ($CD44^{low}$ $CD62L^{high}$) and memory CD4+ T cells ($CD44^{high}$ $CD62L^{low}$) by flow cytometry. **(D)** Flow cytometry of Foxp1 expression in regulatory (CD4+ CD25+) and conventional T helper cells (CD4+ CD25-). Foxp1 expression is shown as histogram overlay of the respective T cell subset according to their CD62L expression.

To investigate protein expression of Foxp1 during different stages of T cell development, wildtype thymocytes were FACS-sorted according to their extracellular expression of CD4 and CD8. By staining for these two markers, it is possible to discriminate double-negative (CD4- CD8-), double-positive (CD4+ CD8+) and single-positive (CD4+ CD8- and CD8+ CD4-) thymocyte populations. Subsequently, sorted thymocytes were lysed and Foxp1 expression was analysed by Western Blotting (Figure 6A). Again, expression of the most prominent Foxp1 isoform 1A was observed at a height of approximately 97 kDa in lysates of all thymocytes subsets. Interestingly, double-positive thymocytes expressed markedly lower levels of Foxp1A, whereas double-negative and single-postive thymocytes showed comparable amounts of this isoform. Additionally, minor expression of the isoform Foxp1C was observed in all sorted thymocytes, similar to what was observed in peripheral T cells.

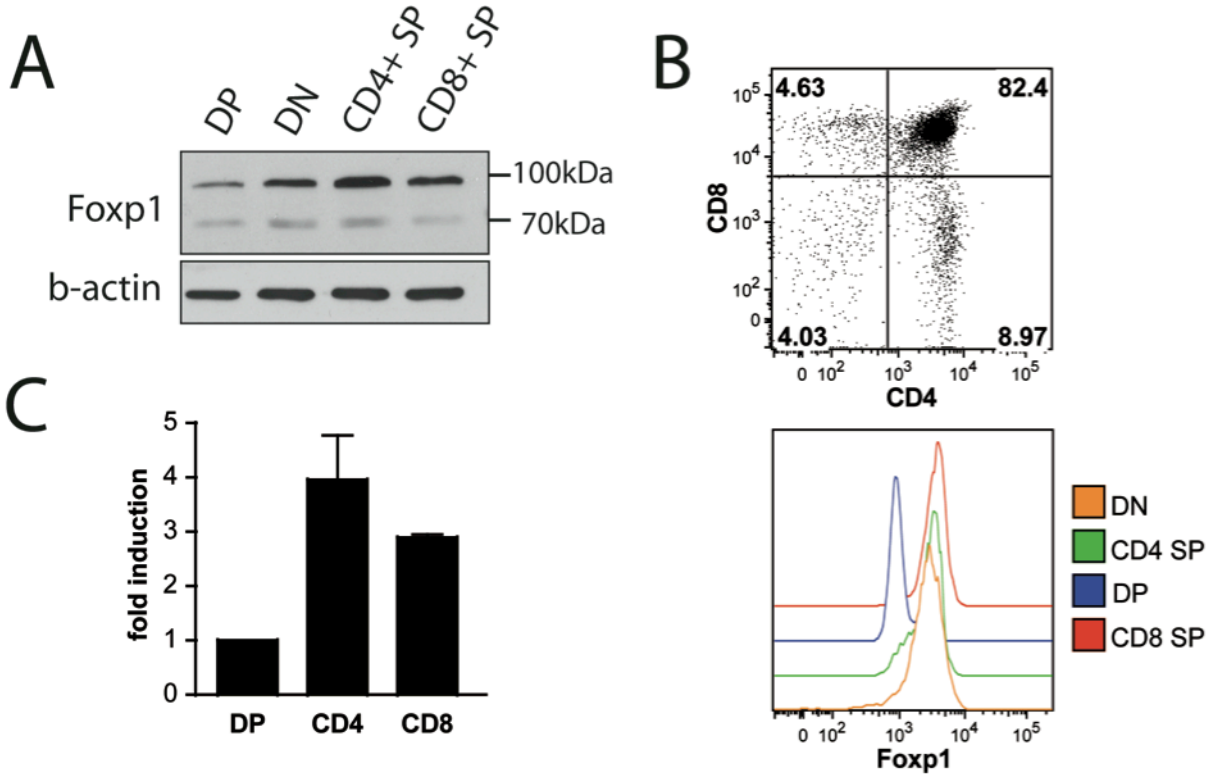

Figure 6 Differential Foxp1 expression in thymocytes subsets. (A) Western blot analysis of Foxp1 expression in thymocyte subsets. Thymic cells were FACS-sorted according to expression of CD4 and CD8 into double-negative, double-positive, and single-positive thymocytes and subjected to western blotting for Foxp1 and β-actin. **(B)** Intracellular flow cytometry of Foxp1 expression in the four different thymocytes subsets given as histogram overlays. Plots show representative data of three independent experiments. **(C)** Quantitative real-time PCR analysis of FACS-sorted double-positive and single-positive thymocytes for Foxp1 message, relative to Tbp and normalized to double-positive thymocytes (DP). Bar graphs show pooled data (mean values +/- SEM) of two independent experiments.

Again, this finding was supported by intracellular flow cytometry for Foxp1 expression in the different thymocyte populations. In this experiment, cells from wildtype thymi were stained for their surface expression of CD4 and CD8, before intracellular staining for Foxp1 was performed. Here, Foxp1 expression was again reduced in double-positive thymocytes (Figure 6B). A similar outcome was observed, when thymocytes were FACS-sorted and cDNA was prepared from isolated RNA of those cells. By quantitative real-time PCR analysis with Foxp1-specific primers, lower presence of Foxp1 message in double-positive thymocytes was observed, when compared to single-positive CD4+ and CD8+ thymocytes (Figure 6C). This finding indicates lower abundance of Foxp1 mRNA in double-positive thymocytes.

Taken together, Foxp1 was differentially expressed in various lymphocyte and T cell subset. Whereas CD4+ T helper and CD8+ cytotoxic T cells showed similar expression of Foxp1, lower Foxp1 expression was observed in CD4+ CD25+ regulatory T cells. Most importantly, naïve and memory T cells differed in their Foxp1 expression pattern: Foxp1 expression was down-regulated in the memory T cell compartment, differentiated by CD4+ $CD44^{high}$ $CD62L^{low}$ in contrast to the naïve T cell compartment marker by their expression of CD4+ $CD44^{low}$ $CD62L^{high}$. Additionally, lower expression of Foxp1 was measured in the double-positive thymocyte fraction, whereas other thymocyte populations showed comparable expression levels of Foxp1.

In summary, different isoforms of Foxp1 are broadly expressed in cells of the lymphoid lineage. However, in several cell types like double-negative thymocytes, memory T cells, and a fraction of regulatory T cells expression of Foxp1 is down-regulated implicating a specific role of the transcription factor during T cell differentiation and maturation.

5.2 T cell-specific Foxp1 knock-out

5.2.1 Generation of a T cell-specific conditional Foxp1 knock-out mouse

Whereas all lymphocytes showed expression of Foxp1, a downregulation of the transcription factor was observed in CD4+ CD44^{high} CD62L^{low} T cells, implicating a role for the protein in the transition from naïve to effector/memory T cells. To investigate the role of the transcription factor Foxp1 in T cells in an *in vivo* setting, a previously generated Foxp1 conditional mouse model was used (Patzelt, 2010). Briefly, the conditional knock-out mouse was generated by targeting the endogenous Foxp1 locus via homologous recombination (Figure 7A). The resulting Foxp1^{flox} allele contained newly introduced loxP sites flanking exons 10 – 12 representing a major part of the forkhead-DNA-binding domain, which is conserved in all Foxp family members. In presence of a Cre recombinase, both loxP sites are cleaved and excision of the three flanked exons takes place. The newly generated allele is

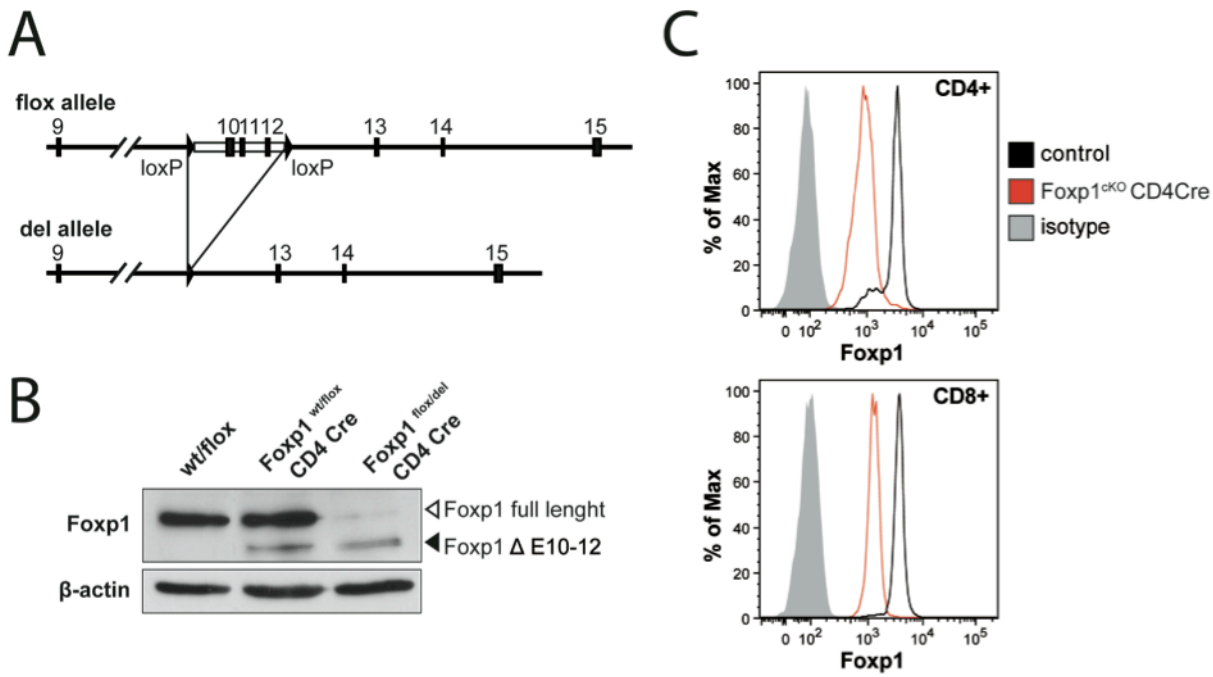

Figure 7 Generation and validation of a T cell-specific Foxp1 conditional knock-out mouse. (A) Schematic representation of the transgenic Foxp1 locus showing the loxP-site flanked exons 10-12 (flox allele) according to Patzelt (Patzelt 2010). In the presence of Cre recombinase the floxed locus is excised, resulting in a modified allele lacking exon 10-12 (del allele). **(B)** Western blot analysis for the expression of Foxp1 and β-actin in purified CD4+ T cells from Foxp1-conditional knock-out mice carrying CD4 Cre recombinase. The open arrow indicates the full-length form of Foxp1, whereas the filled arrow marks the low-abundant truncated Foxp1 protein in conditional knock-out cells. **(C)** Intracellular flow-cytometry of Foxp1 expression in CD4+ and CD8+ T cells in conditional knock-out mice and controls. Grey lines indicate isotype controls. Histograms are representative of three independent experiments.

referred to as Foxp1^{del}, lacking exons 10 - 12. Importantly, Foxp1$^{del/del}$ mice, generated by breeding of Foxp1^{flox} mice to a Cre deleter strain (B6.C-Tg(CMV-cre)1Cgn/J), resemble phenotypically the previously described full knock-out genotype for Foxp1, as both animals die *in utero* at E14.5 due to severe malfunction of the cardiac outflow tract, endocardial morphogenesis and myocyte malfunction (Patzelt, 2010; Wang, 2004).

For the generation of T cell-specific Foxp1 conditional knock-out mice, animals were bred to a CD4 Cre recombinase mouse strain, which expresses Cre recombinase specifically in T cells (Lee et al., 2001). Cre recombinase expression in the CD4 Cre mouse starts during double-positive thymocyte stages when the CD4 antigen is first expressed in thymocyte maturation. The recombination typically results in nearly complete deletion of loxP-flanked DNA loci.

In this work, Foxp1 conditional mice are generally referred to as Foxp1^{cKO} mice and represent the allelic combinations Foxp1$^{flox/del}$ and Foxp1$^{flox/flox}$. Animals of both allelic combinations, Foxp1$^{flox/del}$ and Foxp1$^{flox/flox}$ in a CD4 Cre background were tested in the assays described in this work, but no differences were apparent (data not shown). The allelic combination Foxp1$^{+/flox}$ CD4 Cre was preferably used as control in all experiments shown in this work. Additionally, Foxp1$^{+/+}$ CD4 Cre and Foxp1$^{flox/flox}$ in the absence CD4 Cre recombinase were used as controls. None of theses groups showed significant differences to the Foxp1$^{+/flox}$ CD4 Cre group in any assay tested (data not shown).

Western blot analysis of CD4+ T cells of Foxp1$^{flox/del}$ CD4 Cre mice and controls showed nearly complete absence of Foxp1 expression (Figure 7B, open arrow). Additionally, a faint band representing the truncated Foxp1 protein lacking exons 10 – 12 was observed (closed arrow). The truncated form of Foxp1 was of much lower abundance than the full-length form in control lysates potentially indicating reduced protein stability of the truncated form. Furthermore, absence of Foxp1 expression in CD4+ and CD8+ T cells of Foxp1^{cKO} CD4 Cre mice was observed by intracellular FACS-analysis when compared to cells from control animals (Figure 7C).

In summary, a T cell-specific Foxp1 conditional knock-out mouse model was generated by breeding Foxp1^{cKO} mice to animals carrying CD4 Cre recombinase and the absence of Foxp1 expression in T cells was validated by western blotting and intracellular flow cytometry.

5.2.2 Immunophenotypical characterization of Foxp1^{cKO} CD4 Cre mice

In order to investigate the phenotype of Foxp1^{cKO} CD4 Cre animals in greater detail, young adult mice were immunophenotypically analyzed. First, total body and spleen weights of 6-9 week old Foxp1^{cKO} CD4 Cre and control mice were measured (Figure 8). Foxp1^{cKO} CD4 Cre mice showed moderate splenomegaly marked by an increase in splenic weight and total splenic cell numbers, whereas total body weight remained unaltered. In this context, it became obvious that lymph node sizes were generally reduced in Foxp1^{cKO} CD4 Cre mice (data not shown).

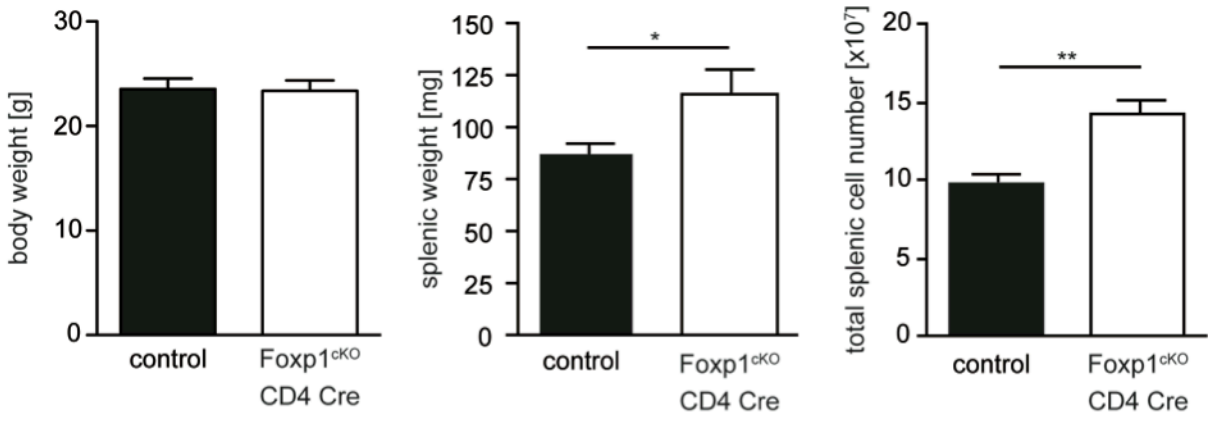

Figure 8 Mild splenomegalia in Foxp1^{cKO} CD4 Cre mice. Body weights of male control (n = 10) and Foxp1^{cKO} CD4 Cre mice (n = 5) at the age of 6 – 9 weeks (left panel). Splenic weights of control (n = 11) and Foxp1^{cKO} CD4 Cre mice (n = 7) (middle panel). Total splenic cell numbers of control (n = 10) and Foxp1^{cKO} CD4 Cre mice (n = 5) (right panel). Bar charts show mean values +/- SEM. * $P < 0.05$, ** $P < 0.01$.

Early T cell developmental stages in the thymus did not show obvious alterations (Figure 9A, left panel). Here, double-negative, double-positive, CD4+ and CD8+ single-positive were present in comparable percentages in Foxp1^{cKO} CD4 Cre mice and control mice. Additionally, no alteration in the percentage of thymus-derived 'natural' regulatory T cells was observed (Figure 9A, right panel).

Further investigation of the immune cell composition of spleens from Foxp1^{cKO} CD4 Cre mice showed a shift in B/T cell ratio towards B cells (Figure 9B, left panel). This shift is marked by an increase of the percentage of B220+ B cells in contrast to a general reduction of TCRβ+ T cells in spleens of Foxp1^{cKO} CD4 Cre mice. The reduced overall abundance of T cells was also observed in CD4+ T helper cells and CD8+ cytotoxic T cells, as percentages of both subsets were clearly diminished.

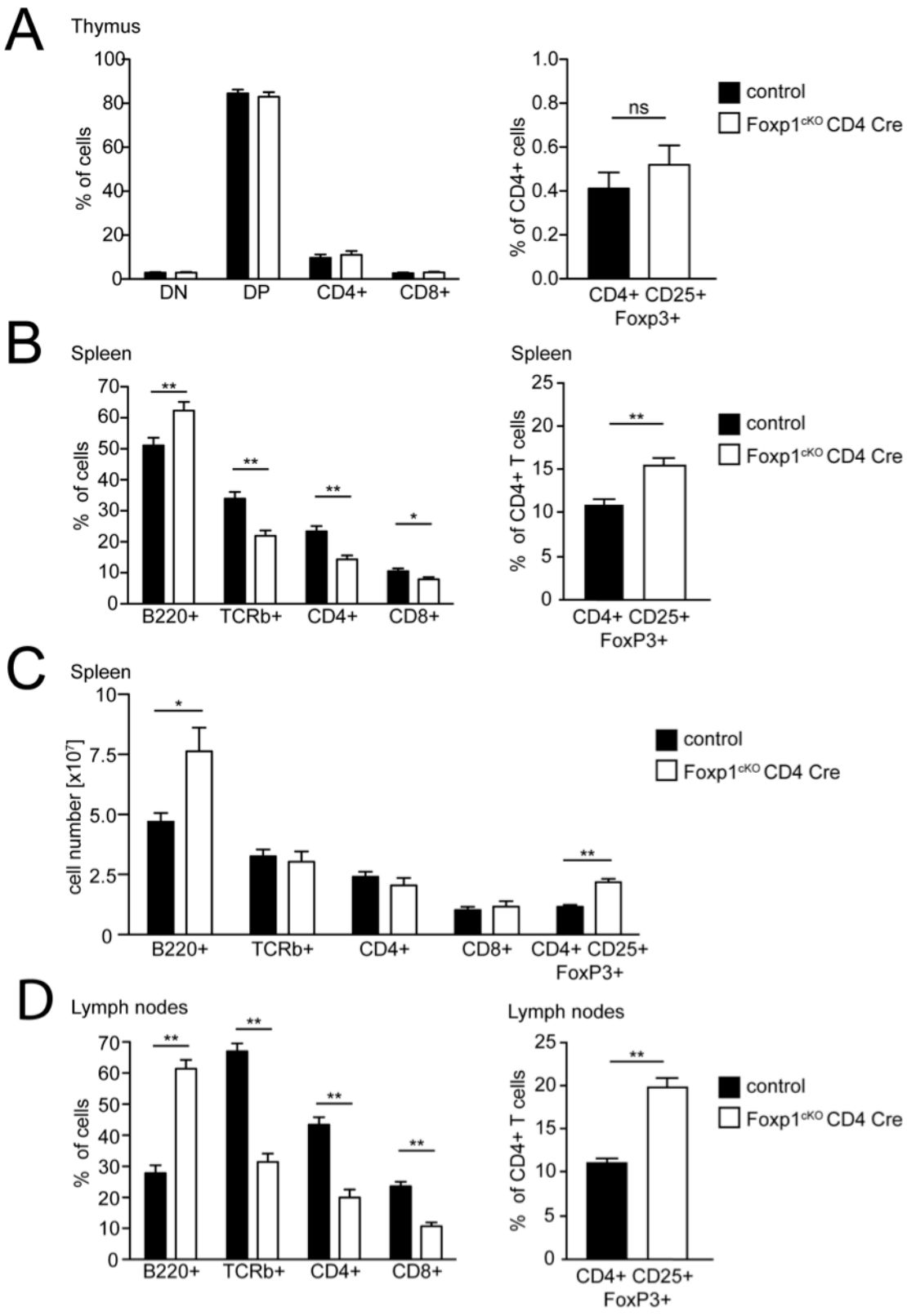

Figure 9 Foxp1^{cKO} CD4 Cre mice showed altered immune cell distributions. (A) Thymocyte distribution of control (n = 7) and Foxp1^{cKO} CD4 Cre mice (n = 4). Thymocytes subsets were distinguished by CD4 and CD8 expression (left panel) and CD4+ CD25+ Foxp3+ for regulatory T cells (right panel). **(B)** Percentages of splenocytes detected by flow cytometry by their expression of B220, TCRβ, CD4, and CD8 in control (n = 15) and Foxp1^{cKO} CD4 Cre mice (n = 8) (left panel). Splenic CD4+ CD25+ Foxp3+ regulatory T cells of control (n = 12) and Foxp1^{cKO} CD4 Cre mice (n = 7) (right panel). **(C)** Cell numbers of different lymphocyte subsets in spleens of control (n = 10) and Foxp1^{cKO} CD4 Cre mice (n = 5). **(D)** Cell distribution in lymph nodes of control (n = 15) and Foxp1^{cKO} CD4 Cre mice (n = 8) (left panel) and regulatory T cells in control (n = 12) and Foxp1^{cKO} CD4 Cre mice (n = 7). Bars show means ± SEM. * $P < 0.05$, ** $P < 0.01$, ns = not significant.

Interestingly, the fraction of CD4+ CD25+ Foxp3+ regulatory T cells was increased by 1/3 within the CD4+ T helper cell compartment of Foxp1^{cKO} CD4 Cre mice (Figure 9B, right panel).

Total splenic cell numbers of Foxp1^{cKO} CD4 Cre mice also showed a marked increase of B220+ B cell number, as expected from the increased percentage of B cells (Figure 9C). In contrast, TCRβ+ T cells were present in comparable numbers in Foxp1^{cKO} CD4 Cre mice and control animals. Also CD4+ and CD8+ T cell subsets were unaltered, whereas CD4+ CD25+ Foxp3+ regulatory T cells were approximately doubled in numbers.

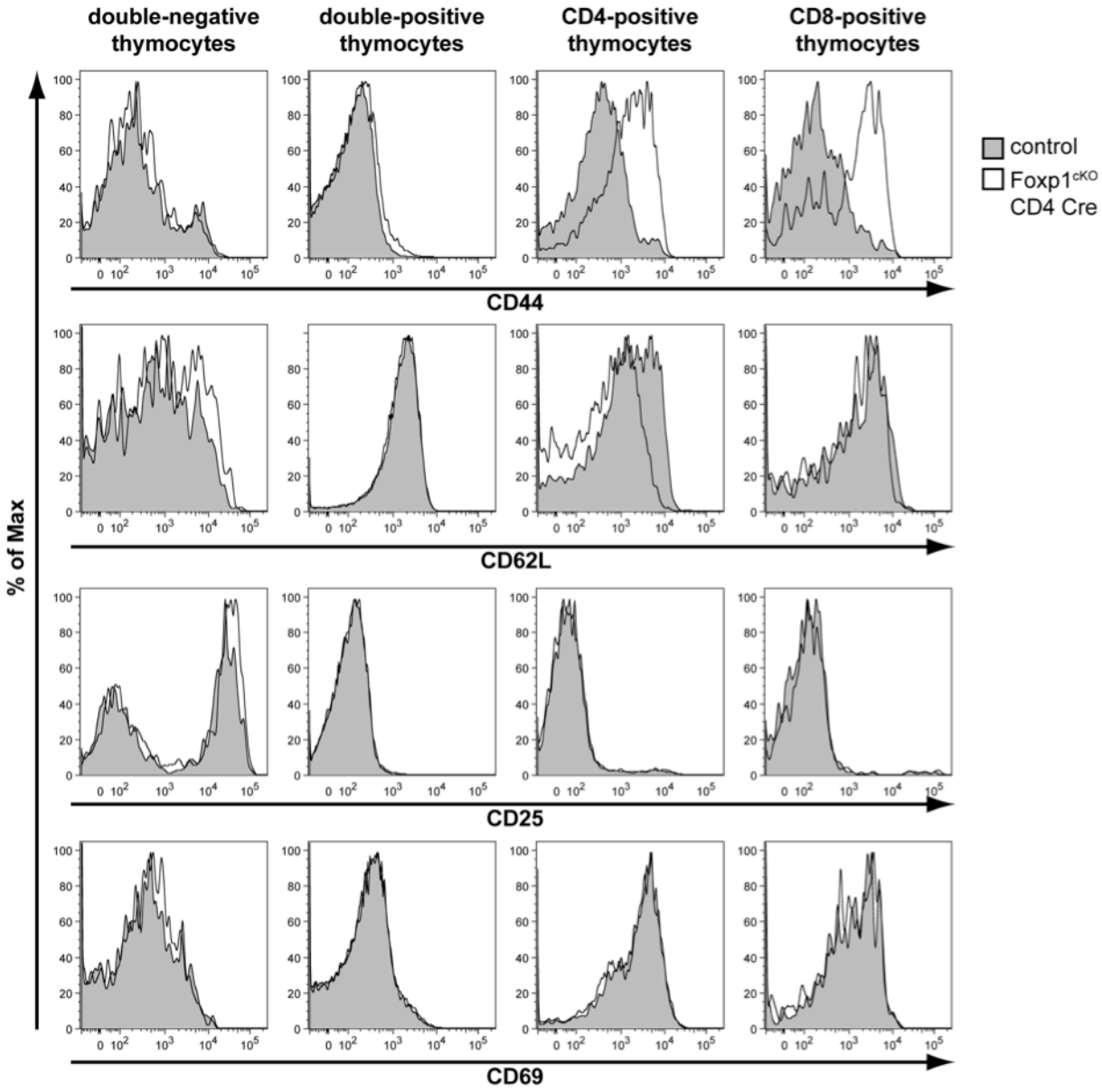

Figure 10 Foxp1^{cKO} CD4 Cre thymocytes showed altered expression pattern. Thymocytes of control and Foxp1^{cKO} CD4 Cre mice were differentiated in double-negative, double-positive, CD4 single-positive, and CD8 single-positive subsets by flow cytometry. Histogram overlays show CD44, CD62L, CD25 and CD69 expression for every thymocytes subsets in control and Foxp1^{cKO} CD4 Cre mice. Results show representative data of at least three independent experiments.

The shift in cell populations observed in spleens of Foxp1^{cKO} CD4 Cre mice were even more pronounced in the lymph nodes of those animals (Figure 9D, left panel). Here, the percentage of TCRβ + T cells was reduced by half, whereas the percentage of B cells was more than doubled. The overall reduced T cell percentage was apparent in the subsets of CD4+ and CD8+ T cells, while regulatory T cells were drastically increased in Foxp1^{cKO} CD4 Cre lymph nodes (Figure 9D, right panel).

Next, in a more detailed analysis, expression of early activation markers CD25 and CD69, as well as maturation markers CD44 and CD62L was investigated in the four different thymocyte subsets (Figure 10). Both CD4 and CD8 single-positive thymocytes showed a distinct upregulation of CD44 in Foxp1^{cKO} CD4 Cre mice. Additionally, Foxp1-deficient CD4 single-positive thymocytes exhibited reduced CD62L, whereas CD8 single-positive thymocytes showed no altered CD62L expression. Expression of CD69 and CD25 was not changed in any thymocyte subpopulation in Foxp1^{cKO} CD4 Cre mice.

In summary, Foxp1^{cKO} CD4 Cre mice showed CD44^{high} single-positive thymocytes, suggesting an altered stage of differentiation in these cells. Still, the absence of a shift towards single-positive thymocytes and the unaltered expression of early activation markers suggest regular T cell maturation and functional mechanisms of positive and negative selection in the thymus. A shift towards single-positive thymocytes can be indicative for disturbed negative selection processes in the thymus as skewing can be observed in mice with altered thymic selection due to overexpression of anti-apoptotic proteins or transgenic TCRs (compare thymocytes of vav-Bcl2 in Figure 21A and of 2D2 mice in Figure 28A).

5.2.3 Detailed analysis of altered T cell compartment in Foxp1^{cKO} CD4 Cre mice

After intra-thymic maturation stages, properly selected single-positive thymocytes exit the thymus and enter the periphery as CD4+ and CD8+ T cells. The majority of these cells circulating through the body have not yet encountered their cognate antigen and are therefore termed naïve T cells. This population is generally marked by their expression pattern being CD44^{low} CD62L^{high}. Investigation of splenic cell suspensions of Foxp1^{cKO} CD4 Cre mice surprisingly showed an almost complete absence of naïve CD4+ T helper cells (Figure 11, upper panel). Instead, splenic CD4+ T cells from Foxp1^{cKO} CD4 Cre mice were completely shifted towards the memory T cell compartment. The majority (~70%) of Foxp1^{cKO} CD4 Cre CD4+ T helper cells showed a CD44^{high} CD62L^{low} phenotype resembling the characteristics of effector-memory T cells. The residual CD4+ T helper cells in Foxp1^{cKO} CD4 Cre mice

showed an expression pattern of CD44^{high} CD62L^{high}, and thereby resembled phenotypically a fraction of central-memory T cells. Normally, the fraction of central-memory T cells is hardly detectable in control animals (~2%), whereas the percentage of effector-memory T cell fraction ranges about 20% of all CD4+ T helper cells. This tendency was also observed in lymph nodes of Foxp1^{cKO} CD4 Cre mice (Figure 11, lower panel). Here, the ratio between effector-memory and central-memory T cells was similarly shifted towards the central-memory T cell compartment. In conclusion, approximately 1/3 of all lymph node CD4+ T cells were phenotypically central memory T cells.

The memory T cell compartment can be roughly subdivided in effector-memory and central-memory T cells by their expression pattern of CD44 and CD62L (Mueller et al., 2013; Sallusto et al., 2004). Both markers are used as hallmark characteristics of the memory T cell fractions of both, CD4 and CD8 lineages. Still, memory T cell subsets have been described to express several different proteins depending on their state of activation, origin, and

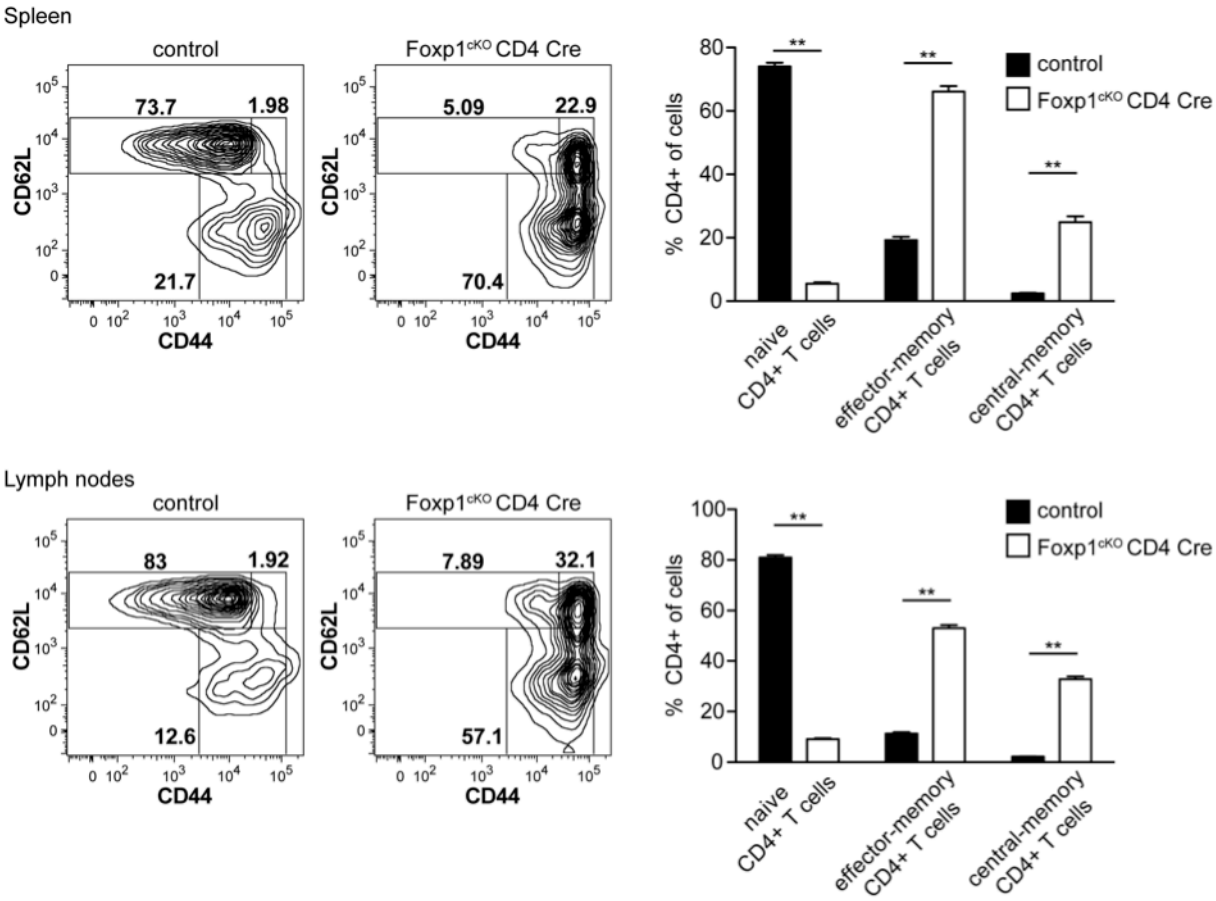

Figure 11 CD4+ T cells of Foxp1^{cKO} CD4 Cre mice showed a memory phenotype. Flow cytometry of CD4+ T cells isolated from spleens (top) and lymph nodes (bottom) of control (n = 12) and Foxp1^{cKO} CD4 Cre (n = 13). Cells were distinguished by their levels of CD44 and CD62L into naïve (CD62L^{high} CD44^{low}), effector-memory (CD62L^{low} CD44^{high}), and central-memory (CD62L^{high} CD44^{high}) CD4+ T cells. Contour plots on the left depict representative results and gating strategies. Bar charts on the right show mean values ± SEM. ** P < 0.01.

microenviroment (Mueller et al., 2013). Remarkably, Foxp1^{cKO} CD4 Cre mice showed a complete loss of naïve T cells and an almost complete shift of all T cells towards a memory T cell phenotype. Further characterization of the memory T cells present in Foxp1^{cKO} CD4 Cre mice revealed first, that Foxp1-deficient CD4+ T cells had a blasted appearance: histogram overlays of forward scatter signals of CD4+ T cells of Foxp1^{cKO} CD4 Cre mice and control animals showed an increase in size (Figure 12, top row). This blasting can be indicative of an activated state and/or increased proliferation rates of lymphocytes. As described above, CD4+ T cells from Foxp1^{cKO} CD4 Cre mice showed markedly altered expression of CD62L and CD44. Interestingly, early activation marker CD69 was not elevated in CD4+ T cells from Foxp1^{cKO} CD4 Cre mice. This observation indicates that T cells were not recently activated but rather have been established as effector or memory T cells. Of note, an increased CD25 positive population was visible in Foxp1-deficient CD4+ T cells, resembling the increased CD4+ CD25+ Foxp3+ regulatory T cell fraction observed in Foxp1^{cKO} CD4 Cre mice. Nevertheless, there was no increase in CD25 expression in CD4+ Foxp3- cells, indicating no acute T cell activation accompanied by the expression of early activation markers (data not shown).

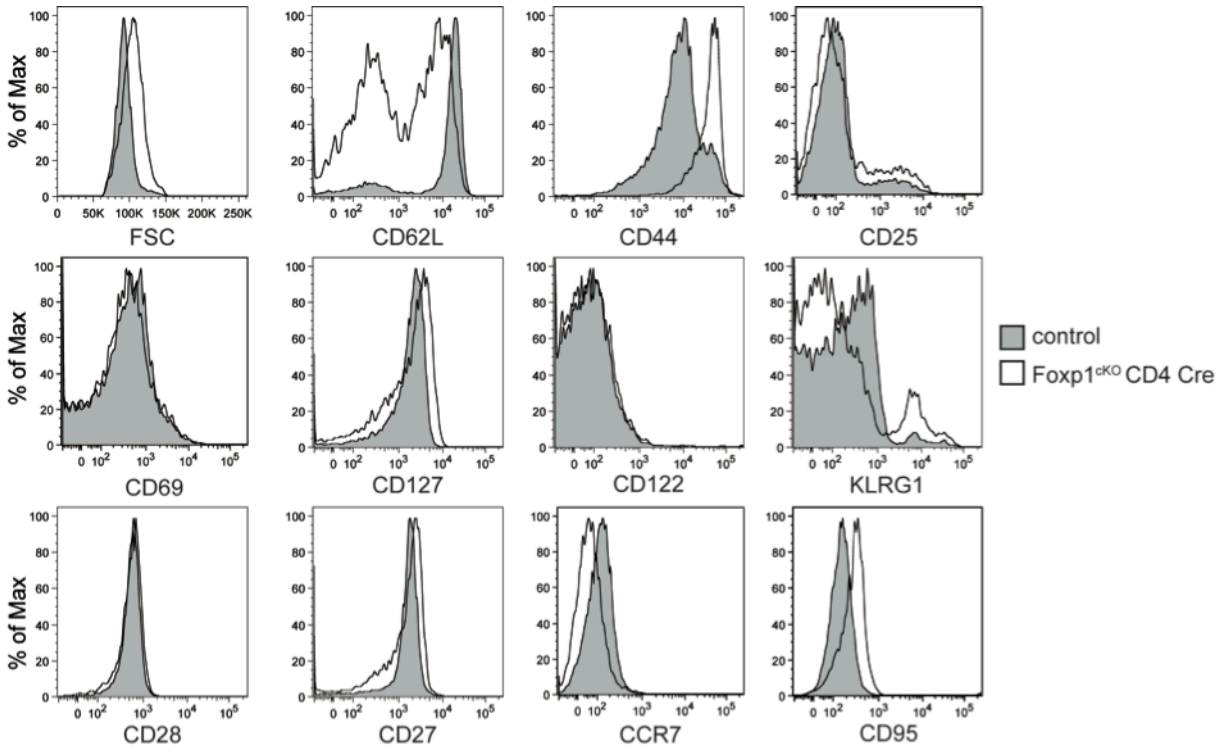

Figure 12 Differential marker expression of CD4+ T helper cells in Foxp1^{cKO} CD4 Cre mice. Analysis of CD4+ T cells isolated from spleens of control and Foxp1^{cKO} CD4 Cre mice by flow cytometry. Histogram overlays show cellular size by FSC signals and expression of surface antigens CD62L, CD44, CD25 (top row), CD69, CD127, CD122, KLRG1 (middle row), CD28, CD27, CCR7, and CD95 (bottom row). Results show representative data of at least three independent experiments.

The cytokine IL-7 plays a crucial role in homeostasis of T cells and its receptor CD127 is constitutively expressed on CD4 and CD8 T cells. Especially memory T cells are known to express higher levels of CD127 and are largely depended on IL-7 as a survival signal. Consistent with that, in Foxp1^{cKO} CD4 Cre mice, CD4 T cells showed an increase in CD127 expression, emphasizing their identity as memory T cells (Figure 12, middle row). CD122 acts as the receptor of IL-15 and is another critical player in memory T cell homeostasis. Both IL-7 and IL-15 are thought to act in a similar way, eventually leading to upregulation of anti-apoptotic proteins. However, Foxp1-deficient CD4+ T cell did not show any changes in CD122 expression, indicating no direct transcriptional dependency on Foxp1.

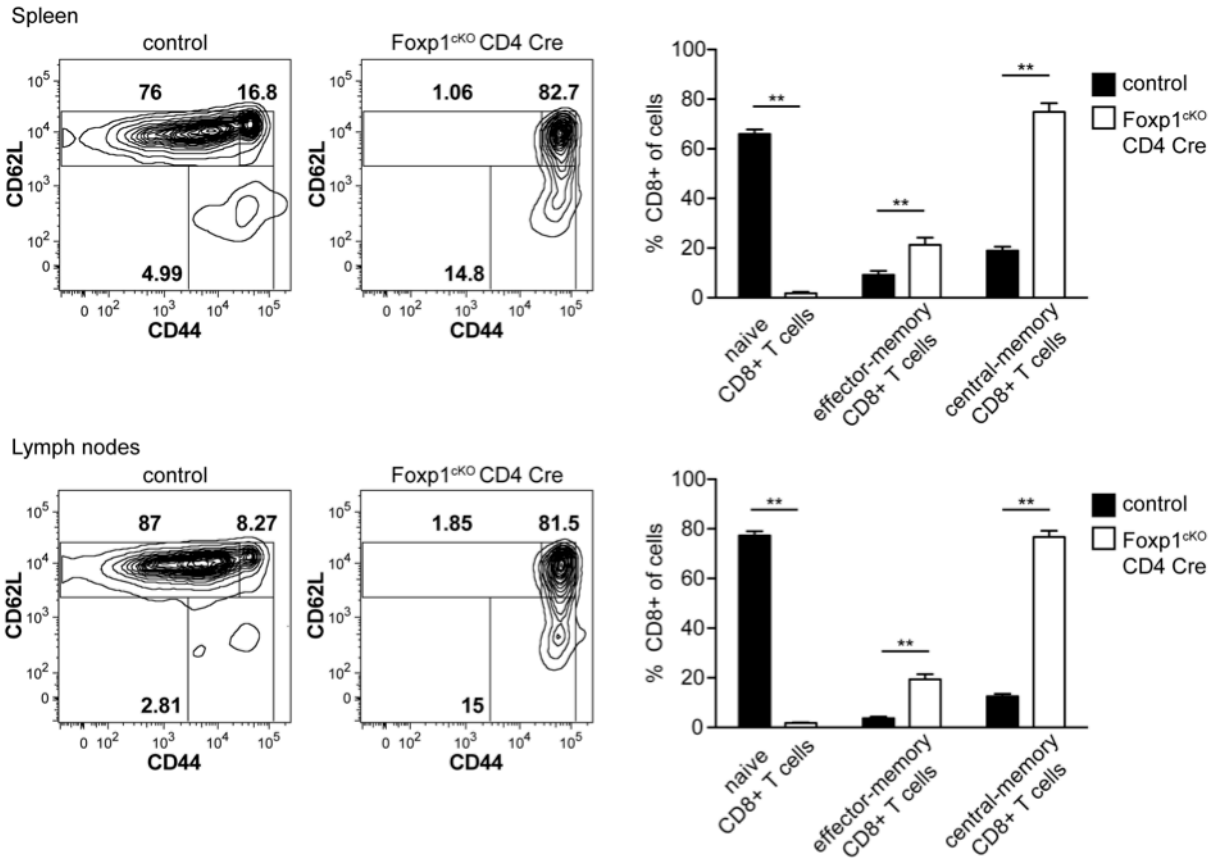

Figure 13 CD8+ T cells of Foxp1^{cKO} CD4 Cre mice showed a memory phenotype. Flow cytometry of CD8+ T cells isolated from spleens (top) and lymph nodes (bottom) of control (n = 12) and Foxp1^{cKO} CD4 Cre (n = 13). Cells were differentiated by their levels of CD44 and CD62L into naïve (CD62L^{high} CD44^{low}), effector-memory (CD62L^{low} CD44^{high}), and central-memory (CD62L^{high} CD44^{high}) CD8+ T cells. Contour plots on the left depict representative results and gating strategies. Bar charts on the right show mean values +/- SEM. ** P <

To further characterize the nature of Foxp1-deficient CD4+ T cells, expression of a number of potentially relevant markers in memory T cell biology was determined. Killer cell lectin-like receptor subfamily G member 1 (KLRG1), which is normally found on virus-activated T cells, was present on more CD4+ T cells than in control mice. However, the majority of Foxp1-deficient CD4+ T cells exhibited decreased expression of KLRG1.

The co-stimulatory B7 receptor CD28 is expressed on different types of T cells and is necessary for full T cell activation. CD28 receptor binds CD80 (B7.1) and CD86 (B7.2) on activated antigen-presenting cells and is crucial for co-stimulation of antigen-inexperienced T cells. Furthermore, CD28 signalling was shown to be involved in trafficking CD4+ memory T cells to non-lymphoid sites (Mirenda et al., 2007). In humans, terminally differentiated memory T cells show a reduction of CD28 and CD27 (Gattinoni et al., 2012). Still, CD4+ T cells of the examined Foxp1^{cKO} CD4 Cre mice showed unchanged expression of CD28 when compared to controls (Figure 12, bottom row). In contrast, CD4+ T cells from Foxp1^{cKO} CD4 Cre mice showed a higher expression of a second co-stimulatory receptor, CD27. So far CD27 signalling has been implicated in the maintenance of CD8+ memory T cells, but its role CD4+ T cells is less clear (Gattinoni et al., 2012; van Gisbergen et al., 2011).

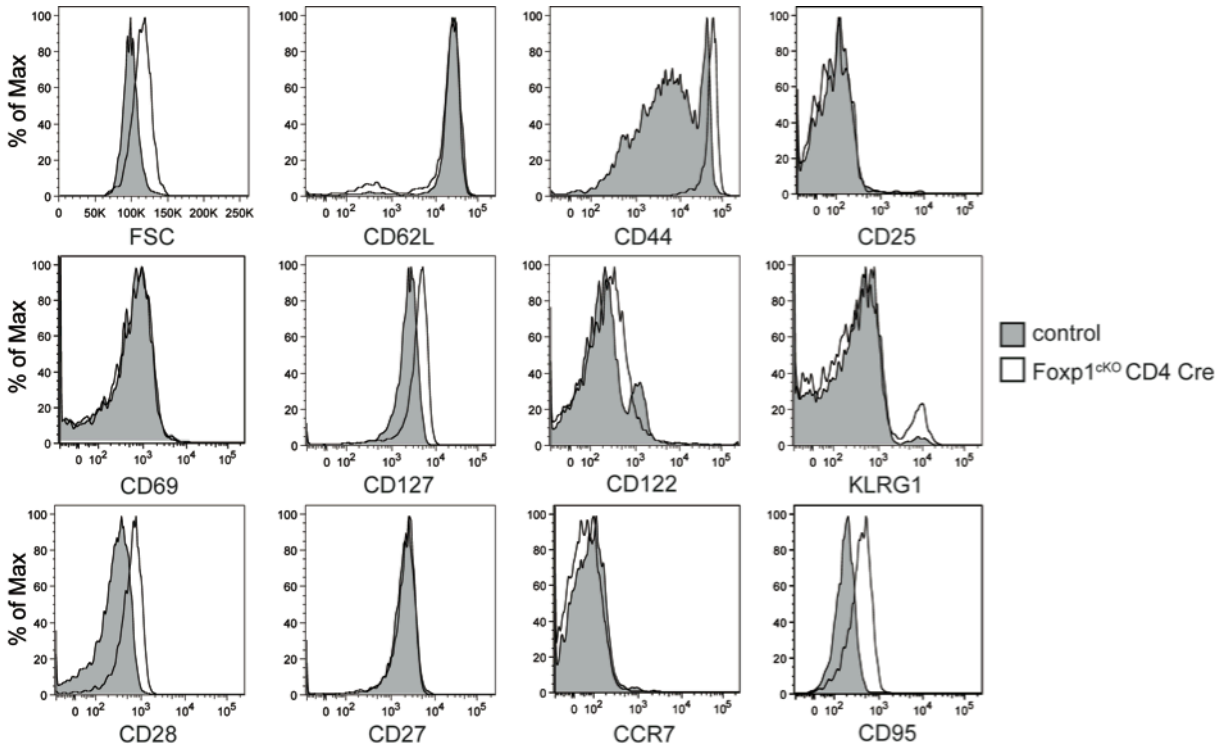

Figure 14 Differential marker expression of CD8+ cytotoxic T cells in Foxp1^{cKO} CD4 Cre mice. Analysis of CD8+ T cells isolated from spleens of control and Foxp1^{cKO} CD4 Cre mice by flow cytometry. Histogram overlays show cellular size by FSC signals and expression of surface antigens CD62L, CD44, CD25 (top row), CD69, CD127, CD122, KLRG1 (middle row), CD28, CD27, CCR7, and CD95 (bottom row). Results show representative data of at least three independent experiments.

C-C chemokine receptor type 7 (CCR7, CD197) acts as a receptor for CCL21 and CCL19 and modulates the cellular tropism towards lymphoid tissues (Woodland and Kohlmeier, 2009). Additionally, CCR7 is expressed on central-memory T cells in concert with CD62L. In contrast, effector memory T cells show a CCR7- CD62L- expression profile that goes along with their tropism towards peripheral tissues. Interestingly, CD4+ T cells from Foxp1^{cKO} CD4 Cre mice showed lower expression of CCR7. This finding is consistent with the observation that the majority of CD4+ T cells in Foxp1^{cKO} CD4 Cre mice are phenotypically effector-memory T cells.

Upon stimulation via their TCR, T cells express the Fas receptor (CD95). Binding of FasL to Fas induces formation of the death-inducing signalling complex, which is one possibility to drive T cells into apoptosis. Therefore, expression of CD95 is thought to work as regulatory mechanism, which renders CD4+ T cells susceptible to apoptosis after a phase of expansion. Importantly, CD4+ T cells of Foxp1^{cKO} CD4 Cre mice showed increased expression of CD95 when compared to control CD4+ T cells. This might indicate a higher susceptibility of Foxp1-deficient T cells to Fas induced cell death.

In parallel to the loss of naïve CD4+ T helper cells, Foxp1^{cKO} CD4 Cre mice showed massive changes in the CD8+ cytotoxic T cell compartment (Figure 13, upper panel). Again, spleens of Foxp1^{cKO} CD4 Cre mice exhibited an almost complete lack of naïve CD8+ T cells and a shift towards the memory CD8+ T cell compartment. Normally, the CD8+ cytotoxic T cell compartment consists of a majority of naïve T cells and two minor fractions of effector-memory and central-memory T cells. Of note, CD8+ cytotoxic T cells in spleen and lymph nodes of wildtype mice include a bigger population of central-memory T cells than of effector-memory T cells. This tendency was even more pronounced in Foxp1^{cKO} CD4 Cre mice, as the majority of CD8+ T cells phenotypically resembled central-memory T cells (~80%). Additionally, Foxp1^{cKO} CD4 Cre mice exhibited an increase in effector-memory CD8+ T cells up to 20%. Similar changes were observed in lymph nodes of Foxp1^{cKO} CD4 Cre mice (Figure 13, lower panel). In contrast to the CD4+ T cells in Foxp1^{cKO} CD4 Cre mice, cytotoxic CD8+ T cells did not show a skewing of memory T cells from effector-memory towards central-memory in lymph nodes of those animals (Figure 11, 13).

Comparable to CD4+ T cells in Foxp1^{cKO} CD4 Cre mice, the expression of various surface markers was altered in CD8+ T cells. Briefly, also CD8+ T cells exhibited a blasted appearance and high expression of CD44, whereas no alterations in CD62L, CD25 and CD69 expression was observed (Figure 14, top and middle row). Similar to CD4+ T cells in

Foxp1^{cKO} CD4 Cre mice, IL7 receptor CD127 showed higher expression in CD8+ T cells, whereas expression of IL-15 receptor CD122 was altered in a way that the CD8+ T cell population shifted slightly as a whole. KLRG1, CCR7, and CD27 expression on CD8+ T cells of Foxp1^{cKO} CD4 Cre mice largely remained unaltered. Instead, cytotoxic T cells showed higher expression of the co-stimulatory receptor CD28 and CD95 (Figure 14, bottom row).

In summary, both CD4+ T helper and CD8+ cytotoxic T cell compartments showed tremendous changes in Foxp1^{cKO} CD4 Cre mice, suggesting a crucial role for the transcription factor Foxp1 during effector or memory T cell differentiation and expression of homing markers.

5.2.4 Altered lifespan of Foxp1^{cKO} CD4 Cre mice and absence of auto-antibodies in sera of aged mice

As described earlier, Foxp1 full knock out mice die before birth due to a cardiovascular phenotype (Wang, 2004). In contrast to that, Foxp1^{cKO} CD4 Cre mice are born in mendelian ratios, are viable and healthy without any obvious signs of pathology, except a mild form of splenomegaly (Figure 8 and data not shown). When mice are housed over a longer period of time, Foxp1^{cKO} CD4 Cre mice showed a reduced overall median survival compared to the control group ($P < 0.001$, Mantel-Cox) (Figure 15). While Foxp1^{cKO} control animals showed a median survival of 740 days (n = 23), Foxp1^{cKO} CD4 Cre mice died after 678 days (n = 22). Occasionally, moribund Foxp1^{cKO} CD4 Cre mice showed heavily enlarged spleens and

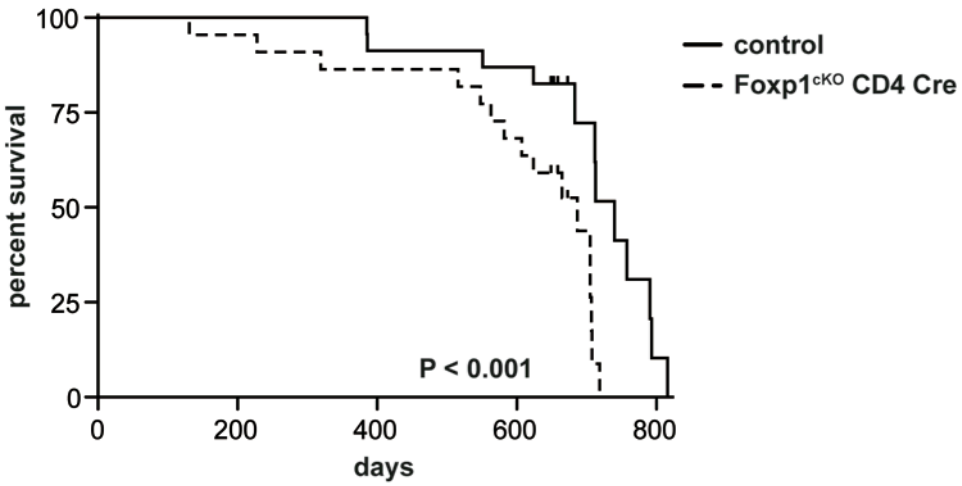

Figure 15 Foxp1^{cKO} CD4 Cre mice succumbed earlier than control animals. Kaplan-Mayer curves of control animals (n = 23) and Foxp1^{cKO} CD4 Cre mice (n = 22). P value was calculated by Logrank/Mantel-Cox

abdominal tumour masses, presumably arising from Peyer's patches or mesenteric lymph nodes (data not shown). These observations might be indicative for a pathological condition in aged Foxp1^{cKO} CD4 Cre mice, potentially induced by the strongly altered T cell compartment, namely the absence of naïve T cells.

Another explanation for the reduced lifespan of Foxp1^{cKO} CD4 Cre mice could be ongoing mild autoimmune processes as a result of the altered T cell compartment. Many autoimmune diseases are marked by the appearance of auto-antibodies (Naparstek and Plotz, 1993). Therefore, sera of Foxp1^{cKO} CD4 Cre mice at the age of one year were tested for the presence of anti-dsDNA, anti-ENA/ANA, anti-histone, and anti-ssDNA antibodies (Figure 16). Noteworthy, none of the tested auto-antibodies were significantly elevated in sera of Foxp1^{cKO} CD4 Cre mice compared to control animals. In summary, these observations so far suggest the absence of an ongoing overt autoimmune reaction and auto-reactive antibodies to dsDNA, ENA/ANA, histones, and ssDNA, whereas other forms of autoimmunity cannot be fully excluded.

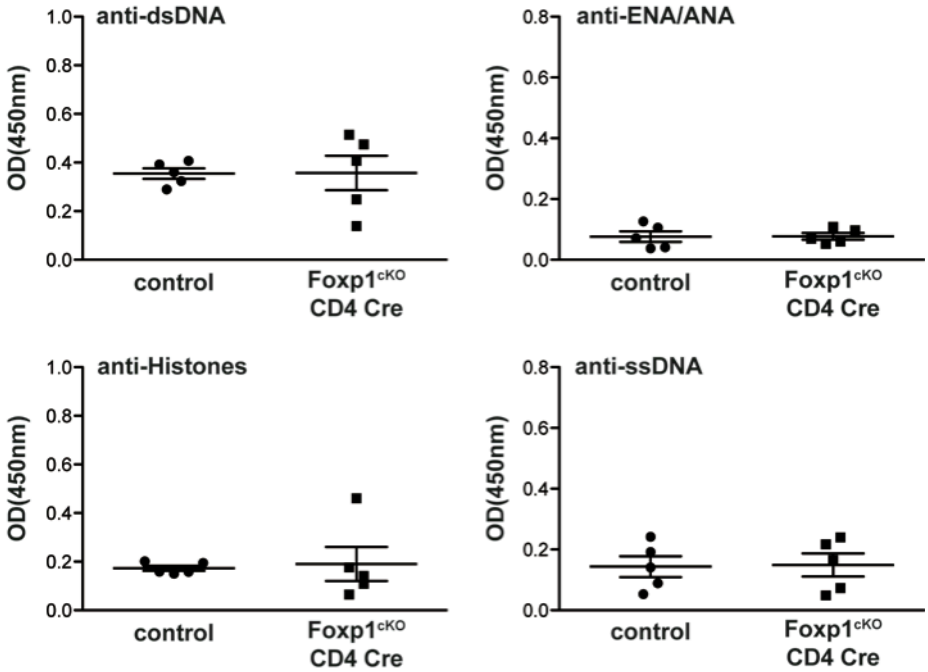

Figure 16 Absence of auto-antibodies in older Foxp1^{cKO} CD4 Cre mice. ELISA measurements of sera from 1-1.5 year old control (n = 5) and Foxp1^{cKO} CD4 Cre mice (n = 5) for specific anti-dsDNA, anti-ENA/ANA, anti-Histones, and anti-ssDNA antibodies. Scatter plots show optical densities (OD_{450}) of single values +/- SEM.

5.2.5 Enhanced cytokine production of CD4+ T cells from Foxp1^{cKO} CD4 Cre

Phenotypically both, CD4+ and CD8+ T cells subsets had shown a complete lack of CD62L^{high} CD44^{low} naïve T cells and a full transition towards the effector or memory T cell compartments. Still, it was unclear whether this phenotype went along with memory-like functionality marked by faster and stronger response upon TCR-ligation. To address this question, purified CD4+ T cells of Foxp1^{cKO} CD4 Cre mice and controls were challenged with soluble anti-CD3 antibodies alone or with a combination of soluble anti-CD3 and anti-CD28 antibodies *in vitro*. As expected, wildtype CD4+ T cells did not show any prominent response upon stimulation with soluble anti-CD3 antibodies, as TCR-cross-linking is normally needed for proper stimulation (Figure 17, dashed lines). However, memory and effector-memory T cells show a lower activation threshold and are stimulated by soluble anti-CD3 antibodies alone.

In this assay, CD4+ T cells isolated from Foxp1^{cKO} CD4 Cre mice showed strongly enhanced production of IL-2 upon stimulation with soluble anti-CD3 alone (Figure 17, left panel). Combination of soluble anti-CD3 with soluble anti-CD28 antibodies even enhanced this effect and elicited a more pronounced IL-2 secretion, whereas wildtype CD4+ T cells only showed IL-2 levels close to baseline (Figure 17, right panel).

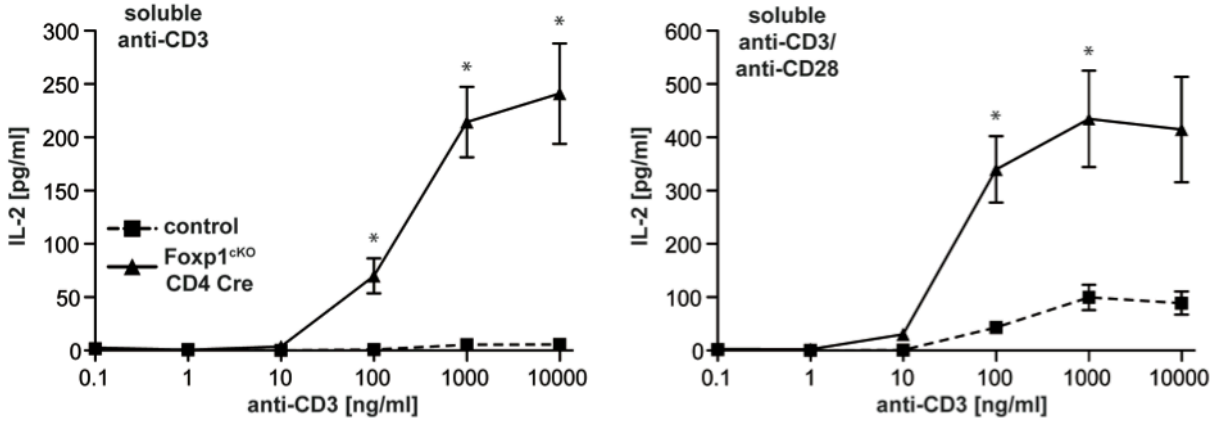

Figure 17 Subtle stimulation triggered massive IL-2 production in CD4+ T cells of Foxp1^{cKO} CD4 Cre mice. IL-2 production by MACS-purified CD4+ T cells from control (n = 3) and Foxp1^{cKO} CD4 Cre mice (n = 3) stimulated with soluble anti-CD3 alone (left panel), or in combination with soluble anti-CD28 antibodies (right panel). Graphs show mean values +/- SEM. * $P < 0.05$.

In addition, isolated CD4+ T cells from Foxp1^{cKO} CD4 Cre mice were stimulated with PMA/Ionomycin in a time-course experiment for 4, 8, 16 and 24 h. Supernatants of all stimulated cells were harvested at the indicated time-points and subsequently analysed for the

presence of different T cell cytokines by cytokine bead array. Again, CD4+ of Foxp1^{cKO} CD4 Cre mice showed massively increased cytokine production for IL-2 (Figure 18A). Additionally, Foxp1-deficient CD4+ T cells produced large amounts of the inflammatory cytokines IFNγ and TNF. Furthermore, enhanced levels of IL-4, IL17, and GM-CSF were

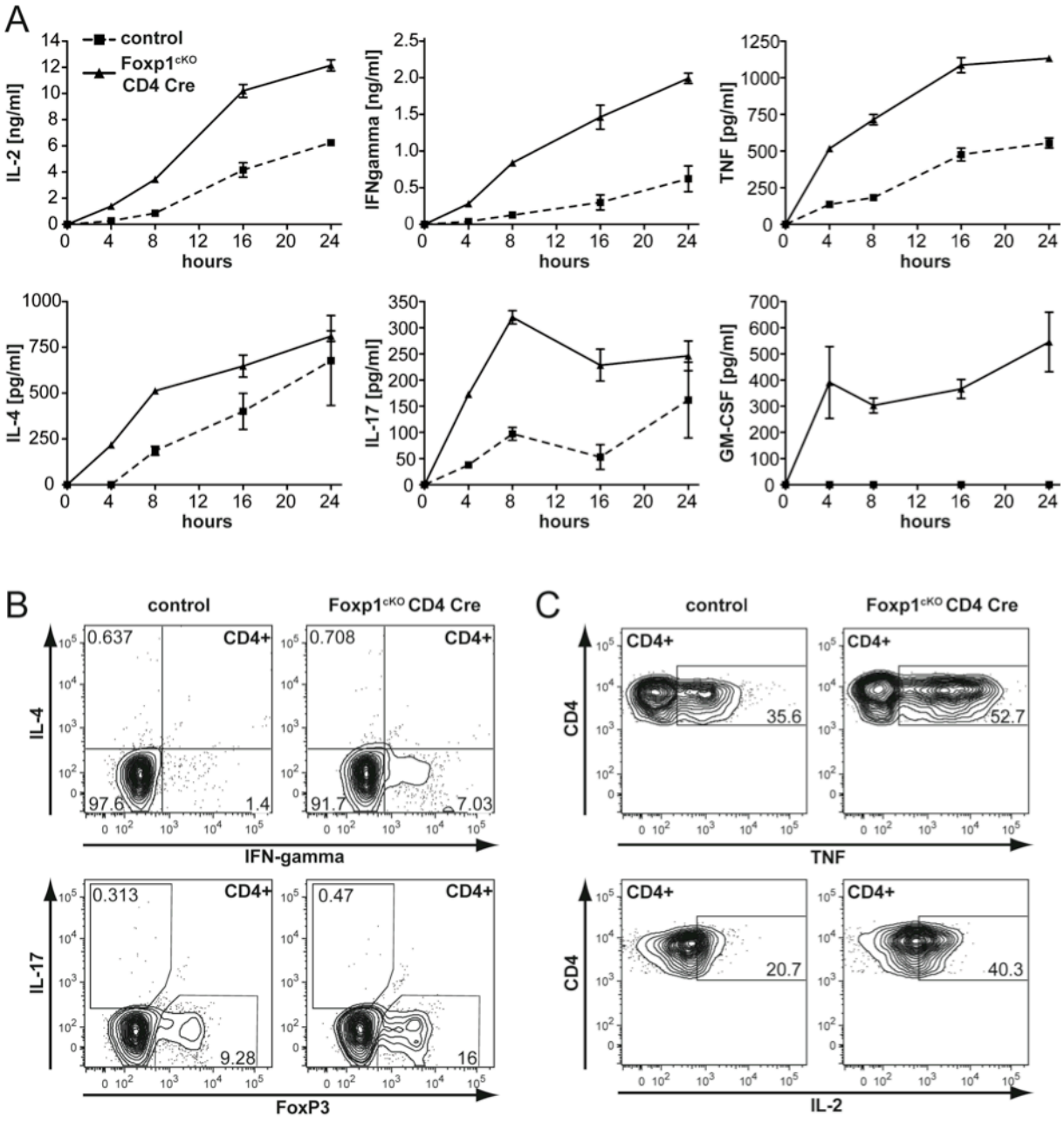

Figure 18 Cytokine production by stimulated CD4+ T cells from Foxp1^{cKO} CD4 Cre mice. (A) Cytokine production of CD4+ T cells isolated from control and Foxp1^{cKO} CD4 Cre mice (both n = 3) and stimulated with PMA and Ionomycin for the indicated time. Cytokine levels in supernatants were determined by cytokine bead array. Graphs show mean values ± SEM. **(B)** Flow cytometry for IFNγ, IL-4, IL-17, and Foxp3 as well as **(C)** TNF, and IL-2 in splenic CD4+ T cells of control and Foxp1^{cKO} CD4 Cre mice. Splenocytes were stimulated with PMA/Ionomycin in the presence of Brefeldin A *in vitro*. Results show pregated CD4+ T cells and representative data of three independent experiments.

measured in the supernatants of CD4+ T cells of Foxp1^{cKO} CD4 Cre mice. Of note, most cytokines secreted from CD4+ T cells of Foxp1^{cKO} CD4 Cre mice became already detectable early after 4 h of stimulation. The increased responsiveness and the fast production of cytokines after stimulation are hallmarks of effector or memory T cells. Together, this supports the notion of their presence in Foxp1^{cKO} CD4 Cre mice phenotypically and functionally, respectively.

In lymphoid organs of wildtype animals only a small fraction of T cells readily produce cytokines upon stimulation. To measure the percentage of CD4+ T cells producing cytokines after stimulation of control and Foxp1^{cKO} CD4 Cre T cells, splenocytes were stimulated with PMA/Ionomycin in the presence of Brefeldin A, which blocks secretion of cytokines by disrupting the golgi apparatus. Here, a defined fraction of Foxp1-deficient CD4+ T cells produced IFNγ upon stimulation, whereas no increased cell fraction was observed to be positive for IL-4, or IL-17 (Figure 18B). The elevated levels of IL-4 and IL-17 measured by ELISA might therefore point to an increased production of cytokines in skewed cells of the Th2 and Th17 T cell differentiation lineages without changes in their overall abundance (Figure 18A, B). Additionally, CD4+ T cells from Foxp1^{cKO} CD4 Cre mice showed a higher percentage of TNF and IL-2 producing cells in the spleen (Figure 18C), which confirmed the results of cytokines measured in the supernatant of stimulated CD4+ T cells. Together, these results indicate some skewing of T helper cells towards a Th1 response that is defined by the increased presence of IFNγ-producing CD4+ T cells expressing the transcription factor T-bet.

In summary, CD4+ T cells isolated from Foxp1^{cKO} CD4 Cre mice produced high levels of classical T cell cytokines and hyper-responded upon subtle soluble TCR ligation. Therefore it can be concluded, that Foxp1-deficient T cells do not only phenotypically resemble an effector/memory T cell fraction, but also functionally.

5.2.6 Analysis of Foxp1-binding to IL-2 promoter region

The excessive cytokine production of Foxp1-deficient T cells suggested a potential direct control of cytokine transcription through the repressive actions of Foxp1. In line with this hypothesis, the hallmark transcription factor of regulatory T cells, Foxp3, was shown to negatively regulate the production of IL-2 (Schubert et al., 2001). In a subsequent study, the related forkhead-box family member Foxp1, had been shown to bind not only to a conserved DNA binding motif in the IL-2 promoter region but also to a site in the SV40 promoter (Wang, 2003). Additionally, Wu et al. showed that Foxp3 cooperates with NFAT and AP-1

and modulates regulatory T cell function by binding to evolutionary conserved sites in the IL-2 promoter amongst others (Wu et al., 2006).

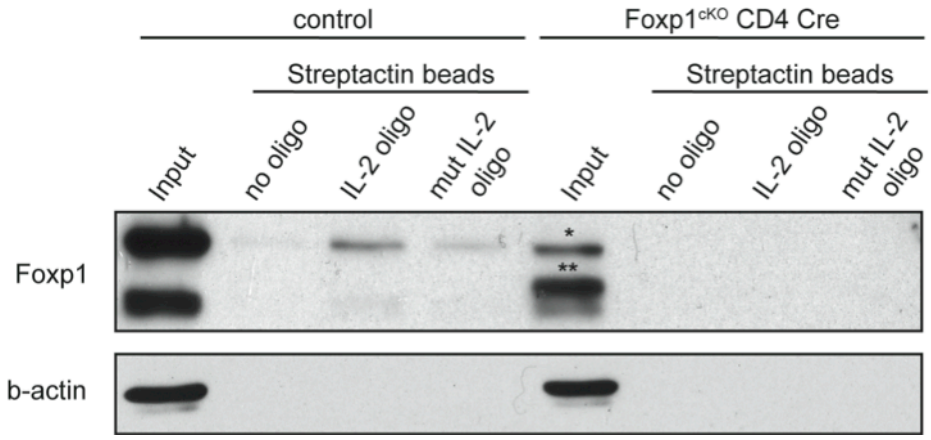

Figure 19 Foxp1 bound to the IL-2 promoter. Western blotting for Foxp1 and β-actin of an oligonucleotide pull-down assay carried out with lysates of CD4+ T cells isolated from control and Foxp1^{cKO} CD4 Cre mice. * indicates residual Foxp1 protein in conditional knock-out cells, while ** mark the band of truncated Foxp1 lacking exons 10-12. Representative blots of two independent experiments are shown.

Therefore, we sought to test binding of Foxp1 in an oligonucleotide pull-down experiment for the reported endogenous IL-2 consensus sites. Indeed, lysates of primary CD4+ T cells showed binding of Foxp1 to oligonucleotides resembling to the sequence of the distal IL-2 promoter (Figure 19). However, binding of Foxp1 to a mutated form of the IL-2 consensus sequence was significantly weaker. Interestingly, only the largest isoform of Foxp1 was pulled down by wildtype IL-2 oligonucleotides in this assay. As expected, CD4+ T cells isolated from Foxp1^{cKO} CD4 Cre mice did not show any Foxp1 binding to IL-2 oligonucleotides. Still, the strong exposition of the Western blot made residual Foxp1 expression visible in lysates of CD4+ T cells isolated from Foxp1^{cKO} CD4 Cre mice. Additionally, a band of the truncated Foxp1 protein lacking exon 10 – 12, and therefore missing a major part of the DNA-binding domain, was present in the lysate input. Importantly, none of those bands showed binding to the IL-2 promoter consensus sequence in the oligonucleotide pull-down assay.

These findings support the previously reported observations of Foxp3- and Foxp1-binding to consensus sequence in the IL-2 promoter. Together with the enhanced IL-2 expression observed in stimulated CD4+ T cells from Foxp1^{cKO} CD4 Cre mice the data suggests the direct control of IL-2 production through Foxp1, acting as a transcriptional repressor in

primary T cells. Physiological down-regulation of Foxp1 in effector/memory T cells or loss of the protein in T cells of Foxp1^{cKO} CD4 Cre mice will therefore eventually lead to elevated IL-2 gene transcription and production.

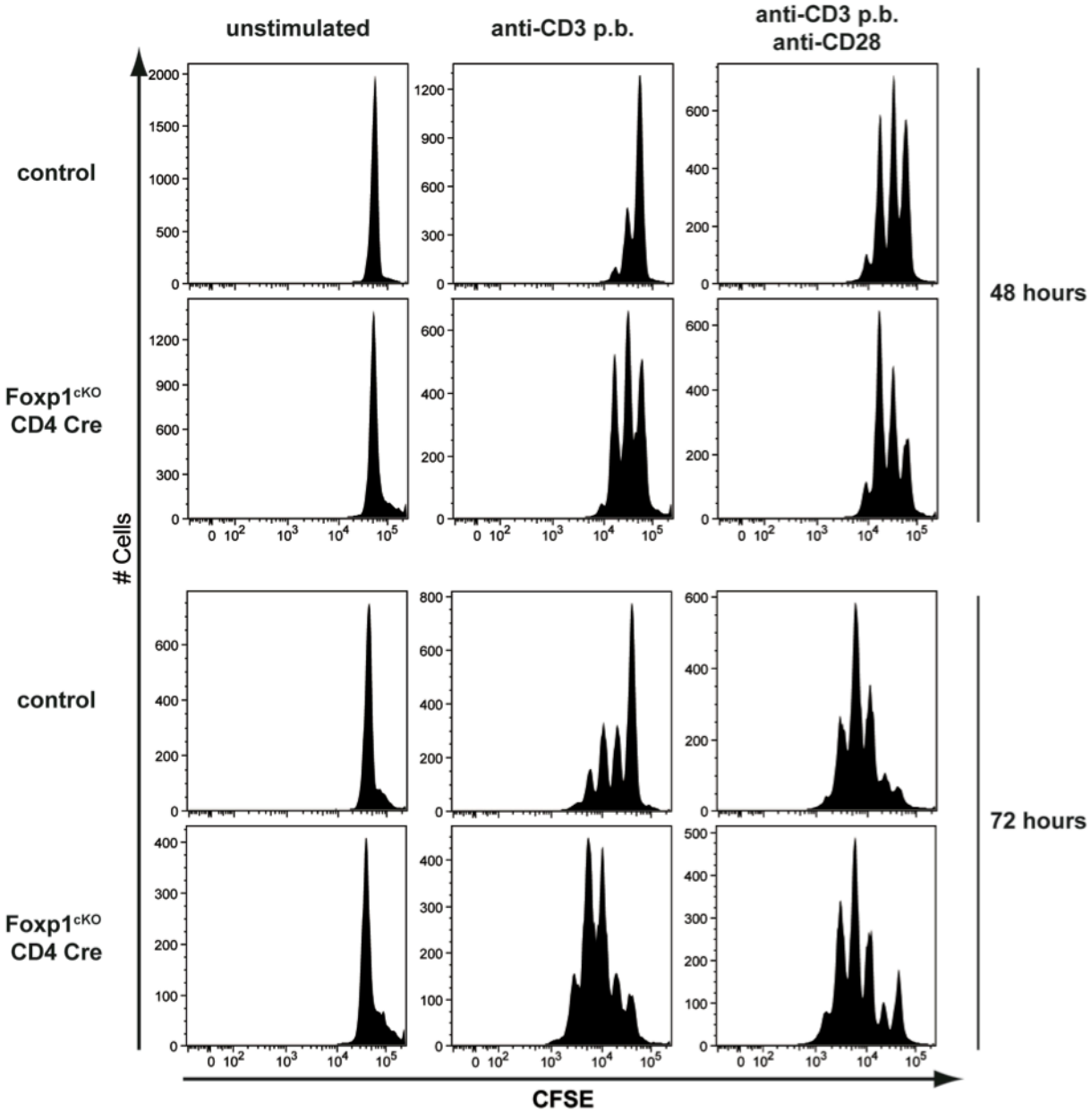

Figure 20 Loss of Foxp1 promoted proliferation of CD4+ T cells from Foxp1^{cKO} CD4 Cre mice. Flow cytometry of CFSE-labelled CD4+ T cells isolated from control and Foxp1^{cKO} CD4 Cre mice after 48 and 72 h of culture. Cells were either left unstimulated or were treated with plate-bound anti-CD3 only, and in combination with soluble anti-CD28 antibodies. Representative data of three experiments are shown.

5.2.7 Proliferation of CD4+ T cells from Foxp1^{cKO} CD4 Cre mice

The observed sensitivity of Foxp1-deficient T cells to TCR stimulation and the excessive cytokine production suggested also altered expansion behaviour of the cells. To analyse Foxp1-deficient T cells in terms of proliferation, isolated CD4+ T cells from Foxp1^{cKO} CD4 Cre mice and controls were labelled with carboxyfluorescein succinimidyl ester (CFSE) and stimulated under different conditions for 48 and 72 h *in vitro*. Here, it became obvious that plate-bound stimulation with anti-CD3 antibodies elicited a strong proliferative response in CD4+ T cells from Foxp1^{cKO} CD4 Cre mice and nearly all labelled cells underwent proliferation after 72 h (Figure 20). In contrast, control cells showed only weak proliferative response upon sub-optimal anti-CD3 stimulation after 48 and 72 h. When CD4+ T cells were treated with plate-bound anti-CD3 antibodies in presence of soluble anti-CD28 antibodies, the proliferative advantage of CD4+ T cells from Foxp1^{cKO} CD4 Cre mice was largely overcome and Foxp1-deficient CD4+ T cells showed only slightly faster proliferation. This result indicates that Foxp1^{cKO} CD4 Cre CD4+ T cells strongly respond with proliferation upon TCR ligation in the absence of co-stimulation. In summary, these findings are consistent with the increased IL-2 cytokine production of Foxp1-deficient CD4+ T cells upon subtle stimulation with soluble anti-CD3 antibodies observed in previous experiments.

5.2.8 Survival assay and *in vitro* culture of Foxp1-deficient CD4+ T cells

Immunophenotyping of Foxp1^{cKO} CD4 Cre mice had revealed a striking reduction of TCRβ+ T cells of both CD4+ and CD8+ lineages in percentages of cells. At the same time the total cell number of TCRβ+ cells had remained unchanged and suggested a potential survival deficiency of T cells in Foxp1^{cKO} CD4 Cre mice. Indeed, we observed in an flow cytometry-based AnnexinV/ 7-AAD survival assay, that CD4+ T cells isolated from Foxp1^{cKO} CD4 Cre mice showed markedly impaired survival in comparison to control CD4+ T cells when kept unstimulated *in vitro* (Figure 21). After 24 h of *in vitro* culture only 35% of unstimulated Foxp1-deficient CD4+ T cells were viable, whereas approximately 60% of control CD4+ T cells were still alive. Furthermore, the impaired survival *in vitro* was already visible after two and three days in culture.

To test *in vitro* survival of cultured cells after activation, CD4+ T cells were stimulated by plate-bound anti-CD3 and soluble anti-CD28. Here, a severe drop in viability was observed for Foxp1-deficient CD4+ T cells after 24 h. However, after 2 days of *in vitro* culture, the

viability of Foxp1 cKO and wildtype controls was comparable. This outcome might by due to the increased proliferation rates of CD4+ T cells from Foxp1^{cKO} CD4 Cre mice compensating for the initial loss of viable cells. Importantly, IL-2-only treatment of CD4+ T cells isolated from Foxp1^{cKO} CD4 Cre mice did not show a major increase in viability during the first 3 days of *in vitro* culture compared to unstimulated cells. This observation is consistent with the absence of CD25 up-regulation in CD4+ T cells of Foxp1^{cKO} CD4 Cre mice, as seen in acutely activated T cells. Very surprisingly, Foxp1-deficient cells showed an increase of percentage of living cells after five days in culture in the presence of IL-2-only. This increase in cells indicates an *in vitro* proliferation of Foxp1-deficient CD4+ T cells in response to IL-2.

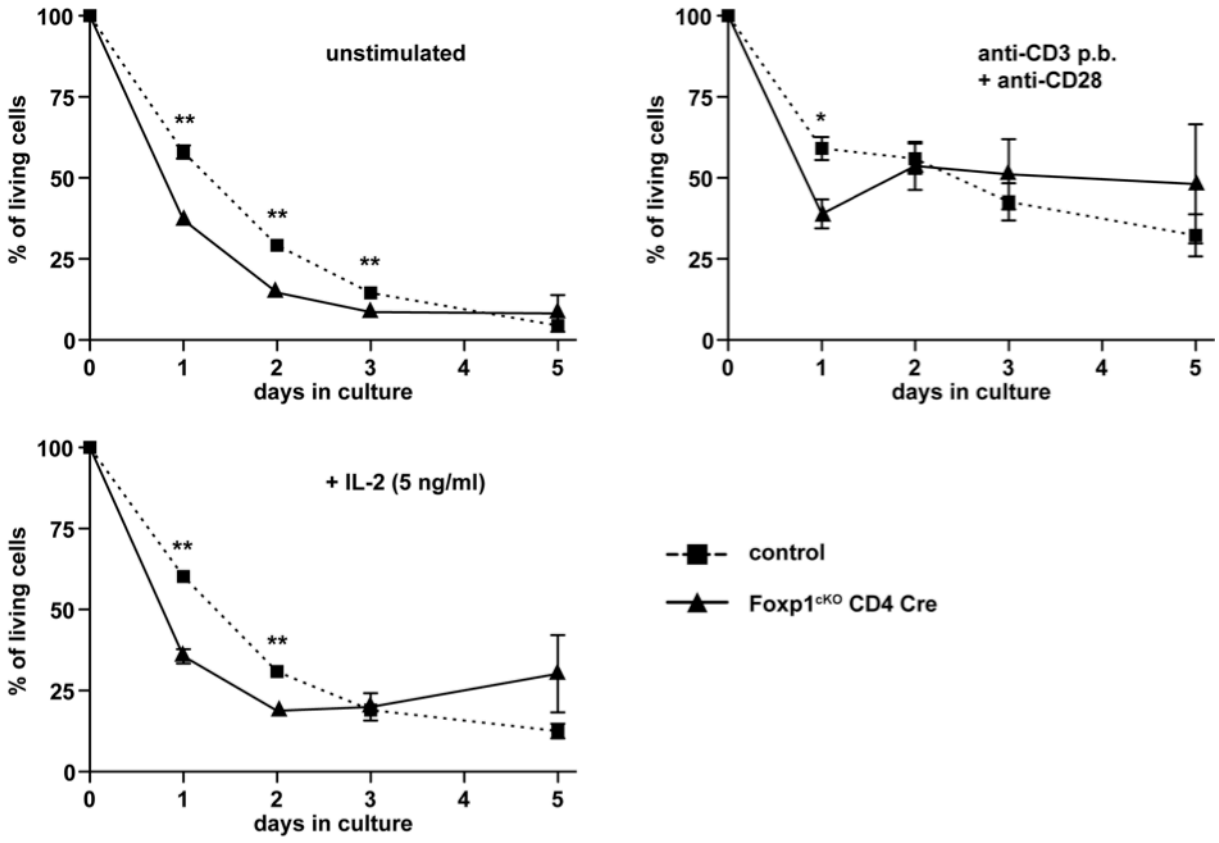

Figure 21 Foxp1-deficient T cells showed reduced survival *in vitro*. Flow cytometric survival assay of MACS-purified CD4+ T cells from control (n = 7; n = 5 for day 5) and Foxp1^{cKO} CD4 Cre mice (n = 4; n = 3 for day 5) cultured for indicated time either unstimulated (top left), in presence of IL-2 (bottom left), or plate-bound anti-CD3 and soluble anti-CD28 antibodies (top right). Live cells were distinguished by AnnexinV and 7-AAD and normalized to the percentage of living cells at the start of the experiment. Graphs show mean values ± SEM. * P < 0.05, ** < 0.01.

To characterize which cells expand in presence of IL-2, CD4+ T cells were isolated from Foxp1^{cKO} CD4 Cre mice and labelled with CFSE. These cells were again treated with IL-2 and investigated after 4 days of *in vitro* culture. Here, it became obvious that mostly CD4+ Foxp3+ regulatory T cells expanded upon IL-2 treatment of Foxp1-deficient CD4+ T cells (Figure 22A, B). Interestingly, these regulatory T cells expanded without the need of any further TCR-ligation or co-stimulation. In summary, Foxp1-deficient regulatory T cells showed *in vitro* expansion upon IL-2 treatment in a TCR-stimulation independent manner. Therefore, the IL-2 dependent proliferation of regulatory T cells might be one explanation for their increased presence in peripheral lymphoid organs of Foxp1^{cKO} CD4 Cre mice.

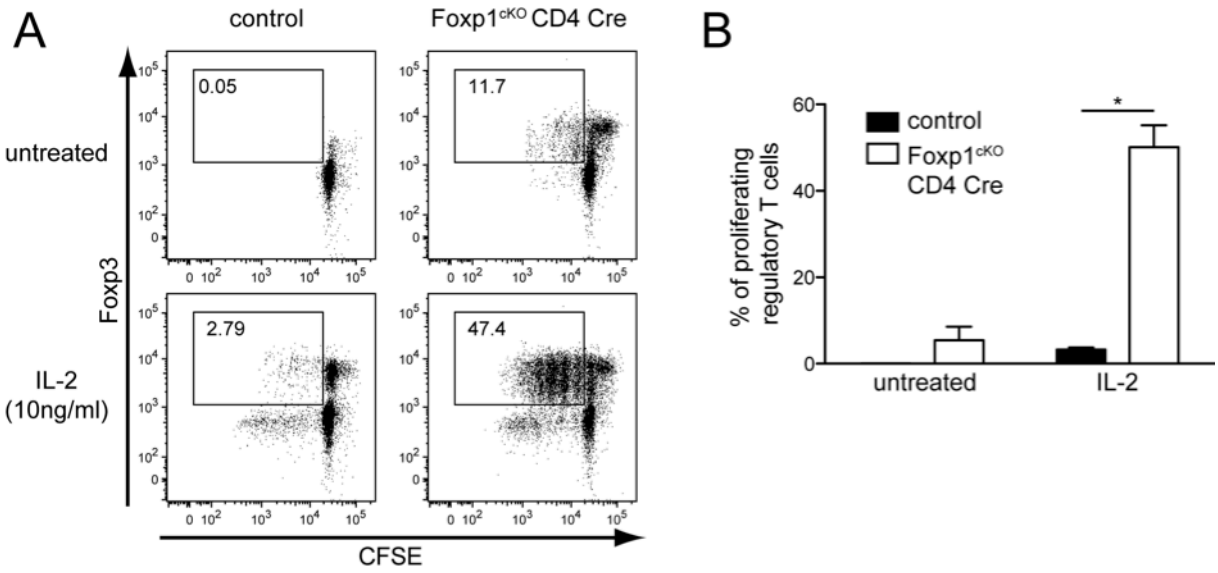

Figure 22 *In vitro* expansion of regulatory T cells upon IL-2 treatment of CD4+ T cells from Foxp1^{cKO} CD4 Cre mice. (A) 4 day *in vitro* proliferation culture of MACS-purified CD4+ T cells from control and Foxp1^{cKO} CD4 Cre mice in the presence of IL-2 (10 ng/ml) and analysis by flow cytometry of CFSE-labelled T cells intracellularly stained for Foxp3. Data show representative of three individual experiments. **(B)** Percentage of proliferating CD4+ Foxp3+ regulatory T cells after 4 days of IL-2 supplemented culture. Bar graphs show mean values ± SEM. * $P < 0.05$.

5.3 Analysis of Foxp1^{cKO} CD4 Cre vav-Bcl2 tg mice

5.3.1 Characterization of Foxp1^{cKO} CD4 Cre vav-Bcl2 tg mice

Foxp1^{cKO} CD4 Cre mice showed an altered B/T cell ratio in peripheral lymphoid organs. As shown in Figure 9B and C, percentages of splenic T cells were reduced, whereas total numbers of T cells remained steady even though mice exhibited signs of splenomegaly. Additionally, unstimulated CD4+ T cells of Foxp1^{cKO} CD4 Cre mice showed greatly reduced survival *in vitro* (Figure 21), suggesting cell death as a possible cause of the reduced T cell percentages *in vivo*. We therefore sought to address the role of apoptosis in Foxp1-deficient T cells in a genetic rescue approach.

For that purpose, Foxp1^{cKO} CD4 Cre mice were bred to vav-Bcl2 transgenic (tg) animals, expressing the human BCL-2 protein under the promoter control of Vav1, targeting expression of the transgene in all cells of the hematopoietic lineage (Ogilvy et al., 1999). Vav-Bcl2 tg mice exhibited multiple effects on their hematopoietic system, including elevated myeloid and lymphocyte cell numbers, splenomegaly, lymphadenopathy as well as altered T cell development in the thymus. The latter is marked by an increase of cells in the double-negative and single-positive stages and a reduction in double-positive thymocytes (Ogilvy et al., 1999).

Investigation of thymocyte development in Foxp1^{cKO} CD4 Cre vav-Bcl2 tg animals revealed no differences between vav-Bcl2 tg and Foxp1^{cKO} CD4 Cre vav-Bcl2 tg mice in terms of thymocyte subset distribution (Figure 23A, left panel). Interestingly, both vav-Bcl2 tg and Foxp1^{cKO} CD4 Cre vav-Bcl2 tg mice showed a 5-fold increase in thymus-derived 'natural' Tregs when compared to Foxp1^{cKO} CD4 Cre and Foxp1^{cKO} controls suggesting survival factors of the Bcl2 family to play a central role in the development or homeostasis of thymus-derived Tregs (Figure 23A, right panel).

Immunphenotyping of spleens and lymph nodes indicated that Bcl2-overexpression was unable to rescue the overall reduction of TCRβ+ cells observed in Foxp1^{cKO} CD4 Cre mice, as Foxp1^{cKO} CD4 Cre vav-Bcl2 tg mice showed even less TCRβ+ cells and therefore an even more pronounced skewing of the T/B cell ratio (Figure 23B, left panel). Remarkably, percentages of CD8+ T cells were found to be reduced in Foxp1^{cKO} CD4 Cre vav-Bcl2 tg mice, while CD4+ T cells were present in comparable percentages as in vav-Bcl2 tg mice. In contrast, the percentage of CD4+ CD25+ Foxp3+ regulatory T cells was massively increased

in Foxp1^{cKO} CD4 Cre vav-Bcl2 tg mice to up to 50% of all splenic CD4+ T cells (Figure 23B, right panel).

In lymph nodes the T/B cell ratio in Foxp1^{cKO} CD4 Cre vav-Bcl2 tg mice was again skewed towards the B cell compartment (Figure 23C, left panel). At the same time, similar to the situation observed in the spleen, CD8+ T cells showed a stronger reduction in Foxp1^{cKO} CD4

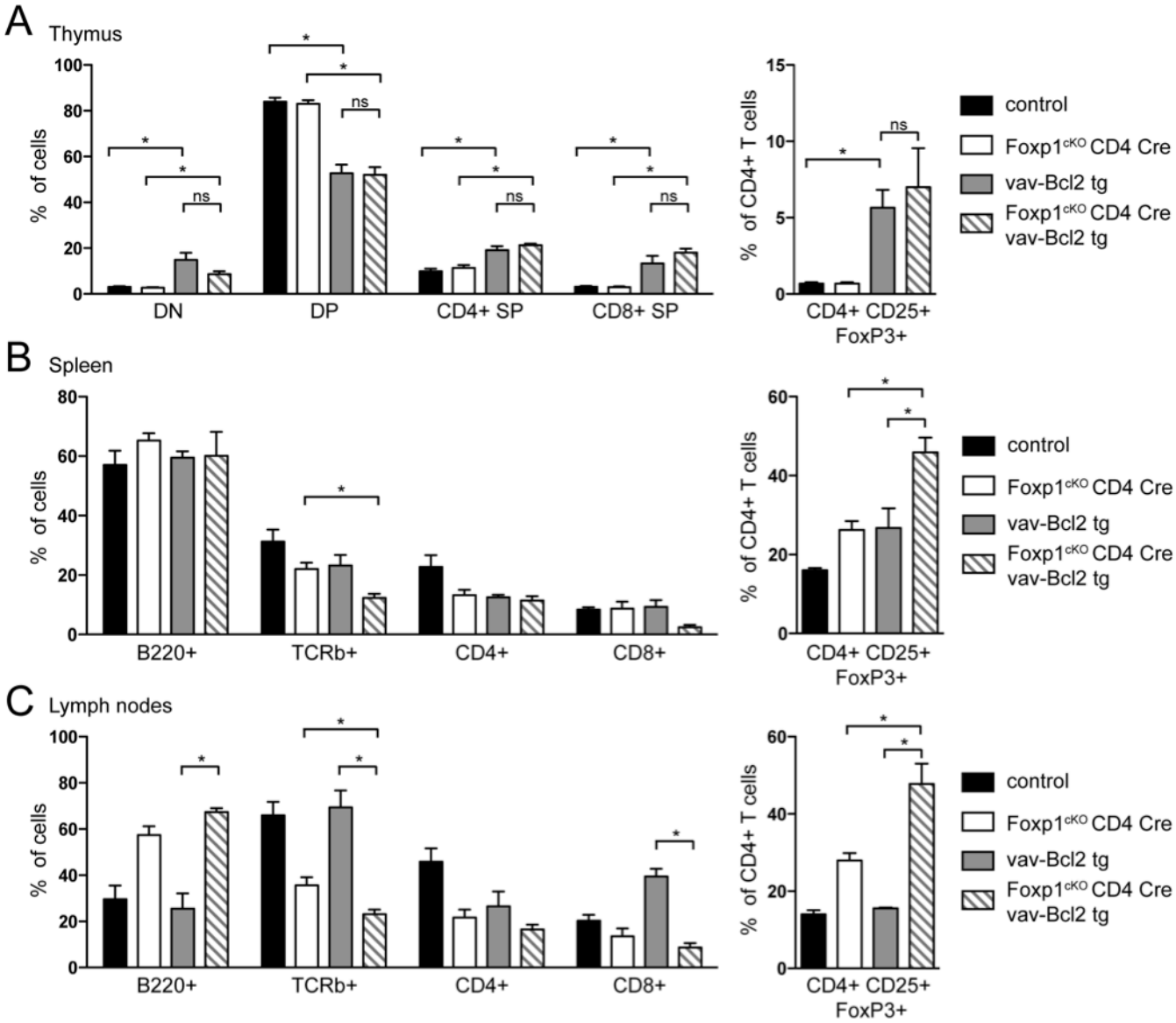

Figure 23 Immune cell distribution of Foxp1^{cKO} CD4 Cre vav-Bcl2 transgenic mice. (A) Flow cytometry of thymocyte distribution in thymi of control (n = 5), Foxp1^{cKO} CD4 Cre (n =4), vav-Bcl2 tg (n = 3), and Foxp1^{cKO} CD4 Cre vav-Bcl2 tg mice (n = 3). Cells were distinguished according to their expression of CD4, CD8, and Foxp3 into double-negative, double-positive, single positive thymocytes (left panel), and thymus-derived regulatory T cells (right panel). Lymphocyte distribution of B cells (B220+), T cells (TCRβ+), T helper cells (CD4+), cytotoxic T cells (CD8+), and regulatory T cells (CD4+ CD25+ Foxp3+) in spleens **(B)** and lymph nodes **(C)** of control (n = 5), Foxp1^{cKO} CD4 Cre (n =4), vav-Bcl2 tg (n = 3), and Foxp1^{cKO} CD4 Cre vav-Bcl2 tg mice (n = 3). Bar graphs show mean values ± SEM. * $P < 0.05$, ns = not significant.

Cre vav-Bcl2 tg mice when compared to vav-Bcl2 tg mice, than Foxp1^{cKO} CD4 Cre showed to their controls. On the contrary, CD4+ T cells were not significantly reduced in Foxp1^{cKO} CD4 Cre vav-Bcl2 tg mice compared to vav-Bcl2 tg mice. Again, about half of CD4+ T cells in lymph nodes of Foxp1^{cKO} CD4 Cre vav-Bcl2 tg mice consisted of a CD4+ CD25+ Foxp3+ regulatory T cell fraction (Figure 23C, right panel).

Taken together, breeding of Foxp1^{cKO} CD4 Cre to vav-Bcl2 tg mice resulted in a complex phenotype that in part recapitulated the immunophenotypic alterations observed in Foxp1^{cKO} CD4 Cre mice. Even though T/B cell ratios remained altered in Foxp1^{cKO} CD4 Cre vav-Bcl2 tg mice and percentages of CD8+ T cells were found to be reduced, CD4+ T cells showed comparable percentages as in vav-Bcl2 tg control mice. Astonishingly, regulatory T cells were massively increased both in spleens and lymph nodes of Foxp1^{cKO} CD4 Cre vav-Bcl2 tg mice and exceeded the percentages observed in Foxp1^{cKO} CD4 Cre by more than two-fold.

These observations support the notion that the reduced percentage of T cells in Foxp1^{cKO} CD4 Cre mice is not or only partially related to increased apoptosis of T cells *in vivo* that could be reversed by overexpression of Bcl-2. It should be emphasized that T cell percentages Foxp1^{cKO} CD4 Cre vav-Bcl2 tg mice did not return to levels measured in Foxp1^{cKO} control mice by expression of the Bcl-2 transgene. Additionally, regulatory T cells were expanded massively in Foxp1^{cKO} CD4 Cre vav-Bcl2 tg mice and contributed to the total percentage of

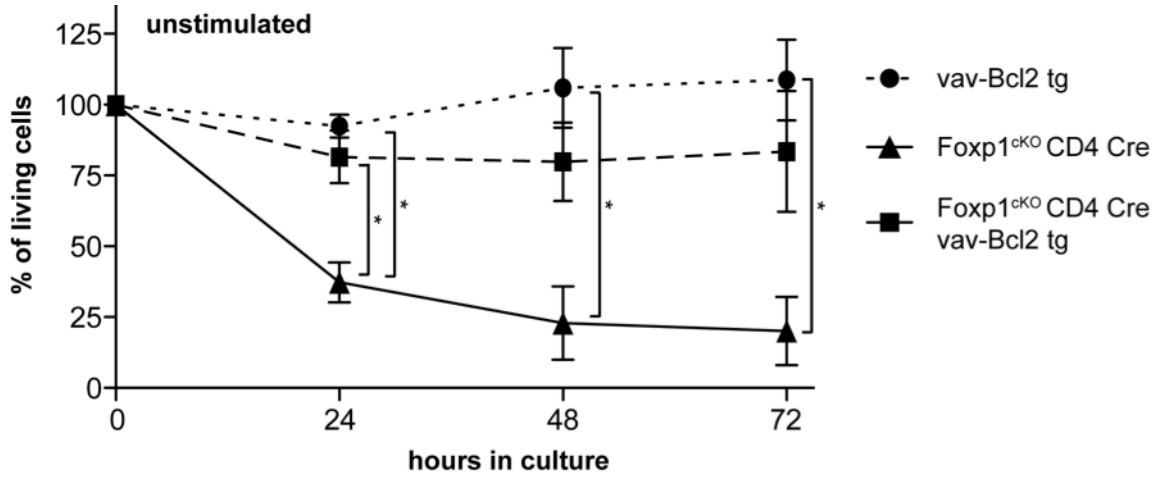

Figure 24 *In vitro* survival of CD4+ T cells from Foxp1^{cKO} CD4 Cre vav-Bcl2 mice. Flow cytometric survival assay of MACS-purified CD4+ T cells from vav-Bcl2 (n = 3), Foxp1^{cKO} CD4 Cre vav-Bcl2 (n = 3), and Foxp1^{cKO} CD4 Cre mice cultured for indicated time in the absence of stimuli. Live cells were distinguished by AnnexinV and 7-AAD and normalized to the percentage of living cells at the start of the experiment. Graphs show mean values ± SEM. * $P < 0.05$.

CD4+ T cells. Therefore, the increase in regulatory T cells may be responsible for the compensation of CD4+ T cell percentages observed in Foxp1^{cKO} CD4 Cre vav-Bcl2 tg mice.

Next, we sought to investigate the influence of the anti-apoptotic Bcl-2 on the *in vitro* survival behaviour of Foxp1-deficient CD4+ T cells as those showed increased apoptosis in this setting. For *in vitro* survival experiments, CD4+ T cells of Foxp1^{cKO} CD4 Cre vav-Bcl2 tg mice and control animals were isolated and kept in culture under unstimulated conditions (Figure 24). Here, the percentages of CD4+ T cells from Foxp1^{cKO} CD4 Cre vav-Bcl2 tg mice remained steady over time showing no signs of cell death. Similar survival rates were observed in CD4+ T cells isolated from vav-Bcl2 tg mice, whereas Foxp1^{cKO} CD4 Cre cells succumbed rapidly, as described before.

In summary, *in vitro* survival assays performed with CD4+ T cells obtained from Foxp1^{cKO} CD4 Cre vav-Bcl2 tg mice exhibited greatly enhanced survival rates of cultured cells comparable to cells isolated from vav-Bcl2 tg mice. These results emphasize the anti-apoptotic influence of Bcl2 overexpression in peripheral CD4+ T cells. However, the reduction of T cell ratios in the periphery of Foxp1^{cKO} CD4 Cre mice was, if at all, only partially overcome by additional expression of Bcl2.

In conclusion, overexpression of the potent anti-apoptotic protein Bcl2 was unable to rescue the loss of CD4+ T cells *in vivo* but resulted in improved survival in *in vitro* survival assays. Together, the genetic rescue approach failed to compensate the apoptotic effect of Foxp1-deletion on T cells *in vivo*. However, the data supports the idea that Foxp1^{cKO} CD4 Cre T cells rather are diminished by another mechanism, e.g. by migration to non-lymphoid sites than by apoptosis. This emigration might in part be due to the altered expression of chemokine-receptors on memory T cells, allowing Foxp1^{cKO} CD4 Cre T cells to enter non-lymphoid tissues and to become tissue-resident memory T cells, presumably.

5.3.2 Survival of Foxp1^{cKO} CD4 Cre and Foxp1^{cKO} CD4 Cre vav-Bcl2 tg mice

Bcl2 is one of the best-studied anti-apoptotic proteins and of key importance in the regulation of live and death, not only in cells of the immune system (Marsden and Strasser, 2003). In humans, overexpression of Bcl2 was found in neoplastic B cells with t(14;18) chromosomal translocations (Tsujimoto et al., 1984). The role of Bcl2 in oncogenesis and its influence on cell of the immune system was studied by generating transgenic animals, expressing the anti-apoptotic protein under the control of different promoters (McDonnell et al., 1989; Ogilvy et

al., 1999; Strasser et al., 1991). Unlike other Bcl2 transgenic animals, mice expressing Bcl2 under the control of the vav promoter exhibit a reduced lifespan and develop follicular lymphoma preceded by excessive germinal centre formation (Egle et al., 2004).

In this study, control vav-Bcl2 tg mice showed an average median survival time of 259.5 days (n = 8) and lived significantly longer than Foxp1^{cKO} CD4 Cre vav-Bcl2 tg mice, as the latter died within 179 days (n = 11) ($P < 0.05$, Mantel-Cox) (Figure 25). As reported previously, moribund vav-Bcl2 mice showed massive splenomegaly, which is in line with the development of follicular lymphoma in these animals. Similarly, Foxp1^{cKO} CD4 Cre vav-Bcl2 tg mice exhibited enlarged spleens (data not shown). A comparison between lifespan in survival statistics revealed a stronger lifetime reduction of T cell-specific Foxp1-deficient mice in a vav-Bcl2 background (32% reduction), than in Foxp1^{cKO} CD4 Cre mice (9% reduction), compared to their respective control groups. In summary, Foxp1-deficiency in T cells affects the survival outcome of vav-Bcl2 transgenic mice in an additive manner.

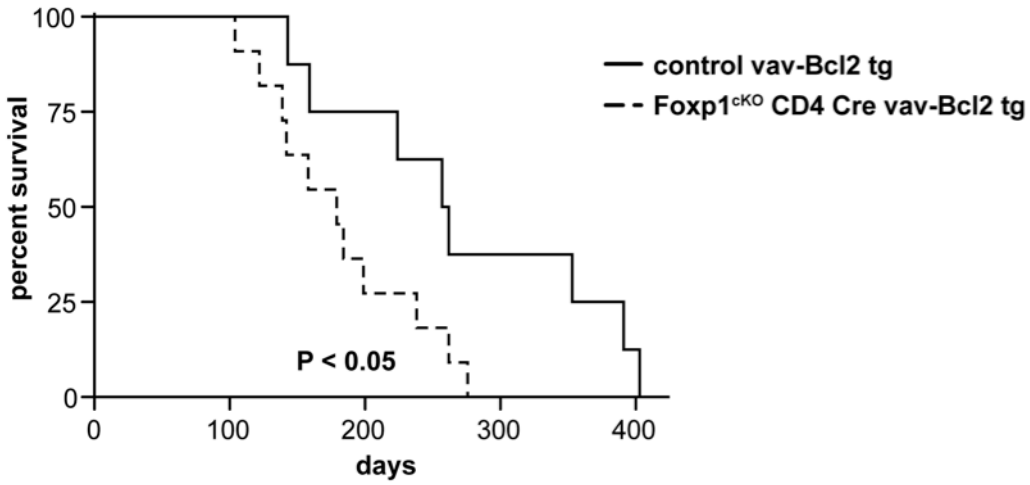

Figure 25 Foxp1^{cKO} CD4 Cre vav-Bcl2 mice succumbed earlier than control animals. Kaplan-Mayer curves of vav-Bcl2 control animals (n = 8) and Foxp1^{cKO} CD4 Cre mice (n = 11). P value was calculated by Log rank/ Mantel-Cox test.

5.4 Analysis of Foxp1^{cKO} Foxp3 Cre mice

5.4.1 Immunophenotypical characterization of Foxp1^{cKO} Foxp3 Cre mice

Foxp1^{cKO} CD4 Cre mice had shown a strikingly altered T cell compartment which not only lacked naïve T cells, but also gave rise to increased numbers of regulatory T cells. Additionally, CD4+ CD25+ Foxp3+ regulatory T cells expanded from isolated CD4+ T cells of Foxp1^{cKO} CD4 Cre mice after *in vitro* culture in presence of IL-2 without any further antigenic stimulation and co-stimulation. To further investigate the role of the transcription factor Foxp1 in regulatory T cells, Foxp1^{cKO} mice were bred to a Foxp3 promoter–driven BAC transgenic mouse strain carrying a GFP-Cre fusion protein (Foxp3 Cre) (Zhou et al., 2008). In Foxp1^{cKO} Foxp3 Cre mice Foxp1 expression was specifically deleted in Foxp3+ regulatory T cells which were at the same time marked by GFP expression (Figure 26A and data not shown).

Immunophenotyping of Foxp1^{cKO} Foxp3 Cre mice revealed no obvious changes in percentages of thymocyte subsets and no alteration of thymus-derived 'natural' regulatory T cells (Figure 26B). Whereas Foxp1^{cKO} CD4 Cre mice showed signs of splenomegaly, altered T/B cell ratios and increased numbers of regulatory T cells in the spleen, no changes in cell distribution and cell number were observed in Foxp1^{cKO} Foxp3 Cre mice (Figure 26C and data not shown). Lymph nodes of Foxp1^{cKO} Foxp3 Cre mice exhibited a faintly diminished percentage of B cells in favour of CD4+ T cells (Figure 26D, left panel). Importantly, the percentage of regulatory T cells in lymph nodes of Foxp1^{cKO} Foxp3 Cre mice remained comparable to those of Foxp1^{cKO} control mice (Figure 26D, right panel).

While Foxp1^{cKO} CD4 Cre mice had shown a major shift of their CD4+ and CD8+ T cell population towards the effector or memory T cell compartment, Foxp1^{cKO} Foxp3 Cre mice showed no prominent changes (Figure 27A, B). Only a minor reduction of naïve CD4+ T cells in favour of the central-memory CD4+ T cells in the spleen of Foxp1^{cKO} Foxp3 Cre mice was observed, whereas T cell populations in lymph nodes remained unaltered. Also, Foxp1^{cKO} Foxp3 Cre animals were viable and healthy and did not show any obvious signs of autoimmunity, suggesting a limited role for Foxp1 in regulatory T cell function and homeostasis.

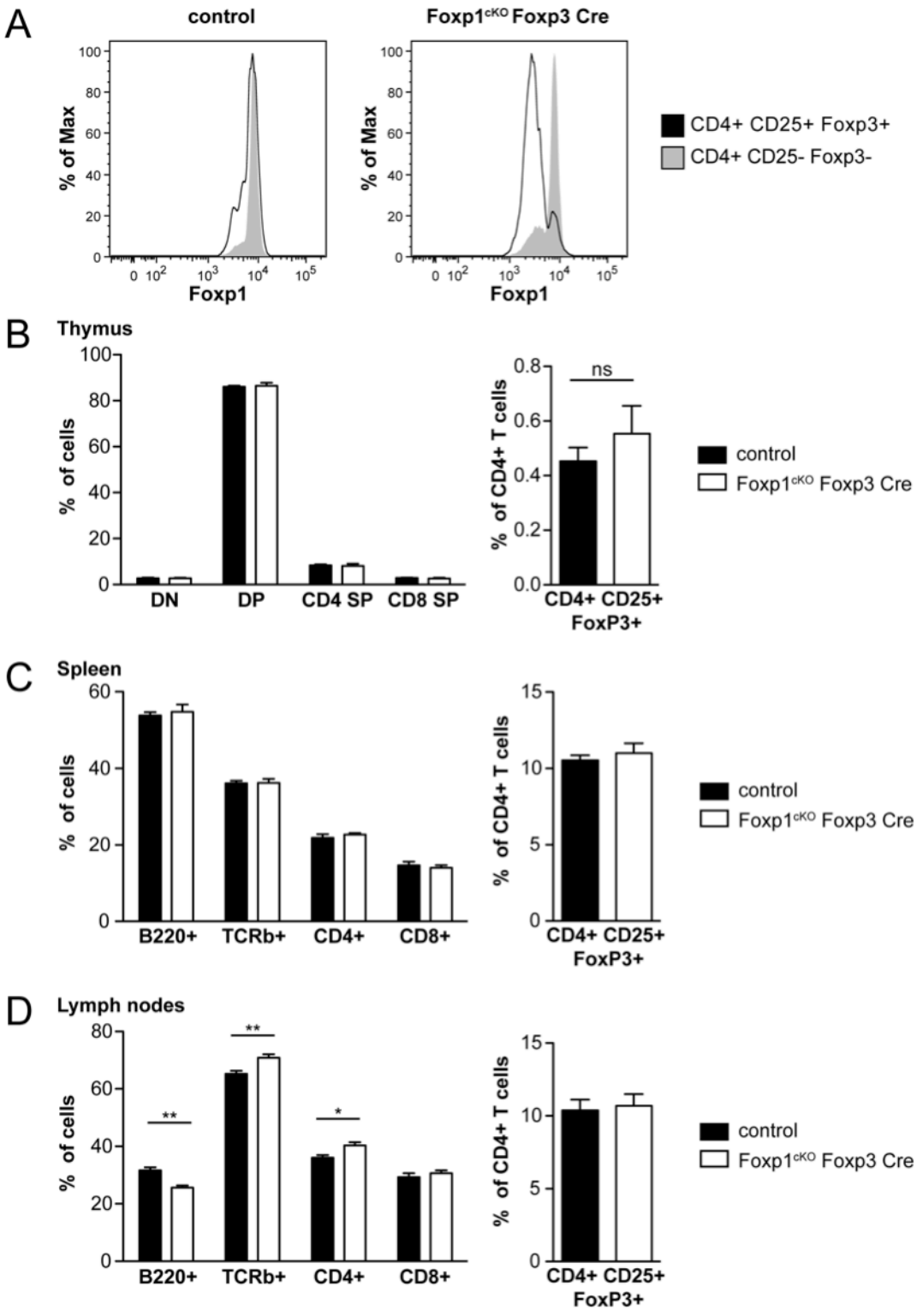

Figure 26 Immune cell phenotype of Foxp1^{cKO} Foxp3 Cre mice. (A) Foxp1 expression in regulatory T cells in Foxp1^{cKO} Foxp3 Cre and control mice by intracellular flow cytometry. Histograms show overlays of CD4+ CD25+ Foxp3+ cells and CD4+ CD25- Foxp3- T cells of the respective genotype. **(B)** Thymocytes of control and Foxp1^{cKO} Foxp3 Cre mice (both n = 5) distinguished into double-negative, double-positive, and single-positive (left panel) and regulatory T cells (CD4+ CD25+ Foxp3+) (right panel) by flow cytometry. **(C)** Percentages of splenic lymphocytes detected by flow cytometry according to their expression of B220, TCRβ, CD4, CD8 (left panel), and CD4+ CD25+ Foxp3+ regulatory T cells (right panel) in control and Foxp1^{cKO} Foxp3 Cre mice. **(D)** Cell distribution of lymphocytes in pooled lymph nodes of control and Foxp1^{cKO} Foxp3 Cre mice. Bar charts show mean values ± SEM. * $P < 0.05$, ** $P < 0.01$, ns = not significant.

In summary, Foxp1^{cKO} Foxp3 Cre mice did not exhibit any prominent changes in immune cell populations. These findings suggest that the transcription factor Foxp1 is necessary for the maintenance of naïve T cells, but largely dispensable for differentiated regulatory T cells.

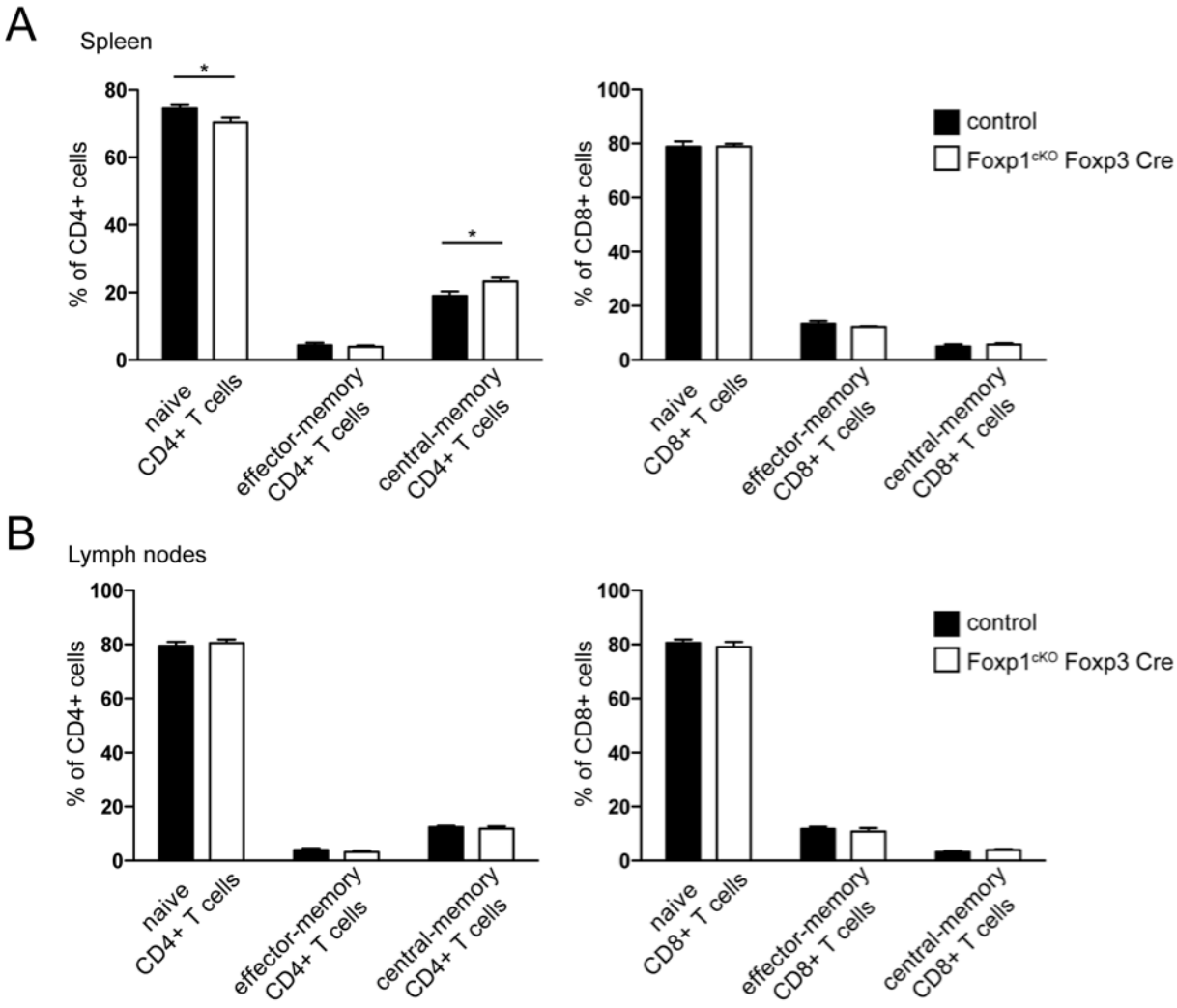

Figure 27 Minor changes in T cell compartments of Foxp1^{cKO} Foxp3 Cre mice. (A) Flow cytometry of CD4+ and CD8+ T cells isolated from spleens (top) and lymph nodes (bottom) of control (n = 5) and Foxp1^{cKO} CD4 Cre (n = 5). Cells are distinguished by their levels of CD44 and CD62L in naïve (CD62L^{high} CD44 ^{low}), effector-memory (CD62L^{low} CD44 ^{high}), and central-memory (CD62L^{high} CD44^{high}) CD4+ and CD8+ T cells. Bar charts show mean values ± SEM. * P < 0.05.

5.5 Analysis of 2D2 MOG-specific Foxp1^{cKO} CD4 Cre mice

5.5.1 Characterization of 2D2 MOG$_{(35-55)}$-specific Foxp1^{cKO} CD4 Cre mice

All T cells of Foxp1^{cKO} CD4 Cre mice obtained a memory T cell phenotype immediately after Foxp1 expression was abolished in the double-positive thymocyte stage. Although the peripheral T cell compartment only consisted effector and/or memory T cells, no overt autoimmune pathology was observed in Foxp1^{cKO} CD4 Cre animals. Nevertheless, functional assays with CD4 T cells from Foxp1^{cKO} CD4 Cre mice revealed an effector/memory T cell-like behaviour in terms of cytokine production upon stimulation. These observations raised the question whether Foxp1-deficient T cells are functional *in vivo* and how a loss of Foxp1 would affect the pathological outcome in an autoimmune-prone context.

In order to address the function of Foxp1 in autoimmunity, Foxp1^{cKO} CD4 Cre mice were bred to the 2D2 mouse strain, carrying a transgenic myelin oligodendrocyte glycoprotein (MOG)-specific TCR (Bettelli et al., 2003). All CD4+ T cells in 2D2 mice express a TCR consisting of Vα3.2 and Vβ11 chains which are specific for the MOG$_{(35-55)}$ peptide. About 35% of all 2D2 mice of a C57BL/6 background spontaneously develop clinical signs of an optic neuritis, whereas only 4% show clinical signs resembling an experimental autoimmune encephalomyelitis (EAE) (Bettelli et al., 2003).

T cell development in the thymus of 2D2 controls and Foxp1^{cKO} CD4 Cre 2D2 mice was altered in a way that double-negative thymocytes were largely reduced. In contrast, CD4 single-positive thymocytes were increased to upon to 60% of all cells in the thymus (Figure

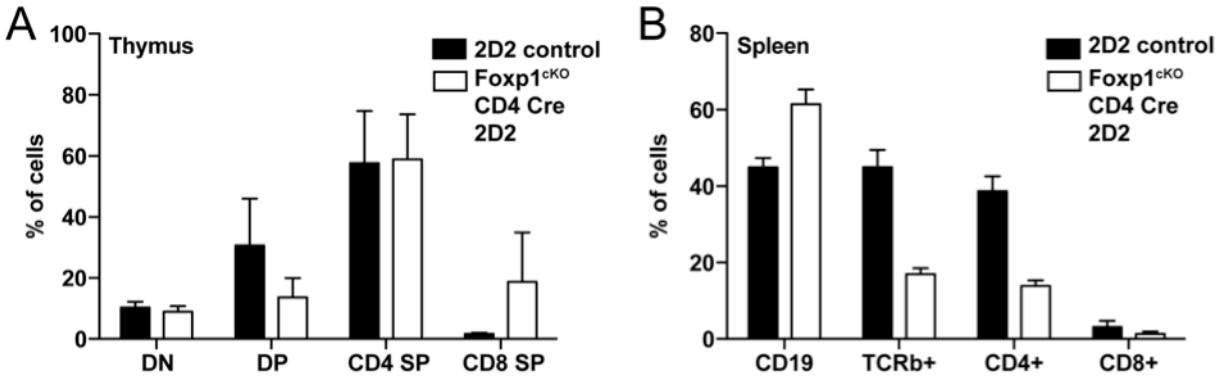

Figure 28 Immune cell distribution of Foxp1^{cKO} CD4 Cre 2D2 mice. (A) Thymocytes in 2D2 control (n = 3) and Foxp1^{cKO} CD4 Cre 2D2 mice (n = 5) distinguished into double-negative, double-positive, and single-positve by their expression of CD4 and CD8 by flow cytometry. **(B)** Percentages of splenic lymphocytes detected by flow cytometry according to their expression of B220, TCRβ, CD4, and CD8 in 2D2 control (n = 4) and Foxp1^{cKO} CD4 Cre 2D2 mice (n = 8). Bar charts show mean values ± SEM.

28A). In spleens of 2D2 control mice equal percentages of T and B cells were observed, whereas the T cell compartment consisted almost exclusively of CD4+ T cells (Figure 28B). Foxp1^{cKO} CD4 Cre 2D2 mice again showed a marked skewing of their T/B cell ration in the spleen, resulting in a reduction of TCRβ+ T cells to 20% of all cells. Similar to the 2D2 control animals, nearly all TCRβ+ T cells in Foxp1^{cKO} CD4 Cre 2D2 mice were of CD4+ T cell origin, whereas CD8+ T cells were almost absent. Comparable to what was observed in Foxp1^{cKO} CD4 Cre mice, Foxp1^{cKO} CD4 Cre 2D2 animals showed a complete shift in T cell differentiation towards effector/memory T cells (data not shown).

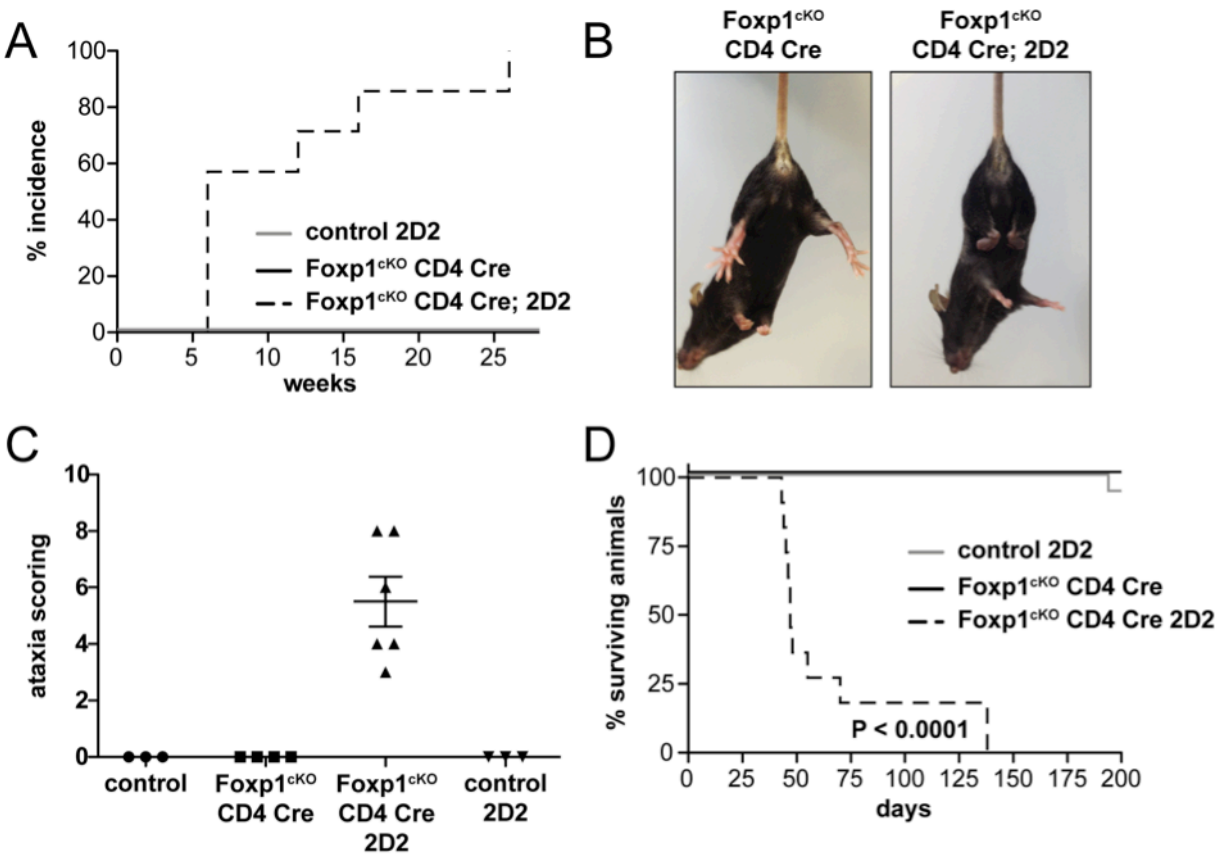

Figure 29 Foxp1^{cKO} CD4 Cre 2D2 mice developed rapid spontaneous neuropathology. (A) Incidence of neuropathological symptoms of control 2D2 (n = 6), Foxp1^{cKO} CD4 Cre (n = 3), and Foxp1^{cKO} CD4 Cre 2D2 mice (n = 7) in weeks of age. **(B)** Photograph of typical hindlimb clasping symptoms in Foxp1^{cKO} CD4 Cre 2D2 mice. **(C)** Ataxia scoring of control (n = 3), Foxp1^{cKO} CD4 Cre (n = 4), Foxp1^{cKO} CD4 Cre 2D2 (n = 6), and control 2D2 mice (n = 3). Composite phenotype scoring system comprised hindlimb clasping, gait ataxia, ledge walk, and kyphosis (each scored 0 – 3). Scatter plot show mean values +/- SEM. **(D)** Kaplan-Mayer curves of control 2D2 (n = 7), Foxp1^{cKO} CD4 Cre (n = 12), and Foxp1^{cKO} CD4 Cre 2D2 (n = 12). P value was calculated by Logrank/Mantel-Cox test.

Strikingly, and unlike the 2D2 control animals, Foxp1^{cKO} CD4 Cre 2D2 mice developed neurological symptoms at an early age (median of 6 weeks) (Figure 29). The course of disease was initially marked by hindlimb clasping, spasms of the hindlimbs and partial paralysis (Figure 29B). About 70% (8 of 11) of all Foxp1^{cKO} CD4 Cre 2D2 animals furthermore showed reduced body weight of less than 75% of their littermate controls. Ataxia scoring confirmed the neurological disorder observed in Foxp1^{cKO} CD4 Cre 2D2 mice (Figure 29C). Briefly, ataxia scoring included clinical parameters of hindlimb clasping, ledge walk, gait ataxia and kyphosis (Guyenet et al., 2010). In none of the control mice any neurological symptoms were observed, whereas Foxp1^{cKO} CD4 Cre 2D2 animals showed a mean ataxia score of 5,5. Additionally, most Foxp1^{cKO} CD4 Cre 2D2 animals became moribund soon after onset of the neurological symptoms and either died or had to be sacrificed, while 2D2 control mice remained phenotypically unapparent (Figure 29D). Even though approximately 20% of all Foxp1^{cKO} CD4 Cre 2D2 mice lived longer than 100 days before they succumbed, the median survival of the animals was only 47 days.

Analysis of CNS-infiltrating lymphocytes showed an increased number of CD4+ T cells present in the brains of Foxp1^{cKO} CD4 Cre 2D2 mice compared to Foxp1^{cKO} CD4 Cre animals

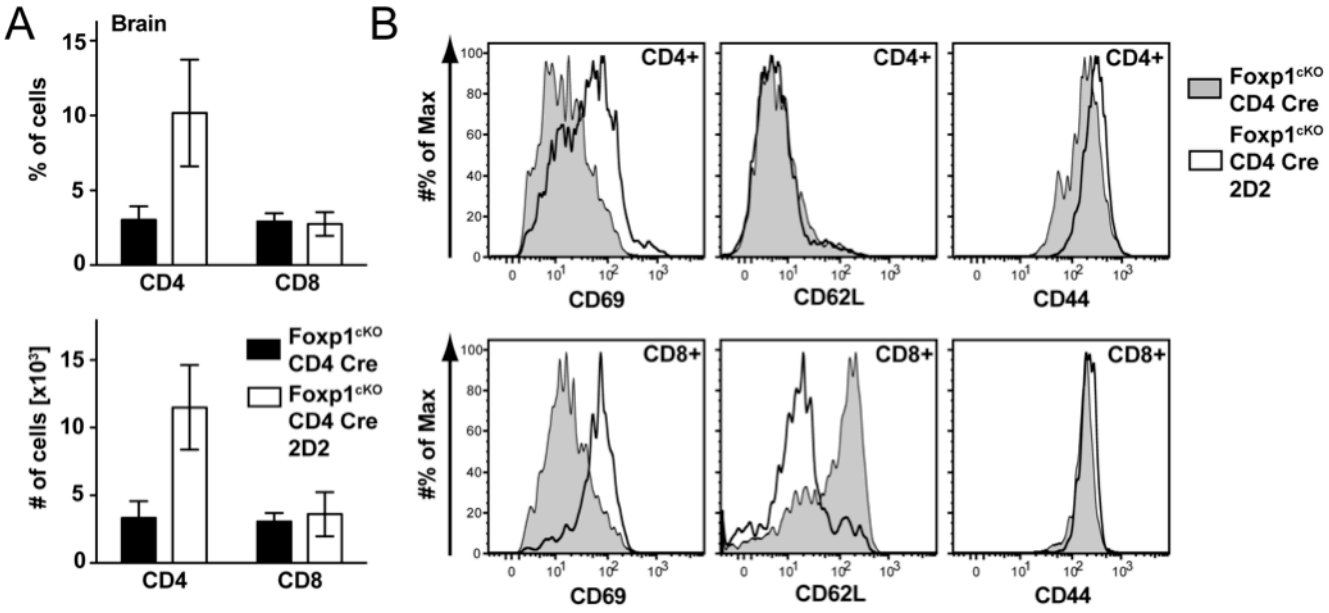

Figure 30 CNS-infiltration of lymphocytes in Foxp1^{cKO} CD4 Cre 2D2 mice. (A) Flow cytometry of CNS-infiltrating CD4+ and CD8+ lymphocytes in Foxp1^{cKO} CD4 Cre and Foxp1^{cKO} CD4 Cre 2D2 mice (n = 3 each). Bar charts show mean values ± SEM. **(B)** Histogram overlays of CD69, CD62L, and CD44 levels on CNS-infiltrating T cells of Foxp1^{cKO} CD4 Cre and Foxp1^{cKO} CD4 Cre 2D2 mice. Results show representative data of three independent experiments.

(Figure 30A). Furthermore, infiltrating CD4+ T cells showed an activated $CD44^{high}$ $CD62L^{low}$ phenotype, represented by upregulation of CD69 in $Foxp1^{cKO}$ CD4 Cre 2D2 mice (Figure 30B). Additionally, CD8+ T cells showed a marked down-regulation of CD62L in $Foxp1^{cKO}$ CD4 Cre 2D2 mice in addition to high CD69 expression suggesting the presence of acutely activated cytotoxic T cells contributing to the observed neuropathology.

Taken together, the expression of a MOG-specific transgenic TCR of T cells in $Foxp1^{cKO}$ CD4 Cre mice triggered spontaneous neuropathology accompanied by early incidence of neurological symptoms and premature death. Concomitant presence of CNS-infiltrating T cells was observed in $Foxp1^{cKO}$ CD4 Cre 2D2 mice indicating ongoing autoimmune processes in the CNS of those mice. These data suggest that Foxp1 in T cells is a critical regulator of quiescence in the context of autoimmunity and its loss in a model for multiple sclerosis is associated with a fatal course of neuropathology.

6 Discussion

6.1 Reduced Foxp1 expression in effector/memory T cells

The forkhead-box transcription factor Foxp1 is expressed in a variety of tissues and in cells of the immune system, like monocytes, B cells and T cells (Feng et al., 2010; Hu et al., 2006; Shi et al., 2004). Consistent with these reports, Foxp1 expression was detected in lymphocytes obtained from wildtype mice. Two different isoforms were observed in T helper cells, cytotoxic T cells, and Tregs, and an additional third isoform in B cells by Western blotting (Figure 5A). Based on their size, the different isoforms most likely represented the previously reported isoforms Foxp1A, C, and D (Wang, 2003). Foxp1A represents the longest isoform, containing a C-terminal poly-Q stretch, followed by a glutamine-rich region. In contrast, Foxp1D lacks only the poly-Q stretch, whereas in Foxp1C both, poly-Q stretch and the glutamine-rich region are missing. Interestingly, B cells showed a third Foxp1 band, presumably corresponding to Foxp1D. Even though different Foxp1 isoforms are of great importance for ESC pluripotency and are also implicated to have oncogenic potential, little is known about their function (Brown et al., 2008; Gabut et al., 2011). Most likely, the variations in Foxp1 isoform expression are indicative for a differential role of the transcription factors in the tested lymphocyte subsets. A variation in poly-Q stretches potentially indicates differences in protein-protein interaction behaviour of Foxp1 isoforms in the respective cell types, which eventually might result in a diverging transcriptional outcome.

In addition to differences in isoform composition, also total expression levels varied systematically between cell types. Effector and memory T cells, being CD4+ CD44+ CD62L-, showed strikingly diminished Foxp1 expression compared to naïve T cells identified as CD4+ CD44- CD62L+ (Figure 5B, C). This finding of reduced Foxp1 expression in effector/memory T cells suggests a critical role for the transcription factor in T cell differentiation. Here, the regulation of Foxp1 expression might be analogous to down-modulation during the differentiation of monocytes to macrophages (Shi et al., 2004). Likewise in T cells, Foxp1 expression might be restricted to naïve T cells before the encounter of their cognate antigen, potentially regulating the tissue tropism, responsiveness and quiescence of the respective T cell.

Moreover, expression of Foxp1 was also reduced in Tregs (Figure 5A). This finding has to be interpreted in conjunction with the observation, that Foxp1 expression is generally reduced in CD62L- T cells: As the Treg fraction consists of a larger proportion of CD62L- cells, lower

Foxp1 levels are the consequence (Figure 5D). The concomitant regulation of Foxp1 and CD62L suggests a role for the transcription factor in regulation of migratory behaviour, T cell activation, and during transition from naïve to effector or memory T cells, respectively.

In addition to differential expression in various T cell subtypes, Foxp1 expression is also regulated during their maturation stages in the thymus. Here, T cells pass through different phases in which genetic recombination takes place and cells are selected positively and negatively. A comparison of Foxp1 expression in the four main stages of thymocyte differentiation revealed reduced levels of the transcription factor in double-positive thymocytes (Figure 6A, B, C). While the effects of lower Foxp1 expression during this stage of differentiation is not known, one can hypothesize that antigen-stimulation of the recently generated TCR in double-positive cells might result in down-regulation of Foxp1, comparable to what was observed in monocytes upon integrin ligation (Shi et al., 2004). Potentially, reduced levels of Foxp1 in thymocytes are a consequence of activatory signals via their TCR and might be indicative for cells undergoing selection processes in the thymus. Interestingly, Foxp1 expression was restored in single-positive thymocytes, which might either result from re-expression of the protein or from loss of $Foxp1^{low}$ thymocytes by thymic selection mechanisms. However, the transcription factor Foxp1 seems to be largely dispensable in earlier stages of thymocyte development, as the foetal liver chimeric approach by Hu et al. reported no alteration in thymocyte maturation (Hu et al., 2006).

6.2 Analysis of Foxp1-deficiency in T cells

Banham et al. reported in 2001 the expression of a newly described winged helix transcription factor Foxp1 in various types of cancer and DLBCLs (Banham et al., 2001). Later, Foxp1 was shown to be involved in recurrent chromosomal aberrations leading to increased expression in DLBCL and MALT lymphoma, indicating a potential oncogenic role of the protein (Fenton et al., 2006; Streubel et al., 2005; Wlodarska et al., 2005). These observations initially drew our interest to the role of this transcription factor in haematopoiesis and its function in lymphocytes. As the full knock-out was reported to succumb at day E14.5, a conditional knock-out mouse strain was generated in our laboratory (Patzelt, 2010).

For the current study, T cell-specific deletion of Foxp1 was achieved by mating Foxp1 conditional knock-out animals with a CD4 Cre mouse strain. Similarly to what Patzelt reported initially for B cells in a CD19 Cre system, CD4+ T cells purified from $Foxp1^{cKO}$

CD4 Cre mice showed an abolished full-length form of Foxp1, while a marginally expressed truncated form of the protein was still visible in western blotting (Figure 7B, C) (Patzelt, 2010). This low-grade expression is potentially due to decreased stability of the protein lacking its core functional forkhead-box domain. While ablation of the DNA-binding domain clearly abolishes binding of Foxp1 to DNA in an electromobility shift assays (Patzelt, 2010), it cannot be completely excluded that the truncated Foxp1 form partially executes other functions mediated by protein-protein interaction. However, the greatly reduced amount of the residual truncated protein makes a prominent effect unlikely. In addition, a $Foxp1^{del/del}$ mutant generated by Patzelt also exhibited the reported cardiovascular malfunctions of the full knock-out and died during embryonic development (Patzelt, 2010; Wang, 2004). Finally, T cells from $Foxp1^{+/flox}$ CD4 Cre mice, which also showed low-level expression of the truncated Foxp1 form, are undistinguishable from those obtained from $Foxp1^{+/+}$ CD4 Cre mice, thereby reducing the likelihood of a dominant-negative effect of the residual protein as a reason for the observed phenotypes.

Even though mice with Foxp1-deficient T cells were apparently of good health, all animals suffered from a mild form of splenomegaly whereas lymph node sizes were generally reduced (Figure 8 and data not shown). At the same time, while thymocyte development was normal, $Foxp1^{cKO}$ CD4 Cre mice exhibited altered B/T cell ratios with a reduction of T cells in favour of B cells (Figure 9A, B, D). Indeed, the increased splenic cell number was mainly due to the exuberant presence of B220+ B cells and CD4+ CD25+ Tregs, whereas total number of TCRβ+ T cells remained unaltered compared to control animals (Figure 9C). Consistent with that, $Foxp1^{cKO}$ CD4 Cre mice showed a strong relative increase in Tregs in the periphery, whereas thymus-derived Tregs did not exhibit a change in percentage (Figure 9A, B, D). However, the observations did not allow the conclusion that the splenomegaly depends on the sole expansion of B cells and Tregs. Potentially, T cells could expand as well, but migrate to non-lymphoid sites or even undergo apoptosis. Alternatively, the expansion of splenic B cells and Tregs in $Foxp1^{cKO}$ CD4 Cre mice could also be attributed to an altered microenvironment, as Foxp1-deficient T cells might generate a cytokine milieu that promotes their proliferation.

A more detailed analysis of immune cell markers revealed that all CD4+ and CD8+ T cells in $Foxp1^{cKO}$ CD4 Cre mice showed an effector and memory T cell-like phenotype. Concomitantly, T cells of $Foxp1^{cKO}$ CD4 Cre mice showed no residual naïve T cell

population. This altered phenotype was already visible in the thymus, where CD4 and CD8 single-positive thymocytes expressed higher levels of CD44 (Figure 10). Importantly, no expression of CD25 and/or CD69 was detected on thymocytes or peripheral T cells of Foxp1^{cKO} CD4 Cre mice, indicating the absence of an acutely activated phenotype (Figure 10, 12, 14). Further subdivision of Foxp1-deficient CD4+ T cells according to the memory marker scheme revealed that the majority were effector/memory T cells (CD62L^{low} CD44^{high}) in the spleens of Foxp1^{cKO} CD4 Cre mice, whereas the residual cells showed a central-memory phenotype (CD62L^{high} CD44^{high}). Also the CD8+ T cell compartment in Foxp1^{cKO} CD4 Cre mice showed a complete loss of naïve T cells in favour of effector/memory T cells. In contrast to CD4+ T cells, all Foxp1-conditional knock-out CD8+ T cells were found to exhibit a complete shift towards a central-memory phenotype.

One difficulty in defining the actual nature of the arising T cell fraction is the similarity of effector and memory T cells as explained in Chapter 1.2.4 of the introduction to this thesis. Effector T cells normally arise from early activated T cells, typically during the expansion phase of an immune reaction. This effector cell population shares phenotypic and functional characteristics with memory T cells and therefore cannot be easily distinguished from them (Kaech et al., 2002). According to Sallusto et al., memory T cells can be further distinguished in central memory and effector-memory T cells by their expression of CD44 and CD62L (Sallusto et al., 1999). Additionally, memory T cells are often characterized by their specificity towards a certain antigen after immunization, which is not applicable in an unimmunized animal.

Morphological analysis of the T cell populations showed that all Foxp1-deficient T cells were of blasted appearance. This phenotypical change is often correlated with activated effector cells, which also exhibit a higher rate of proliferation and increased cellular metabolism. Additionally, CD127 (IL7R) expression was increased in both CD4 and CD8 T cells of Foxp1^{cKO} CD4 Cre mice. This observation is in line with a report (published while this work was in preparation) which shows that Foxp1 is a direct regulator of IL7R expression and competes with Foxo1 for binding to the enhancer region of *Il7r* (Feng et al., 2011). Upon binding of IL-7 to its receptor, receptor-bound Jak1 and Jak3 are activated and signal through STAT5a/b resulting in expression of anti-apoptotic proteins Bcl2 and Mcl-1 (Surh and Sprent, 2008). It has also been reported that higher expression of IL7R goes along with increased IL-7 dependence of T cells. This mechanism regulates the survival of antigen-responding T cells

after removal of their cognate antigen and is critical for the maintenance of memory T cells (Mazzucchelli and Durum, 2007). This finding may be one explanation for the relative loss of T cells in the periphery and for the reduced cellularity of lymph nodes, as the present memory T cells potentially compete for IL-7. The exuberant number of memory T cells might lead to a relative shortness in IL-7 and subsequent deprivation of survival signals. Hence, a lack of survival signals might eventually lead to the apoptosis of undersupplied memory T cells and therefore conditions a relative loss of peripheral T cells.

In addition to differences in the expression pattern of CD62L and CD44, memory T cells can be distinguished according to their expression levels of CCR7 (Sallusto et al., 2004), a chemokine receptor critical for cellular tissue tropisms and the entrance of lymphocytes through HEVs into lymph nodes (Woodland and Kohlmeier, 2009). Foxp1^{cKO} CD4 Cre CD4+ T cells generally showed reduced expression of CCR7, further corroborating the effector-memory T cell phenotype of Foxp1-deficient T cells.

Notably, T helper cells from Foxp1^{cKO} CD4 Cre mice showed both CD27 and CD95 upregulation. CD27 belongs to the TNF-receptor super-family, has co-stimulatory functions and was shown to maintain effector and memory CD8^{+} T cells of low affinity *in vivo* by enabling proliferation and providing survival signals (van Gisbergen et al., 2011). It is intriguing to speculate that Foxp1 could dampen the expression of CD27 in naïve T cells to prevent inappropriate co-stimulation. This regulation might be lost in effector/memory T cells by the down-regulation of Foxp1. The increased expression of CD95 on the other hand, usually found on acutely activated T cells, might contribute to an increased susceptibility to apoptosis in T cells and thereby contribute to the observed alterations in the B/T cell ratio. Also in CD8+ T cells of Foxp1^{cKO} CD4 Cre, higher expression of IL7R and CD95 was observed, but in contrast to CD4+ T cells, no altered expression of CD27 or CCR7 was detectable. While Foxp1-deficient CD4+ T cells mainly turned into T cells with an effector-memory phenotype, CD8+ T cells rather resembled a central-memory T cell population, which are known to express higher levels of CCR7 than effector-memory T cells. Additionally, Foxp1-deficient CD8+ T cells showed increased levels of co-stimulatory receptor CD28. These elevated levels of CD28 could contribute to a lowered threshold of co-stimulation for T cells having contact with APCs. Altogether, the changes in expression levels suggest that several of the altered proteins might be direct targets Foxp1 on a transcriptional level, comparable to *Il2* and *Il7r*.

Generally, the finding that loss of Foxp1 expression converts naïve T cells into effector or memory T cells is of great interest to the field of T cell biology, as it contributes to a deeper understanding of how immunological memory in T cells is created and controlled. The transcription factor Foxp1 seems to act as a 'transcriptional break' which maintains the quiescent state of naïve T cells that is lost during the activation phase of a T cell and its transition to an effector and memory cell stage (Figure 31).

A separate study by Feng et al., conducted in parallel to this work, also described the transcription factor Foxp1 as a regulator of naïve T cell quiescence (Feng et al., 2010). In a similar conditional knock-out approach, Foxp1 was depleted in T cells, which resulted in the acquisition of an activated T cell phenotype. Furthermore, Foxp1-deficient T cells proliferated faster, exhibited elevated cytokine production and increased cell death. Additionally, the authors showed in a mixed bone-marrow approach a cell-autonomous mechanism for the acquisition of the activated phenotype of Foxp1-deficient T cells (Feng et al., 2010). In the most recent study of the same group, Foxp1 has additionally been described as a negative regulator of Tfh development, controlling IL-21 expression in direct manner by binding to its genetic locus (Wang et al., 2014).

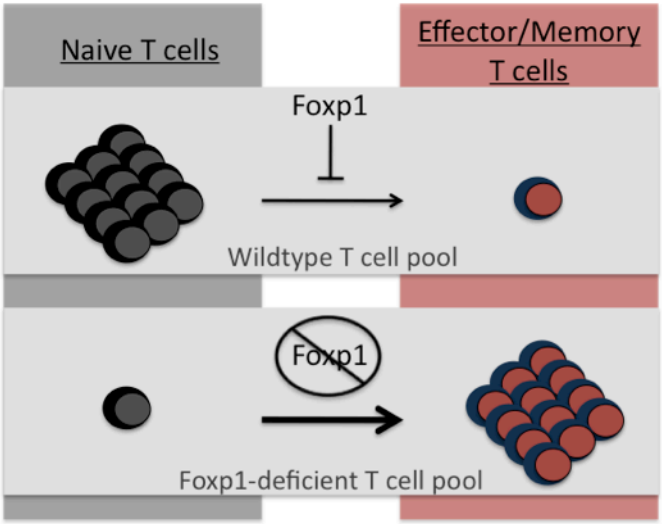

Figure 31 Model of Foxp1 limiting the effector/memory T cell pool. Expression of the transcription factor Foxp1 in naive T cells maintains their identity as antigen-inexperienced naive T cells. Loss of Foxp1 results in a transition of naive to effector/memory T cells starting from double-positive stages of thymocyte development. The Foxp1-deficient T cell pool eventually consists only of CD4+ and CD8+ effector/memory T cells.

A study by Wu et al. gives further insights into the mechanism by which Foxp proteins might contribute to the regulation of effector function in conventional and regulatory T cells (Wu et al., 2006). The authors report that after TCR stimulation NFAT forms a complex with AP-1 proteins to induce a transcriptional program directing acute T cell activation. In contrast, in regulatory T cells AP-1 is replaced by Foxp3, resulting in a NFAT:Foxp3 complex that directs down-regulations of effector functions and initiates a suppressor program to maintain T cell tolerance (Wu et al., 2006). Interestingly, this model could be extended to also explain the role of Foxp1 in regulating the quiescence of naïve T cells. Here, Foxp1 might interact with NFAT proteins to prevent T cell activation upon self-antigen:MHC engagement in the periphery. Loss of Foxp1 thereby would result in the induction of an activatory T cell program, which eventually would lead to the generation of effector or memory T cells in the absence of their cognate antigen.

The regulation of Foxp1 itself and how the expression of the transcription factor is maintained at low levels in the effector/memory T cell compartment is not clear yet. One can hypothesize that epigenetic modifications of the Foxp1 locus - which are introduced during the effector phase of an acutely activated T cell - might silence gene transcription. Also, mechanisms of post-transcriptional regulation of Foxp1 might play a role in T cells comparable to miR-34a in the B cell lineage (Ackermann et al., 2010). However, the exact mechanisms of this regulation remain to be investigated.

6.3 Foxp1-deficient T cells exert effector/memory functions

After the initial phenotypic characterization of Foxp1-deficient T cells, functional *in vitro* assays of isolated T helper cells confirmed the effector/memory T cell phenotype in Foxp1^{cKO} CD4 Cre mice. Foxp1-deficient T cells were easily stimulated by anti-CD3 antibodies to produce IL-2 without any additional cross-linking of the TCR (Figure 17). This behaviour was observed in both effector and memory type T cells, as they execute their function independent of any further co-stimulation, which in contrast would be necessary for antigen-inexperienced naïve T cells. Additionally, Foxp1-deficient CD4+ T cells were able to produce vast amounts of a variety of cytokines upon stimulation in addition to IL-2, like IFNγ, IL-4, TNF, IL-17, and GM-CSF (Figure 18A). Even though *ex vivo* stimulation of splenic T cells provided evidence of Th1-skewing in Foxp1^{cKO} CD4 Cre mice, only 7% of all CD4+ T cells were readily producing IFNγ (Figure 18B). Enhanced Th1-skewing can be correlated with ongoing inflammatory responses, but no overt inflammation was present in Foxp1^{cKO} CD4

Cre mice. Therefore, one can speculate that low levels of inflammatory cytokines produced by the effector/memory T cells themselves drive a skewing process towards Th1 in a positive feedback loop. Even though Th1-skewing did not seem to contribute to systemic inflammation, it is nevertheless possible that the elevated abundance of Th1-cytokines, like IFNγ, contributed to the observed splenomegaly.

The immediate effect of Foxp1-deficiency on the overshooting IL-2 secretion of CD4+ T cells in Foxp1^{cKO} CD4 Cre mice was additionally confirmed by an oligo pull-down experiment (Figure 19). Here, direct binding of endogenous Foxp1 isolated from CD4+ T cells to the murine IL-2 distal promoter confirmed previous observations by Wu et al., who observed binding of Foxp subfamily members to an antigen receptor response element in the IL-2 promoter/enhancer (ARRE2) site in the presence of NFAT (Wu et al., 2006). Similarly, Foxp1A binding sites in SV40 and human IL2 promoter regions were reported to mediate repression of the promoters (Wang, 2003). As several critical T cell cytokines were strongly expressed by Foxp1-deficient CD4+ T cells upon stimulation, one can hypothesize a general mechanism of Foxp1 acting as a transcriptional repressor of T cell cytokines.

Further functional assays on isolated T helper cells from Foxp1^{cKO} CD4 Cre mice showed strongly increased proliferation upon stimulation with anti-CD3 antibodies (Figure 20). The enhanced response emphasizes the effector/memory character of T cells in Foxp1^{cKO} CD4 Cre mice, as strong proliferation was achieved by triggering the TCR without additional co-stimulation through CD28. Under physiological conditions, the rapid activation of memory T cells after reencounter of their cognate antigen ensures a proper memory response. According to Jameson et al., memory T cells are of greater longevity, but show diminished proliferation in comparison to naïve T cells (Jameson and Masopust, 2009). In this idealized view on memory T cell features, effector memory T cells exhibit both longevity and proliferation rates to a lesser degree than central-memory T cells. Even though Foxp1-deficient CD4+ T cells show increased proliferation upon anti-CD3 stimulation, the proliferation response towards a mixed stimulation of anti-CD3 and anti-CD28 resembled almost the one observed in control CD4+ T cells. This indicates that T cells found in Foxp1^{cKO} CD4 Cre mice are more sensitive to suboptimal TCR ligation and show a lower activation threshold - as expected from cells in the effector or memory compartment - but do not exhibit stronger proliferation upon full stimulation.

In vitro cultured CD4+ T cells isolated from Foxp1^{cKO} CD4 Cre mice interestingly showed diminished survival under unstimulated conditions (Figure 21). On first sight, the impaired

survival is not in line with the above-mentioned model of memory T cells showing increased longevity. Still, this model is referring to the situation observed *in vivo* and cannot be compared to the non-physiological conditions *in vitro*. As mentioned earlier, memory T cells strongly depend on IL-7 and IL-15 signals as survival factors that eventually lead to upregulation of anti-apoptotic proteins, whereas they are less dependent on peptide-MHC signals (Surh and Sprent, 2008). Absence of both IL-7 and IL-15 therefore has a stronger impact on memory-type T cells than on a classical T cell compartment found in control animals and might therefore explain the results obtained from the *in vitro* culture. Further stimulation of CD4+ T cells from controls and Foxp1^{cKO} CD4 Cre mice with anti-CD3/CD28 antibodies showed largely comparable survival behaviour in vitro (Figure 21).

The addition of IL-2 to the *in vitro* culture of CD4+ T cells isolated from Foxp1^{cKO} CD4 Cre mice initially resembled the unstimulated condition and was marked by decreasing percentages of living cells, but a reverse trend became obvious after 3 days (Figure 21). Additional analysis showed an expansion of Tregs in the presence of IL-2 (Figure 22). This observation is of great interest as Tregs are generally described to be hypo-proliferative and *in vitro* expansion of them can usually be achieved only by cross-linking TCR-stimulation, co-stimulatory signals, and additional IL-2 administration (Tang et al., 2004; Walker et al., 2003). In general, Tregs are expressing the high-affinity IL-2 receptor CD25 and compete with neighbouring T cells for IL-2, which acts in an autocrine and paracrine manner. Even though Tregs are dependent on IL-2 for their development and protective function, they do not show extensive *in vitro* proliferation upon treatment with IL-2 alone (Furtado et al., 2002; Josefowicz et al., 2012). In the case of Foxp1^{cKO} CD4 Cre mice, Tregs undergo proliferation in an antigen-independent fashion, being only dependent on exogenous IL-2 addition. This finding suggests that Foxp1 regulates Treg proliferation and its loss overcomes their hypo-proliferative condition.

In line with the increased proliferation of conventional and regulatory T cells from Foxp1-deficient animals, Feng et al. reported a role for Foxp1 in negative regulation of MEK and Erk kinases in double-positive thymocytes and mature CD8+ T cells (Feng et al., 2011). The authors state that the Foxp1-regulated activity of MEK and Erk is involved in proliferation of CD8+ T cells upon stimulation with IL-7. Interestingly, the downstream signalling cascades of both cytokines IL-2 and IL-7 eventually lead to activation of Stat5 (Lin and Leonard, 2000). Whereas IL-7 promotes Stat5 activation in mature CD8+ T cells expressing CD127, a comparable outcome is achieved in Tregs by addition of IL-2. It can therefore be hypothesized that the observed proliferation of Tregs in an *in vitro* culture of Foxp1^{cKO} CD4

Cre CD4+ T cells is related to the observation described for mature CD8+ T cells. Loss of Foxp1 thereby could overcome a proliferative block, which normally prevents Tregs from extensive expansion upon contact with IL-2. In line with this observation, Treg numbers in Foxp1^{cKO} CD4 Cre mice are strongly increased in lymphoid organs, suggesting locally elevated IL-2 concentrations presumably secreted by the massive effector/memory T cell compartment (Figure 11). Finally, it is possible, that the proliferation of Tregs relies not only on IL-2, but also on other cytokines produced by the Foxp1-deficient T helper cells in cell culture *per se* or upon IL-2 stimulation.

Even though Foxp1^{cKO} CD4 Cre mice lack naïve T cells, no overt autoimmunity was observed in theses animals. However, Foxp1^{cKO} CD4 Cre mice were found to succumb slightly earlier than animals in the control group (Figure 15). Still, both groups reached a median lifespan of about two years and no acute activation of isolated lymphocytes was observed in Foxp1^{cKO} CD4 Cre mice at any time whatsoever. Also, auto-antibodies were undetectable in the serum obtained from one year old Foxp1^{cKO} CD4 Cre mice (Figure 16). Together, these observations did not indicate a direct involvement of Foxp1 in systemic autoimmunity mediated by loss of the transcription factor in T cells. However, the overall change in T cell phenotype and function, as well as the complete loss of naïve T cells might impair adaptive immune responses and processes of tumour immunosurveillance, thereby potentially contributing to the observed reduction in lifespan.

6.4 T cell apoptosis or T cell migration?

The reduced percentage of T cells in Foxp1^{cKO} CD4 Cre mice together with the diminished survival of CD4+ T cells in culture evoked the notion of an increased apoptosis rate in Foxp1-deficient T cells. As mentioned earlier, memory T cells strongly depend on IL-7 which promotes expression of anti-apoptotic proteins, like Bcl-2 and Mcl-1. However, breeding Foxp1^{cKO} CD4 Cre mice to a vav-BCL2 transgenic mouse strain failed to ameliorate the reduction of T cells in peripheral lymphoid organs (Figure 21). Exogenous expression of Bcl-2 still resulted in a drop of total T cell population, mainly because of a drastic reduction of CD8+ T cells. In contrast, the T helper cell compartment remained steady due to a strong expansion of regulatory T cells of up to 50 % of all T helper cells in Foxp1^{cKO} CD4 Cre vav-Bcl2 transgenic mice. Interestingly, survival assays with CD4+ T cells isolated from Foxp1^{cKO} CD4 Cre vav-Bcl2 animals revealed a block of apoptosis by overexpression of Bcl2 *in vitro*. This absence of cell death in CD4+ T cells from Foxp1^{cKO} CD4 Cre vav-Bcl2 mice

indicated a clear anti-apoptotic function of Bcl-2 overexpression. Together, the results from the *in vivo* cell distribution and T cell survival *in vitro* exclude a Bcl2-dependent apoptosis as a major cause of T cell loss in Foxp1^{cKO} CD4 Cre mice. Therefore, it is unlikely that shortage of IL-7 promotes cell death *in vivo*, as this should have been compensated by Bcl-2 overexpression. Since apoptosis can be partially ruled out as a major cause for the loss of peripheral T cells in Foxp1^{cKO} CD4 Cre mice, it is intriguing to speculate that altered migratory behaviour of T cells resulted in this phenotype. Indeed, effector-memory T cells, phenotypically constituting the majority of CD4+ T cells in Foxp1^{cKO} CD4 Cre mice, have the capacity to enter non-lymphoid tissues. It is therefore likely, that the observed loss of CD4+ T cells in Foxp1^{cKO} CD4 Cre mice was due to an altered migratory behaviour.

Besides their cellular characteristics, Foxp1^{cKO} CD4 Cre vav-Bcl2 transgenic mice showed a significantly reduced median survival time, compared to vav-Bcl2 animals (Figure 23). Egle et al. previously reported a reduced lifespan in vav-Bcl2 mice associated with the development of follicular B cell lymphoma and excessive germinal centre formation (Egle et al., 2004). Additionally, the authors claim that CD4+ T cells are critical in the exaggerated formation of germinal centres in vav-Bcl2 tg mice. It is therefore likely that the altered T cell phenotype observed in Foxp1^{cKO} CD4 Cre animals contributes to the germinal centre hyperplasia by providing additional survival signals to B cells in their vicinity. In addition, the reduced survival observed in Foxp1^{cKO} CD4 Cre vav-Bcl2 tg mice might also support the hypothesis that Foxp1^{cKO} CD4 Cre mice suffer from reduced tumour-immunity and are unable to prevent the development of follicular B cell lymphoma.

6.5 Foxp1 in Foxp3+ regulatory T cells

As discussed in chapter 6.2, Foxp1-deficiency in T cells resulted in a significant increase of Tregs in spleen and lymph nodes, but not in the thymus (Figure 9). In addition, Tregs proliferated in an IL-2 supplemented *in vitro* culture of T helper cells isolated from Foxp1^{cKO} CD4 Cre animals (Figure 22). Taken together, these results suggested a role for Foxp1 in Treg homeostasis and proliferation. However, analysis of Foxp1^{cKO} Foxp3 Cre mice neither revealed significant changes in Treg numbers nor showed alterations in the effector/memory T cell compartment. From this it can be concluded, that loss of Foxp1 does not largely affect Treg homeostasis and mechanisms of peripheral tolerance. The results rather suggest that the *in vivo* expansion of Tregs in Foxp1^{cKO} CD4 Cre animals is triggered by the loss of naïve T cells and the vast presence of effector/memory T cells than by a cell-intrinsic mechanism in

Tregs. As Foxp1 acts as a direct transcriptional repressor of IL-2 it might be possible that its loss results in continuous low level IL-2 production by the prevalent T cells. Therefore, one can hypothesize that effector/memory T cells contribute to locally elevated levels of IL-2 and thereby drive the expansion of Tregs. However, one has to keep in mind that IL-2 stimulation alone is insufficient to drive Treg expansion in wildtype CD4+ T cells. Therefore, it is likely that either a second additional factor expressed in cultures of CD4+ T cells from Foxp1^{cKO} CD4 Cre animals or an intrinsic change in Foxp1-deficient Tregs is needed for their expansion.

Song et al. recently demonstrated heterodimerization of Foxp3 with Foxp1 and suggested a competition between Foxp1/Foxp3 and Foxp3/Foxp3 dimers which might affect the repressor activity of Foxp3 complexes (Song et al., 2012). In contrast to this assumption, the present data obtained from Foxp1^{cKO} Foxp3 Cre mice argues against a prominent role of Foxp1/Foxp3 heterodimers in the repressor activity of regulatory T cells, as peripheral tolerance was largely unaffected by the specific loss of Foxp1 in regulatory T cells. However, it cannot be excluded that Foxp1/Foxp3 heterodimers are of relevance in other situations than steady-state.

The observations in Foxp1^{cKO} CD4 Cre and Foxp1^{cKO} Foxp3 Cre mice suggest that Foxp1 is necessary for the maintenance of naïve T cells, but dispensable for T cells which have already undergone a terminal differentiation step towards regulatory T cells. Another reason for the unobtrusive phenotype of Foxp1^{cKO} Foxp3 Cre mice might be the expression of Foxp3 itself and its similarity to Foxp1. The master-regulator of regulatory T cells could potentially compensate for the loss of the related forkhead-family member Foxp1 and might thereby indicate a redundancy in the action of both transcription factors.

6.6 Foxp1-deficient T cells in an encephalitogenic mouse model

As mentioned earlier, Foxp1-deficiency in T cells results in complete loss of naïve T cells and a conversion to effector/memory T cells indicating a master-regulatory role for Foxp1 in maintaining T cell quiescence. Surprisingly, so far no overt autoimmunity was detected in Foxp1^{cKO} CD4 Cre mice suggesting that Foxp1-deficiency has no direct impact on mechanisms of central and peripheral T cell tolerance.

However, abrogation of quiescence in T cells is characteristic of autoimmune diseases, and can be detected e.g. in patients at high risk for multiple sclerosis after an initial neurological

event (Corvol et al., 2008). Corvol et al. demonstrated that Tob1, a critical regulator of cell proliferation and quiescence, was down-regulated in T cells of multiple sclerosis patients. In a recent study, the same group investigated $Tob1^{-/-}$ mice after induction of EAE and observed a aggravated outcome of the disease and aberrant immune responses (Schulze-Topphoff et al., 2013).

To similarly investigate the role of Foxp1 in T cells in an autoimmune-prone context, $Foxp1^{cKO}$ CD4 Cre mice were bred to 2D2 mice, expressing a MOG-specific transgenic TCR, which were generated as a model system for multiple sclerosis (Bettelli et al., 2003). Besides a complete shift to the memory T cell compartment and a general reduction in peripheral T cells, $Foxp1^{cKO}$ CD4 Cre 2D2 mice developed severe neurological symptoms (Figure 28, 29). In contrast to 2D2 mice, which have been found to develop paralysis in only about 4% of mice, all $Foxp1^{cKO}$ CD4 Cre 2D2 mice showed neurological manifestations (Figure 29) (Bettelli et al., 2003). In about 60% of $Foxp1^{cKO}$ CD4 Cre 2D2 mice, the disease onset was observed early at about 5-6 weeks of age, while the residual mice developed symptoms within half a year. Mice that showed symptoms at an early age also exhibited weight loss, potentially indicating additional auto-inflammation of the gastrointestinal tract leading to systemic wasting and cachexia.

Analysis of CNS-infiltrating lymphocytes revealed increased T cell numbers in brains of $Foxp1^{cKO}$ CD4 Cre 2D2 mice that exhibited an activated phenotype (Figure 30). From this it can be concluded, that Foxp1-deficient T cells were largely functional *in vivo*, as they were able to elicit autoimmunity in a 2D2 context. While MOG-specific 2D2 T cells alone were hardly capable of provoking neurological symptoms like paralysis in mice (Bettelli et al., 2003), T cells from $Foxp1^{cKO}$ CD4 Cre 2D2 mice elicited spontaneous neuropathology with rapid onset. Since ablation of Foxp1 resulted in excessive differentiation of effector/memory T cells, their presence might be of critical importance in the course of T cell-driven neuroinflammation. Of note, the neurological manifestations observed in $Foxp1^{cKO}$ CD4 Cre 2D2 mice greatly differed from the one observed in affected 2D2 animals as no signs of full-blown paralysis were observed and tail tonus was retained. In contrast, $Foxp1^{cKO}$ CD4 Cre 2D2 mice exhibited a neurological disorder which was dominated by clasping and severe spasms of the hindlimbs. The molecular cause of this discrepancy remains elusive and has to be addressed in future studies. One can hypothesize a role of Foxp1 in the regulation of chemokine receptors and integrins, which mediate the migration of T cells to specific sites of the body. Moreover, several chemokine and integrin receptors, such as CCR6 and LFA-1, have been implicated to play a crucial role in multiple sclerosis and EAE (Emma H Wilson,

2010; Reboldi et al., 2009; Rothhammer et al., 2011). Therefore it will be highly interesting to investigate the expression of such receptors in Foxp1-deficient T cells. The reason for the difference in quantity and quality of neurological symptoms might as well depend on the mere numbers of auto-reactive effector/memory T cells present in Foxp1^{cKO} CD4 Cre 2D2 mice. Even though all T cells in the 2D2 mouse strain are auto-reactive, many CD4+ T cells are of naïve nature and are not capable of eliciting an effector response upon encountering their cognate antigen, but rather become anergic. In contrast, it is likely that in Foxp1^{cKO} CD4 Cre 2D2 mice CD4+ T cells immediately produce cytokines and recruit immune cells to the site of inflammation, which eventually cause neuroinflammation and potentially demyelination after entering the CNS.

In summary, Foxp1^{cKO} CD4 Cre 2D2 mice constitute a new mouse model for spontaneous atypical EAE-like neuropathology and are of great interest to study T cell functions in a neuroimmunological context. Follow-up experiments will focus on the exact sites of neuroinflammation and the molecular mechanisms that underlie the altered neuropathological outcome. Altogether, this novel EAE-like model might contribute to a better understanding of the role effector and memory T cells play in the pathogenesis of autoimmune diseases like multiple sclerosis.

7 Summary and Outlook

The present work provides novel insights into the role of the transcription factor Foxp1 in T cell development and function. In a conditional knock-out approach Foxp1 was specifically ablated in T cells. The ablation resulted in a complete transition of naïve T cells to the effector/memory T cell compartment, starting at the level of single-positive thymocytes during development. Notably, Foxp1-deficient T cells not only phenotypically but also functionally resembled effector/memory T cells. This included the ability to become activated in the absence of co-stimulation and resulted in an increased production of inflammatory cytokines. Interestingly, Foxp1 conditional knock-out mice showed elevated levels of regulatory T cells. However, Treg-specific ablation of Foxp1 resulted in no overt immunophenotypic changes. To further test the function of memory T cell *in vivo*, Foxp1 conditional knock-out CD4 Cre mice were bred to a encephalitogenic 2D2 background, expressing a MOG-specific TCR. Animals with this genetic combination showed an early onset of atypical neuropathology and in contrast to the 2D2 model, succumbed within a few months, suggesting a pathogenic role of the excessively present effector/memory T cells in the Foxp1-deficient background. In conclusion, I here describe Foxp1 as a novel master-regulator of effector and memory T cell differentiation, whose presence is critical for the maintenance of a naïve T cell stage in CD4+ and CD8+ T cells.

The importance of Foxp1 in T cell differentiation processes is of great interest for the field of T cell biology. Until recently, only few molecular factors were known to interfere with the transition of naïve to effector and memory T cells, without disturbing central and peripheral tolerance mechanisms. Therefore, future investigations will have to address the exact molecular mechanisms by which Foxp1 is regulated and exerts its function. Sharing this rare property, Foxp1 has a great potential to become a target for the generation of specific memory T cells and for clinical applications, ranging from adoptive T cell transfers in cancer therapy over genetically engineered T cells to autologous immune enhancement therapy, and innovative vaccination strategies.

Finally, this work introduces a novel genetic mouse model for multiple sclerosis, as Foxp1-decifient T cells in a 2D2 background spontaneously elicit an EAE-like neuropathology with unusual early onset. Therefore, this mouse model might in the future contribute to a better understanding of the role of effector/memory T cells play in neuroinflammatory diseases.

8 Acknowledgements

First, I would like to thank my supervisor Prof. Dr. med. Jürgen Ruland for providing me with this interesting project and for the opportunity to work in his lab.

I would like to thank all past and present members of the Ruland lab for their support throughout the years that we spent together.

Many thanks I owe to Dr. Stefan Wanninger, Dr. Nathalie Knies, Dr. med. Michael Bscheider, Dr. Olaf Groß, Dr. Andreas Gewies, Drs. Katrin and Marc Schweneker for their constant support and friendship.

Especially, I need to express my gratitude to Verena Laux, Kristina Brunner, and Tanja Ruff who were a great technical support in many lab situations.

Furthermore, I would like to acknowledge Dr. Thomas Patzelt who generated the Foxp1 conditional knock-out mouse strain.

I also would like to thank PD Dr. Daniel Krappmann, Prof. Dr. Vigo Heissmeyer, and Prof. Dr. Thorsten Buch for critical discussions.

Many thanks to Dr. Franziska Petermann and Prof. Dr. med. Thomas Korn for scientific input to the neuroimmunological part of this work.

Additionally, I would like to thank the members of AG Jost, AG Groß, AG Haas/Poeck, AG Duyster, AG Heissmeyer and AG Keller.

I also have to express my great gratitude to my parents who always supported me during my studies and the time of my PhD thesis.

Many thanks to Dr. Sebastian Warth for critical input to my work and the great time we spent together in Munich.

Finally, I would like to thank Fiona Müllner, who is a constant source of energy and love to me and greatly supported me during this thesis.

9 Publications

Manuscripts published during this thesis:

1. *Gewies, A., ***Gorka, O.,** Bergmann, H., Pechloff, K., Petermann, F., Jeltsch, K.M., Rudelius, M., Kriegsmann, M., Weichert, W., Horsch, M., Beckers, J., Wurst, W., Heikenwälder, M., Korn, T., Heissmeyer, V., Ruland, J. *Uncoupling Malt1 threshold function from paracaspase activity results in destructive autoimmune inflammation.* **Cell Reports,** 9(4):1292-305. doi: 10.1016/j.celrep.2014.10.044 (*authors contributed equally)

2. **Gorka, O.**, Wanninger, S., Ruland, J. (2014). *Detection of NF-κB pathway activation in T helper cells.* **Methods in Molecular Biology**

3. Sledzinska, A., Hemmers, S., Mair, F., **Gorka, O.**, Ruland, J., Fairbarn, L., Nissler, A., Müller, W., Waisman, A., Becher, B., Buch T. (2013). *TGF-β is required for CD4+ T cell homeaostasis but dispensable for regulatory T cell function.* **PLoS Biology,** 11(10): e1001674. doi:10.1371/journal.pbio.1001674

4. Jabara, H. H., Ohsumi, T., Chou, J., Massaad, M. J., Benson, H., Megarbane, A., Chouery, E., Mikhael, R., **Gorka, O.**, Gewies, A., Portales, P., Nakayama, T., Hosokawa, H., Revy, P., Herrod, H., Le Deist, F., Lefranc, G., Ruland, J., Geha, R.S. (2013). A homozygous mucosa-associated lymphoid tissue 1 (MALT1) mutation in a family with combined immunodeficiency. **The Journal of allergy and clinical immunology,** 132(1), 151–158.

5. Jankovic, D., Ganesan, J., Bscheider, M., Stickel, N., Weber, F. C., Guarda, G., Follo, M., Pfeifer, D., Tardivel, A., Ludigs, T., Bouazzaoui, A., Kerl, K., Fischer, J.C., Haas, T., Schmitt-Gräff, A., Manoharan, A., Müller, L., Finke, J., Martin, S.F., **Gorka, O.,** Peschel, C., Ruland, J., Idzko, M., Duyster, J., Holler, E., French, L.E., Poeck, H., Contassot, E., Zeiser, R. (2013). *The Nlrp3 inflammasome regulates acute graft-versus-host disease.* **Journal of Experimental Medicine,** doi: 10.1084/ jem.20130084

6. Kratzat, S., Nikolova, V., Miething, C., Hoellein, A., Schoeffmann, S., **Gorka, O**., Pietschmann, E., Illert, A., Ruland, J., Peschel, C., Nilsson, J., Duyster, J., Keller, U. (2012). *Cks1 is required for tumor cell proliferation but not sufficient to induce hematopoietic malignancies.* **PloS one**, 7(5): e37433. doi:10.1371/journal.pone.0037433

7. Schweneker, K., **Gorka, O.**, Schweneker, M., Poeck, H., Tschopp, J., Peschel, C., Ruland, J., Groß, O (2012). *The mycobacterial cord factor adjuvant analogue trehalose-6,6'-dibehenate (TDB) activates the Nlrp3 inflammasome.* **Immunobiology**, 218(4), 664–673. doi:10.1016/ j.imbio.2012.07.029

Manuscripts in preparation:

1. **Gorka, O.**, Patzelt, TC., Petermann, F., Gewies A., Korn, T., Ruland, J., *Foxp1 regulates memory T cell differentiation and controls tolerance in an encephalitogenic model.*

2. Patzelt, TC., **Gorka O.,** Gewies A., Ruland, J., *Foxp1 is required for the formation and maintenance of an intact B cell compartment.*

10 Abbreviations

°C	Degree celsius
A	Alanine
ABC-DLBCL	Activated B cell-type Diffuse Large B cell lymphoma
ANA	Anti-nuclear antibodies
APC	Allophycocyanin
APC-Cy7	Allophycocyanin-Cyanine7
BAC	Bacterial artificial chromosome
Bcl2	B cell lymphoma 2
bp	Base pairs
C	Cytosine
Ca^{2+}	Calcium
CD	Cluster of differentiation
cDNA	Complementary DNA
CFSE	Carboxyfluorescein succinimidyl ester
cKO	Conditional knock-out
CNS	Central nervous system
Cre	Cre recombinase
DAG	Diacyl-glycerol
DLBCL	Diffuse Large B cell lymphoma
DMSO	Dimethyl sulfoxide
DN	Double-negative thymocytes
DNA	Deoxyribonucleic acid
dNTP	Deoxynucleotide mix
DP	Double-positive thymocytes
dsDNA	Double-stranded DNA
EAE	Experimental autoimmune encephalomyelitis

EDTA	Ethylenediaminetetraacetic acid
EGFP	Enhanced green fluorescent protein
ENA	Extractable nuclear antigens
ESC	Embryonic stem cell
FACS	Fluorescence activated cell sorting
FCS	Foetal calf serum
FITC	Fluorescein isothiocyanate
Fox	Forkhead-box
FSC	Forward scatter
fwd	Forward
G	Guanine
GC-DLBCL	Germinal-centre Diffuse Large B cell lymphoma
GFP	green fluorescent protein
GM-CSF	Granulocyte macrophage colony-stimulating factor
HEV	High endothelial venules
HRP	Horseradish peroxidase
h/hs	Hour/Hours
IFN	Interferon
Ig	Immunoglobulin
IL	Interleukin
Iono	Ionomycin
IP_3	Inositoltriphosphate
IPEX	Polyendocrinopathy, enteropathy X-linked
ITAM	Immunoreceptor tyrosine-based activation motifs
Jak	Janus kinase
kDa	Kilo Dalton
KLRG1	Killer cell lectin-like receptor subfamily G member 1

LAT	Linker of activated T cells
LKLF	Lung Kruppel-like factor
Mcl1	Myeloid cell leukemia sequence 1
mg	Milligramm
MHC	Major-Histocompatibility-complex
min	Minute
ml	Milliliter
mM	Millimolar
mm	Millimeter
MOG	Myelin oligodendrocyte glycoprotein
mut	Mutant
NFAT	Nuclear factor of activated T cells
NFκB	nuclear factor 'kappa-light-chain-enhancer' of activated B cells
ng	Nanogramm
NHL	Non-Hogkins lymphoma
NK	Natural killer cells
nM	Nanomolar
nm	Nanometer
oligo	Oligonucleotide
p.b.	Plate-bound
PBS	Phosphate buffered saline
PCR	Polymerase chain reaction
PE	Phycoerythrin
PE-Cy5	Phycoerythrin-Cyanine5
PE-Cy7	Phycoerythrin-Cyanine7
PerCP	Peridinin Chlorophyll
PIP_2	Phosphatidylinositol-4,5-bisphosphate

PMA	Phorbol-12-myristat-13-acetat
poly-Q	Poly-glutamine
qPCR	Quantitative polymerase chain reaction
rev	Reverse
RNA	Ribonucleic acid
SDS	Sodium dodecyl sulfate
sec	Second
SEM	Standard error of the mean
SSC	Sideward scatter
ssDNA	Single-strand DNA
T	Thymine
TCR	T cell receptor
tg	Transgene
TNF	Tumour necrosis factor
Treg	Regulatory T cell
V	Volt
v/v	Volume per volume
w/v	Weight per volume
wt	Wildtype
ZAP70	Zeta-chain-associated protein kinase of 70 kDa
µg	Microgramm
µl	Microliter
µM	Micromolar

11 Figure index

Figure 1	Simplified overview of T cell receptor signalling pathways.	18
Figure 2	Crystal structure of Foxp2 fork-head domain bound to DNA.	23
Figure 3	Multiple sequence alignments of Foxp subfamily members.	24
Figure 4	Phylogeny of Foxp subfamily members.	26
Figure 5	Reduced Foxp1 expression in memory T cells.	49
Figure 6	Differential Foxp1 expression in thymocytes subset.	50
Figure 7	Generation and validation of a T cell-specific Foxp1 conditional knock-out mouse.	52
Figure 8	Mild splenomegalia in Foxp1^{cKO} CD4 Cre mice.	54
Figure 9	Foxp1^{cKO} CD4 Cre mice showed altered immune cell distributions.	55
Figure 10	Foxp1^{cKO} CD4 Cre thymocytes showed altered expression pattern.	56
Figure 11	CD4+ T cells of Foxp1^{cKO} CD4 Cre mice showed a memory phenotype.	58
Figure 12	Differential marker expression of CD4+ T helper cells in Foxp1^{cKO} CD4 Cre mice.	59
Figure 13	CD8+ T cells of Foxp1^{cKO} CD4 Cre mice showed a memory phenotype.	60
Figure 14	Differential marker expression of CD8+ cytotoxic T cells in Foxp1^{cKO} CD4 Cre mice.	61
Figure 15	Foxp1^{cKO} CD4 Cre mice succumbed earlier than control animals.	63
Figure 16	Absence of auto-antibodies in older Foxp1^{cKO} CD4 Cre mice.	64
Figure 17	Subtle stimulation triggered massive IL-2 production in CD4+ T cells of Foxp1^{cKO} CD4 Cre mice.	65
Figure 18	Excessive cytokine production by stimulated CD4+ T cells from Foxp1^{cKO} CD4 Cre mice.	66
Figure 19	Foxp1 bound to the IL-2 promoter.	68
Figure 20	Loss of Foxp1 promoted proliferation of CD4+ T cells from Foxp1^{cKO} CD4 Cre mice.	69
Figure 21	Foxp1-deficient T cells showed reduced survival *in vitro*.	71
Figure 22	*In vitro* expansion of regulatory T cells upon IL-2 treatment of CD4+ T cells from Foxp1^{cKO} CD4 Cre mice.	72

Figure 23 Immune cell distribution of Foxp1^{cKO} CD4 Cre vav-Bcl2 transgenic mice. 74

Figure 24 *In vitro* survival of CD4+ T cells from Foxp1^{cKO} CD4 Cre vav-Bcl2 mice. 75

Figure 25 Foxp1^{cKO} CD4 Cre vav-Bcl2 mice succumbed earlier than vav-Bcl2 control animals. 77

Figure 26 Immune cell phenotype in Foxp1^{cKO} Foxp3 Cre mice. 79

Figure 27 Minor changes in T cell compartments of Foxp1^{cKO} Foxp3 Cre mice. 80

Figure 28 Immune cell distribution of Foxp1^{cKO} CD4 Cre 2D2 mice. 81

Figure 29 Foxp1^{cKO} CD4 Cre 2D2 mice developed rapid spontaneous neuropathology. 82

Figure 30 CNS-infiltration of lymphocytes in Foxp1^{cKO} CD4 Cre 2D2 mice. 83

Figure 31 Model of Foxp1 limiting the memory T cell pool. 90

12 Bibliography

Ackermann, S., Kocak, H., Hero, B., Ehemann, V., Kahlert, Y., Oberthuer, A., Roels, F., Theißen, J., Odenthal, M., Berthold, F., et al. (2010). MicroRNA-34a Perturbs B Lymphocyte Development by Repressing the Forkhead Box Transcription Factor Foxp1. Immunity *14*, 1–12.

Ahmed, R., Bevan, M.J., Reiner, S.L., and Fearon, D.T. (2009). The precursors of memory: models and controversies. Nat Rev Immunol *9*, 662–668.

Anderson, M.S., Venanzi, E.S., Klein, L., Chen, Z., Berzins, S.P., Turley, S.J., Boehmer, von, H., Bronson, R., Dierich, A., Benoist, C., et al. (2002). Projection of an immunological self shadow within the thymus by the aire protein. Science *298*, 1395–1401.

Banham, A.H., Beasley, N., Campo, E., Fernandez, P.L., Fidler, C., Gatter, K., Jones, M., Mason, D.Y., Prime, J.E., Trougouboff, P., et al. (2001). The FOXP1 winged helix transcription factor is a novel candidate tumor suppressor gene on chromosome 3p. Cancer Res. *61*, 8820–8829.

Banham, A.H., Connors, J.M., Brown, P.J., Cordell, J.L., Ott, G., Sreenivasan, G., Farinha, P., Horsman, D.E., and Gascoyne, R.D. (2005). Expression of the FOXP1 transcription factor is strongly associated with inferior survival in patients with diffuse large B-cell lymphoma. Clin. Cancer Res. *11*, 1065–1072.

Barrans, S.L., Fenton, J.A.L., Banham, A., Owen, R.G., and Jack, A.S. (2004). Strong expression of FOXP1 identifies a distinct subset of diffuse large B-cell lymphoma (DLBCL) patients with poor outcome. Blood *104*, 2933–2935.

Basso, K., and Dalla-Favera, R. (2010). BCL6: master regulator of the germinal center reaction and key oncogene in B cell lymphomagenesis. Adv. Immunol. *105*, 193–210.

Benayoun, B.A., Caburet, S., and Veitia, R.A. (2011). Forkhead transcription factors: key players in health and disease. Trends Genet. *27*, 224–232.

Bennett, C.L., Christie, J., Ramsdell, F., Brunkow, M.E., Ferguson, P.J., Whitesell, L., Kelly, T.E., Saulsbury, F.T., Chance, P.F., and Ochs, H.D. (2001). The immune dysregulation, polyendocrinopathy, enteropathy, X-linked syndrome (IPEX) is caused by mutations of FOXP3. Nat. Genet. *27*, 20–21.

Best, J.A., Blair, D.A., Knell, J., Yang, E., Mayya, V., Doedens, A., Dustin, M.L., Goldrath, A.W., Monach, P., Shinton, S.A., et al. (2013). Transcriptional insights into the CD8+ T cell response to infection and memory T cell formation. Nature Immunology *14*, 404–412.

Bettelli, E., Dastrange, M., and Oukka, M. (2005). Foxp3 interacts with nuclear factor of activated T cells and NF-kappa B to repress cytokine gene expression and effector functions of T helper cells. Proc. Natl. Acad. Sci. U.S.a. *102*, 5138–5143.

Bettelli, E., Pagany, M., Weiner, H.L., Linington, C., Sobel, R.A., and Kuchroo, V.K. (2003). Myelin oligodendrocyte glycoprotein-specific T cell receptor transgenic mice develop spontaneous autoimmune optic neuritis. J. Exp. Med. *197*, 1073–1081.

Brown, P.J., Ashe, S.L., Leich, E., Burek, C., Barrans, S., Fenton, J.A., Jack, A.S., Pulford, K., Rosenwald, A., and Banham, A.H. (2008). Potentially oncogenic B-cell activation-induced smaller isoforms of FOXP1 are highly expressed in the activated B cell-like subtype of DLBCL. Blood *111*, 2816–2824.

Brunkow, M.E., Jeffery, E.W., Hjerrild, K.A., Paeper, B., Clark, L.B., Yasayko, S.A., Wilkinson, J.E., Galas, D., Ziegler, S.F., and Ramsdell, F. (2001). Disruption of a new

forkhead/winged-helix protein, scurfin, results in the fatal lymphoproliferative disorder of the scurfy mouse. Nat. Genet. *27*, 68–73.

Buckley, A.F., Kuo, C.T., and Leiden, J.M. (2001). Transcription factor LKLF is sufficient to program T cell quiescence via a c-Myc-dependent pathway. Nature Immunology *2*, 698–704.

Bürckstümmer, T., Baumann, C., Blüml, S., Dixit, E., Dürnberger, G., Jahn, H., Planyavsky, M., Bilban, M., Colinge, J., Bennett, K.L., et al. (2009). An orthogonal proteomic-genomic screen identifies AIM2 as a cytoplasmic DNA sensor for the inflammasome. Nature Immunology *10*, 266–272.

Carlsson, P., and Mahlapuu, M. (2002). Forkhead transcription factors: key players in development and metabolism. Dev. Biol. *250*, 1–23.

Ceredig, R., and Rolink, T. (2002). A positive look at double-negative thymocytes. Nat Rev Immunol *2*, 888–897.

Chan, A.C., Dalton, M., Johnson, R., Kong, G.H., Wang, T., Thoma, R., and Kurosaki, T. (1995). Activation of ZAP-70 kinase activity by phosphorylation of tyrosine 493 is required for lymphocyte antigen receptor function. Embo J. *14*, 2499–2508.

Chan, A.C., Iwashima, M., Turck, C.W., and Weiss, A. (1992). ZAP-70: a 70 kd protein-tyrosine kinase that associates with the TCR zeta chain. Cell *71*, 649–662.

Chan, A.C., Irving, B.A., Fraser, J.D., and Weiss, A. (1991). The zeta chain is associated with a tyrosine kinase and upon T-cell antigen receptor stimulation associates with ZAP-70, a 70-kDa tyrosine phosphoprotein. Proc. Natl. Acad. Sci. U.S.a. *88*, 9166–9170.

Chang, T.-C., Wentzel, E.A., Kent, O.A., Ramachandran, K., Mullendore, M., Lee, K.H., Feldmann, G., Yamakuchi, M., Ferlito, M., Lowenstein, C.J., et al. (2007). Transactivation of miR-34a by p53 broadly influences gene expression and promotes apoptosis. Mol. Cell *26*, 745–752.

Chen, J., Knowles, H.J., Hebert, J.L., and Hackett, B.P. (1998). Mutation of the mouse hepatocyte nuclear factor/forkhead homologue 4 gene results in an absence of cilia and random left-right asymmetry. Journal of Clinical Investigation *102*, 1077–1082.

Chen, W., Jin, W., Hardegen, N., Lei, K.-J., Li, L., Marinos, N., McGrady, G., and Wahl, S.M. (2003). Conversion of peripheral CD4+ CD25− naive T cells to CD4+ CD25+ regulatory T cells by TGF-β induction of transcription factor Foxp3. J. Exp. Med. *198*, 1875–1886.

Chen, Z., Xiao, Y., Zhang, J., Li, J., Liu, Y., Zhao, Y., Ma, C., Luo, J., Qiu, Y., Huang, G., et al. (2011). Transcription factors E2A, FOXO1 and FOXP1 regulate recombination activating gene expression in cancer cells. PLoS ONE *6*, e20475.

Clark, K.L., Halay, E.D., Lai, E., and Burley, S.K. (1993). Co-crystal structure of the HNF-3/fork head DNA-recognition motif resembles histone H5. Nature *364*, 412–420.

Collison, L.W., Workman, C.J., Kuo, T.T., Boyd, K., Wang, Y., Vignali, K.M., Cross, R., Sehy, D., Blumberg, R.S., and Vignali, D.A.A. (2007). The inhibitory cytokine IL-35 contributes to regulatory T-cell function. Nature *450*, 566–569.

Corvol, J.-C., Pelletier, D., Henry, R.G., Caillier, S.J., Wang, J., Pappas, D., Casazza, S., Okuda, D.T., Hauser, S.L., Oksenberg, J.R., et al. (2008). Abrogation of T cell quiescence characterizes patients at high risk for multiple sclerosis after the initial neurological event. Proc. Natl. Acad. Sci. U.S.a. *105*, 11839–11844.

Dasen, J.S., De Camilli, A., Wang, B., Tucker, P.W., and Jessell, T.M. (2008). Hox repertoires for motor neuron diversity and connectivity gated by a single accessory factor, FoxP1. Cell *134*, 304–316.

Derbinski, J., Pinto, S., Rösch, S., Hexel, K., and Kyewski, B. (2008). Promiscuous gene expression patterns in single medullary thymic epithelial cells argue for a stochastic mechanism. Proc. Natl. Acad. Sci. U.S.a. *105*, 657–662.

Egle, A., Harris, A.W., Bath, M.L., O'Reilly, L., and Cory, S. (2004). VavP-Bcl2 transgenic mice develop follicular lymphoma preceded by germinal center hyperplasia. Blood *103*, 2276–2283.

Emma H Wilson, W.W.C.A.H. (2010). Trafficking of immune cells in the central nervous system. J. Clin. Invest. *120*, 1368.

Feng, X., Ippolito, G.C., Tian, L., Wiehagen, K., Oh, S., Sambandam, A., Willen, J., Bunte, R.M., Maika, S.D., Harriss, J.V., et al. (2010). Foxp1 is an essential transcriptional regulator for the generation of quiescent naive T cells during thymocyte development. Blood *115*, 510–518.

Feng, X., Wang, H., Takata, H., Day, T.J., Willen, J., and Hu, H. (2011). Transcription factor Foxp1 exerts essential cell-intrinsic regulation of the quiescence of naive T cells. Nature Immunology *12*, 544–550.

Fenton, J.A.L., Schuuring, E., Barrans, S.L., Banham, A.H., Rollinson, S.J., Morgan, G.J., Jack, A.S., van Krieken, J.H.J.M., and Kluin, P.M. (2006). t(3;14)(p14;q32) results in aberrant expression of FOXP1 in a case of diffuse large B-cell lymphoma. Genes Chromosomes Cancer *45*, 164–168.

Fox, S.B., Brown, P., Han, C., Ashe, S., Leek, R.D., Harris, A.L., and Banham, A.H. (2004). Expression of the forkhead transcription factor FOXP1 is associated with estrogen receptor alpha and improved survival in primary human breast carcinomas. Clin. Cancer Res. *10*, 3521–3527.

Frank, J., Pignata, C., Panteleyev, A.A., Prowse, D.M., Baden, H., Weiner, L., Gaetaniello, L., Ahmad, W., Pozzi, N., Cserhalmi-Friedman, P.B., et al. (1999). Exposing the human nude phenotype. Nature *398*, 473–474.

French, C.A., Groszer, M., Preece, C., Coupe, A.-M., Rajewsky, K., and Fisher, S.E. (2007). Generation of mice with a conditional Foxp2 null allele. Genesis *45*, 440–446.

Furtado, G.C., de Lafaille, M.A.C., Kutchukhidze, N., and Lafaille, J.J. (2002). Interleukin 2 Signaling Is Required for CD4+ Regulatory T Cell Function. Journal of Experimental Medicine *196*, 851–857.

Gabut, M., Samavarchi-Tehrani, P., Wang, X., Slobodeniuc, V., O'Hanlon, D., Sung, H.-K., Alvarez, M., Talukder, S., Pan, Q., Mazzoni, E.O., et al. (2011). An alternative splicing switch regulates embryonic stem cell pluripotency and reprogramming. Cell *147*, 132–146.

Gattinoni, L., Klebanoff, C.A., and Restifo, N.P. (2012). Paths to stemness: building the ultimate antitumour T cell. Nat. Rev. Cancer *12*, 671–684.

Genot, E., and Cantrell, D.A. (2000). Ras regulation and function in lymphocytes. Curr. Opin. Immunol. *12*, 289–294.

Germain, R.N. (2002). T-cell development and the CD4–CD8 lineage decision. Nat Rev Immunol *2*, 309–322.

Giatromanolaki, A., Koukourakis, M.I., Sivridis, E., Gatter, K.C., Harris, A.L., and Banham, A.H. (2006). Loss of expression and nuclear/cytoplasmic localization of the FOXP1 forkhead transcription factor are common events in early endometrial cancer: relationship with estrogen receptors and HIF-1alpha expression. Mod. Pathol. *19*, 9–16.

Guyenet, S.J., Furrer, S.A., Damian, V.M., Baughan, T.D., La Spada, A.R., and Garden, G.A. (2010). A simple composite phenotype scoring system for evaluating mouse models of

cerebellar ataxia. J Vis Exp.

Hannenhalli, S., and Kaestner, K.H. (2009). The evolution of Fox genes and their role in development and disease. Nat. Rev. Genet. *10*, 233–240.

Haralambieva, E., Adam, P., Ventura, R., Katzenberger, T., Kalla, J., Höller, S., Hartmann, M., Rosenwald, A., Greiner, A., Muller-Hermelink, H.K., et al. (2006). Genetic rearrangement of FOXP1 is predominantly detected in a subset of diffuse large B-cell lymphomas with extranodal presentation. Leukemia *20*, 1300–1303.

Hori, S., Nomura, T., and Sakaguchi, S. (2003). Control of regulatory T cell development by the transcription factor Foxp3. Science *299*, 1057–1061.

Hu, H., Wang, B., Borde, M., Nardone, J., Maika, S., Allred, L., Tucker, P.W., and Rao, A. (2006). Foxp1 is an essential transcriptional regulator of B cell development. Nature Immunology *7*, 819–826.

Jain, J., McCaffrey, P.G., Valge-Archer, V.E., and Rao, A. (1992). Nuclear factor of activated T cells contains Fos and Jun. Nature *356*, 801–804.

Jameson, S.C., and Masopust, D. (2009). Diversity in T Cell Memory: An Embarrassment of Riches. Immunity *31*, 859–871.

Jin, Y., Birlea, S.A., Fain, P.R., Mailloux, C.M., Riccardi, S.L., Gowan, K., Holland, P.J., Bennett, D.C., Wallace, M.R., McCormack, W.T., et al. (2010). Common variants in FOXP1 are associated with generalized vitiligo. Nat. Genet. *42*, 576–578.

Josefowicz, S.Z., Lu, L.-F., and Rudensky, A.Y. (2012). Regulatory T cells: mechanisms of differentiation and function. Annu. Rev. Immunol. *30*, 531–564.

Kaech, S.M., Wherry, E.J., and Ahmed, R. (2002). Vaccines: Effector and Memory T-Cell Differentiation: Implications for Vaccine Development. Nat Rev Immunol *2*, 251–262.

Kerdiles, Y.M., Beisner, D.R., Tinoco, R., Dejean, A.S., Castrillon, D.H., DePinho, R.A., and Hedrick, S.M. (2009). Foxo1 links homing and survival of naive T cells by regulating L-selectin, CCR7 and interleukin 7 receptor. Nature Publishing Group *10*, 176–184.

Kersh, E.N., Fitzpatrick, D.R., Murali-Krishna, K., Shires, J., Speck, S.H., Boss, J.M., and Ahmed, R. (2006). Rapid demethylation of the IFN-gamma gene occurs in memory but not naive CD8 T cells. J. Immunol. *176*, 4083–4093.

Kuo, C.T. (1997). LKLF: A Transcriptional Regulator of Single-Positive T Cell Quiescence and Survival. Science *277*, 1986–1990.

Kuo, T.C., and Schlissel, M.S. (2009). Mechanisms controlling expression of the RAG locus during lymphocyte development. Curr. Opin. Immunol. *21*, 173–178.

Lai, C.S., Fisher, S.E., Hurst, J.A., Vargha-Khadem, F., and Monaco, A.P. (2001). A forkhead-domain gene is mutated in a severe speech and language disorder. Nature *413*, 519–523.

Lee, P.P., Fitzpatrick, D.R., Beard, C., Jessup, H.K., Lehar, S., Makar, K.W., Pérez-Melgosa, M., Sweetser, M.T., Schlissel, M.S., Nguyen, S., et al. (2001). A critical role for Dnmt1 and DNA methylation in T cell development, function, and survival. Immunity *15*, 763–774.

Leulier, F., and Lemaitre, B. (2008). Toll-like receptors — taking an evolutionary approach. Nat. Rev. Genet. *9*, 165–178.

Li, M.O., Wan, Y.Y., and Flavell, R.A. (2007). T cell-produced transforming growth factor-beta1 controls T cell tolerance and regulates Th1- and Th17-cell differentiation. Immunity *26*, 579–591.

Li, S., Wang, Y., Zhang, Y., Lu, M.M., DeMayo, F.J., Dekker, J.D., Tucker, P.W., and

Morrisey, E.E. (2012). Foxp1/4 control epithelial cell fate during lung development and regeneration through regulation of anterior gradient 2. Development *139*, 2500–2509.

Lin, J.X., and Leonard, W.J. (2000). The role of Stat5a and Stat5b in signaling by IL-2 family cytokines. Oncogene *19*, 2566–2576.

Lin, L., Hron, J.D., and Peng, S.L. (2004a). Regulation of NF-kappaB, Th activation, and autoinflammation by the forkhead transcription factor Foxo3a. Immunity *21*, 203–213.

Lin, L., Spoor, M.S., Gerth, A.J., Brody, S.L., and Peng, S.L. (2004b). Modulation of Th1 activation and inflammation by the NF-kappaB repressor Foxj1. Science *303*, 1017–1020.

Love, P.E., and Hayes, S.M. (2010). ITAM-mediated signaling by the T-cell antigen receptor. Cold Spring Harb Perspect Biol *2*, a002485.

Lu, L., and Osmond, D.G. (2000). Apoptosis and its modulation during B lymphopoiesis in mouse bone marrow. Immunol. Rev. *175*, 158–174.

Lu, M.M., Li, S., Yang, H., and Morrisey, E.E. (2002). Foxp4: a novel member of the Foxp subfamily of winged-helix genes co-expressed with Foxp1 and Foxp2 in pulmonary and gut tissues. Mechanisms of Development *119*, S197–S202.

Ma, C.S., Deenick, E.K., Batten, M., and Tangye, S.G. (2012). The origins, function, and regulation of T follicular helper cells. Journal of Experimental Medicine *209*, 1241–1253.

Macián, F., Im, S.-H., García-Cózar, F.J., and Rao, A. (2004). T-cell anergy. Curr. Opin. Immunol. *16*, 209–216.

Marsden, V.S., and Strasser, A. (2003). Control of apoptosis in the immune system: Bcl-2, BH3-only proteins and more. Annu. Rev. Immunol. *21*, 71–105.

Mathis, D., and Benoist, C. (2007). A decade of AIRE. Nat Rev Immunol *7*, 645–650.

Mazzucchelli, R., and Durum, S.K. (2007). Interleukin-7 receptor expression: intelligent design. Nat Rev Immunol *7*, 144–154.

McDonnell, T.J., Deane, N., Platt, F.M., Nunez, G., Jaeger, U., McKearn, J.P., and Korsmeyer, S.J. (1989). bcl-2-immunoglobulin transgenic mice demonstrate extended B cell survival and follicular lymphoproliferation. Cell *57*, 79–88.

Medzhitov, R. (2007). Recognition of microorganisms and activation of the immune response. Nature *449*, 819–826.

Mirenda, V., Jarmin, S.J., David, R., Dyson, J., Scott, D., Gu, Y., Lechler, R.I., Okkenhaug, K., and Marelli-Berg, F.M. (2007). Physiologic and aberrant regulation of memory T-cell trafficking by the costimulatory molecule CD28. Blood *109*, 2968–2977.

Mombaerts, P., Iacomini, J., Johnson, R.S., Herrup, K., Tonegawa, S., and Papaioannou, V.E. (1992). RAG-1-deficient mice have no mature B and T lymphocytes. Cell *68*, 869–877.

Mueller, S.N., Gebhardt, T., Carbone, F.R., and Heath, W.R. (2013). Memory T Cell Subsets, Migration Patterns, and Tissue Residence. Annu. Rev. Immunol. *31*, 137–161.

Murphy, K.P., Travers, P., Walport, M., and Janeway, C. (2008). Janeway's immunobiology (Garland Pub).

Naparstek, Y., and Plotz, P.H. (1993). The role of autoantibodies in autoimmune disease. Annu. Rev. Immunol. *11*, 79–104.

Nehls, M., Pfeifer, D., Schorpp, M., Hedrich, H., and Boehm, T. (1994). New member of the winged-helix protein family disrupted in mouse and rat nude mutations. Nature *372*, 103–107.

Ogilvy, S., Metcalf, D., Print, C.G., Bath, M.L., Harris, A.W., and Adams, J.M. (1999). Constitutive Bcl-2 expression throughout the hematopoietic compartment affects multiple

lineages and enhances progenitor cell survival. Proc. Natl. Acad. Sci. U.S.a. *96*, 14943–14948.

Ono, M., Yaguchi, H., Ohkura, N., Kitabayashi, I., Nagamura, Y., Nomura, T., Miyachi, Y., Tsukada, T., and Sakaguchi, S. (2007). Foxp3 controls regulatory T-cell function by interacting with AML1/Runx1. Nature *446*, 685–689.

Ouyang, W., and Li, M.O. (2011). Foxo: in command of T lymphocyte homeostasis and tolerance. Trends Immunol. *32*, 26–33.

Ouyang, W., Beckett, O., Flavell, R.A., and Li, M.O. (2009). An Essential Role of the Forkhead-Box Transcription Factor Foxo1 in Control of T Cell Homeostasis and Tolerance. Immunity *30*, 358–371.

Ouyang, W., Beckett, O., Ma, Q., Paik, J.-H., DePinho, R.A., and Li, M.O. (2010). Foxo proteins cooperatively control the differentiation of Foxp3+ regulatory T cells. Nature Immunology *11*, 618–627.

Pancer, Z., and Cooper, M.D. (2006). The evolution of adaptive immunity. Annu. Rev. Immunol. *24*, 497–518.

Patzelt, T.C. (2010). Erzeugung und Analyse eines konditionalen Foxp1 Knockout-Maus-Modells. Dissertation.

Pepper, M., and Jenkins, M.K. (2011). Origins of CD4+ effector and central memory T cells. Nature Immunology *131*, 467–471.

Pfaffl, M.W. (2001). A new mathematical model for relative quantification in real-time RT-PCR. Nucleic Acids Res. *29*, e45.

Reboldi, A., Coisne, C., Baumjohann, D., Benvenuto, F., Bottinelli, D., Lira, S., Uccelli, A., Lanzavecchia, A., Engelhardt, B., and Sallusto, F. (2009). C-C chemokine receptor 6–regulated entry of TH-17 cells into the CNS through the choroid plexus is required for the initiation of EAE. Nature Immunology *10*, 514–523.

Robey, E., and Fowlkes, B.J. (1994). Selective events in T cell development. Annu. Rev. Immunol. *12*, 675–705.

Rothhammer, V., Heink, S., Petermann, F., Srivastava, R., Claussen, M.C., Hemmer, B., and Korn, T. (2011). Th17 lymphocytes traffic to the central nervous system independently of 4 integrin expression during EAE. Journal of Experimental Medicine *208*, 2465–2476.

Rousso, D.L., Gaber, Z.B., Wellik, D., Morrisey, E.E., and Novitch, B.G. (2008). Coordinated actions of the forkhead protein Foxp1 and Hox proteins in the columnar organization of spinal motor neurons. Neuron *59*, 226–240.

Rousso, D.L., Pearson, C.A., Gaber, Z.B., Li, S., Portera-Cailliau, C., Morrisey, E.E., and Novitch, B.G. (2012). Foxp-mediated suppression of N-cadherin regulates neuroepithelial character and progenitor maintenance in the CNS. Neuron *74*, 314–330.

Rubtsov, Y.P., Niec, R.E., Josefowicz, S., Li, L., Darce, J., Mathis, D., Benoist, C., and Rudensky, A.Y. (2010). Stability of the Regulatory T Cell Lineage in Vivo. Science *329*, 1667–1671.

Sagardoy, A., Martinez-Ferrandis, J.I., Roa, S., Bunting, K.L., Aznar, M.A., Elemento, O., Shaknovich, R., Fontan, L., Fresquet, V., Perez-Roger, I., et al. (2013). Downregulation of FOXP1 is required during germinal center B-cell function. Blood *121*, 4311–4320.

Sakaguchi, S., Sakaguchi, N., Asano, M., Itoh, M., and Toda, M. (1995). Immunologic self-tolerance maintained by activated T cells expressing IL-2 receptor alpha-chains (CD25). Breakdown of a single mechanism of self-tolerance causes various autoimmune diseases. J.

Immunol. *155*, 1151–1164.

Sakaguchi, S., Takahashi, T., and Nishizuka, Y. (1982). Study on cellular events in postthymectomy autoimmune oophoritis in mice. I. Requirement of Lyt-1 effector cells for oocytes damage after adoptive transfer. J. Exp. Med. *156*, 1565–1576.

Sallusto, F., Lenig, D., Förster, R., Lipp, M., and Lanzavecchia, A. (1999). Two subsets of memory T lymphocytes with distinct homing potentials and effector functions. Nature *401*, 708–712.

Sallusto, F., Geginat, J., and Lanzavecchia, A. (2004). Central Memory and Effector Memory T Cell Subsets: Function, Generation, and Maintenance. Annu. Rev. Immunol. *22*, 745–763.

Schluns, K.S., Kieper, W.C., Jameson, S.C., and Lefrançois, L. (2000). Interleukin-7 mediates the homeostasis of naïve and memory CD8 T cells in vivo. Nature Immunology *1*, 426–432.

Schubert, L.A., Jeffery, E., Zhang, Y., Ramsdell, F., and Ziegler, S.F. (2001). Scurfin (FOXP3) acts as a repressor of transcription and regulates T cell activation. J. Biol. Chem. *276*, 37672–37679.

Schulze-Topphoff, U., Casazza, S., Varrin-Doyer, M., Sobel, R.A., Hauser, S.L., Oksenberg, J.R., Zamvil, S.S., and Baranzini, S.E. (2013). Tob1 plays a critical role in the activation of encephalitogenic T cells in CNS autoimmunity. Journal of Experimental Medicine.

Seder, R.A., and Ahmed, R. (2003). Similarities and differences in CD4+ and CD8+ effector and memory T cell generation. Nature Immunology *4*, 835–842.

Seder, R.A., Darrah, P.A., and Roederer, M. (2008). T-cell quality in memory and protection: implications for vaccine design. Nat Rev Immunol *8*, 247–258.

Shaffer, A.L., Rosenwald, A., and Staudt, L.M. (2002). Decision making in the immune system: Lymphoid Malignancies: the dark side of B-cell differentiation. Nat Rev Immunol *2*, 920–933.

Shi, C., Sakuma, M., Mooroka, T., Liscoe, A., Gao, H., Sharma, A., Kaplan, D., Greaves, D.R., Wang, Y., et al. (2008). Down-regulation of the forkhead transcription factor Foxp1 is required for monocyte differentiation and macrophage function. Blood *112*, 4699–4711.

Shi, C., Zhang, X., Chen, Z., Sulaiman, K., Feinberg, M.W., Ballantyne, C.M., Jain, M.K., and Simon, D.I. (2004). Integrin engagement regulates monocyte differentiation through the forkhead transcription factor Foxp1. Journal of Clinical Investigation *114*, 408–418.

Shimizu, K., Kato, A., Hinotsume, D., Shigemura, M., Hanaoka, M., Shimoichi, Y., Honoki, K., and Tsujiuchi, T. (2006). Reduced expressions of Foxp1 and Rassf1a genes in lung adenocarcinomas induced by N-nitrosobis(2-hydroxypropyl)amine in rats. Cancer Lett. *236*, 186–190.

Shinkai, Y., Rathbun, G., Lam, K.P., Oltz, E.M., Stewart, V., Mendelsohn, M., Charron, J., Datta, M., Young, F., and Stall, A.M. (1992). RAG-2-deficient mice lack mature lymphocytes owing to inability to initiate V(D)J rearrangement. Cell *68*, 855–867.

Shu, W., Yang, H., Zhang, L., Lu, M.M., and Morrisey, E.E. (2001). Characterization of a new subfamily of winged-helix/forkhead (Fox) genes that are expressed in the lung and act as transcriptional repressors. J. Biol. Chem. *276*, 27488–27497.

Shu, W., Cho, J.Y., Jiang, Y., Zhang, M., Weisz, D., Elder, G.A., Schmeidler, J., De Gasperi, R., Sosa, M.A.G., Rabidou, D., et al. (2005). Altered ultrasonic vocalization in mice with a disruption in the Foxp2 gene. Proc. Natl. Acad. Sci. U.S.a. *102*, 9643–9648.

Shu, W., Lu, M.M., Zhang, Y., Tucker, P.W., Zhou, D., and Morrisey, E.E. (2007). Foxp2 and Foxp1 cooperatively regulate lung and esophagus development. Development *134*, 1991–

2000.

Sievers, F., Wilm, A., Dineen, D., Gibson, T.J., Karplus, K., Li, W., Lopez, R., McWilliam, H., Remmert, M., Söding, J., et al. (2011). Fast, scalable generation of high-quality protein multiple sequence alignments using Clustal Omega. Mol. Syst. Biol. *7*, 539.

Smith-Garvin, J.E., Koretzky, G.A., and Jordan, M.S. (2009). T cell activation. Annu. Rev. Immunol. *27*, 591–619.

Song, X., Li, B., Xiao, Y., Chen, C., Wang, Q., Liu, Y., Berezov, A., Xu, C., Gao, Y., Li, Z., et al. (2012). Structural and biological features of FOXP3 dimerization relevant to regulatory T cell function. Cell Rep *1*, 665–675.

Strasser, A., Whittingham, S., Vaux, D.L., Bath, M.L., Adams, J.M., Cory, S., and Harris, A.W. (1991). Enforced BCL2 expression in B-lymphoid cells prolongs antibody responses and elicits autoimmune disease. Proc. Natl. Acad. Sci. U.S.a. *88*, 8661–8665.

Streubel, B., Vinatzer, U., Lamprecht, A., Raderer, M., and Chott, A. (2005). T(3;14)(p14.1;q32) involving IGH and FOXP1 is a novel recurrent chromosomal aberration in MALT lymphoma. Leukemia *19*, 652–658.

Stroud, J.C., Wu, Y., Bates, D.L., Han, A., Nowick, K., Paabo, S., Tong, H., and Chen, L. (2006). Structure of the forkhead domain of FOXP2 bound to DNA. Structure *14*, 159–166.

Surh, C.D., and Sprent, J. (2008). Homeostasis of naive and memory T cells. Immunity *29*, 848–862.

Surh, C.D., Boyman, O., Purton, J.F., and Sprent, J. (2006). Homeostasis of memory T cells. Immunol. Rev. *211*, 154–163.

Takahashi, K., Liu, F.-C., Hirokawa, K., and Takahashi, H. (2008). Expression of Foxp4in the developing and adult rat forebrain. J. Neurosci. Res. *86*, 3106–3116.

Tamura, S., Morikawa, Y., Iwanishi, H., Hisaoka, T., and Senba, E. (2004). Foxp1 gene expression in projection neurons of the mouse striatum. Neuroscience *124*, 261–267.

Tamura, S., Morikawa, Y., Iwanishi, H., Hisaoka, T., and Senba, E. (2003). Expression pattern of the winged-helix/forkhead transcription factor Foxp1 in the developing central nervous system. Gene Expr. Patterns *3*, 193–197.

Tang, B., Becanovic, K., Desplats, P.A., Spencer, B., Hill, A.M., Connolly, C., Masliah, E., Leavitt, B.R., and Thomas, E.A. (2012). Forkhead box protein p1 is a transcriptional repressor of immune signaling in the CNS: implications for transcriptional dysregulation in Huntington disease. Hum. Mol. Genet. *21*, 3097–3111.

Tang, Q., Henriksen, K.J., Bi, M., Finger, E.B., Szot, G., Ye, J., Masteller, E.L., McDevitt, H., Bonyhadi, M., and Bluestone, J.A. (2004). In vitro-expanded antigen-specific regulatory T cells suppress autoimmune diabetes. J. Exp. Med. *199*, 1455–1465.

Tangye, S.G., Ma, C.S., Brink, R., and Deenick, E.K. (2013). The good, the bad and the ugly - TFH clls in human health and disease. Nat Rev Immunol *13*, 412–426.

Thome, M. (2004). CARMA1, BCL-10 and MALT1 in lymphocyte development and activation. Nat Rev Immunol *4*, 348–359.

Tsujimoto, Y., Finger, L.R., Yunis, J., Nowell, P.C., and Croce, C.M. (1984). Cloning of the chromosome breakpoint of neoplastic B cells with the t(14;18) chromosome translocation. Science *226*, 1097–1099.

Tykocinski, L.-O., Sinemus, A., Rezavandy, E., Weiland, Y., Baddeley, D., Cremer, C., Sonntag, S., Willecke, K., Derbinski, J., and Kyewski, B. (2010). Epigenetic regulation of promiscuous gene expression in thymic medullary epithelial cells. Proc. Natl. Acad. Sci.

U.S.a. *107*, 19426–19431.

Tzachanis, D., Freeman, G.J., Hirano, N., van Puijenbroek, A.A., Delfs, M.W., Berezovskaya, A., Nadler, L.M., and Boussiotis, V.A. (2001). Tob is a negative regulator of activation that is expressed in anergic and quiescent T cells. Nature Immunology *2*, 1174–1182.

van Gisbergen, K.P.J.M., Klarenbeek, P.L., Kragten, N.A.M., Unger, P.-P.A., Nieuwenhuis, M.B.B., Wensveen, F.M., Brinke, ten, A., Tak, P.P., Eldering, E., Nolte, M.A., et al. (2011). The costimulatory molecule CD27 maintains clonally diverse CD8(+) T cell responses of low antigen affinity to protect against viral variants. Immunity *35*, 97–108.

Walker, L.S.K., Chodos, A., Eggena, M., Dooms, H., and Abbas, A.K. (2003). Antigen-dependent Proliferation of CD4+ CD25+ Regulatory T Cells In Vivo. Journal of Experimental Medicine *198*, 249–258.

Wan, Y.Y., and Flavell, R.A. (2009). How Diverse--CD4 Effector T Cells and their Functions. Journal of Molecular Cell Biology *1*, 20–36.

Wang, B. (2003). Multiple Domains Define the Expression and Regulatory Properties of Foxp1 Forkhead Transcriptional Repressors. Journal of Biological Chemistry *278*, 24259–24268.

Wang, B. (2004). Foxp1 regulates cardiac outflow tract, endocardial cushion morphogenesis and myocyte proliferation and maturation. Development *131*, 4477–4487.

Wang, H., Geng, J., Wen, X., Bi, E., Kossenkov, A.V., Wolf, A.I., Tas, J., Choi, Y.S., Takata, H., Day, T.J., et al. (2014). The transcription factor Foxp1 is a critical negative regulator of the differentiation of follicular helper T cells. Nature Immunology *15*, 667–675.

Weaver, C.T., Harrington, L.E., Mangan, P.R., Gavrieli, M., and Murphy, K.M. (2006). Th17: An Effector CD4 T Cell Lineage with Regulatory T Cell Ties. Immunity *24*, 677–688.

Weigel, D., Jürgens, G., Küttner, F., Seifert, E., and Jäckle, H. (1989). The homeotic gene fork head encodes a nuclear protein and is expressed in the terminal regions of the Drosophila embryo. Cell *57*, 645–658.

Weng, N.-P., Araki, Y., and Subedi, K. (2012). The molecular basis of the memory T cell response: differential gene expression and its epigenetic regulation. Nat Rev Immunol *12*, 306–315.

Wlodarska, I., Veyt, E., De Paepe, P., Vandenberghe, P., Nooijen, P., Theate, I., Michaux, L., Sagaert, X., Marynen, P., Hagemeijer, A., et al. (2005). FOXP1, a gene highly expressed in a subset of diffuse large B-cell lymphoma, is recurrently targeted by genomic aberrations. Leukemia *19*, 1299–1305.

Woodland, D.L., and Kohlmeier, J.E. (2009). Migration, maintenance and recall of memory T cells in peripheral tissues. Nat Rev Immunol *9*, 153–161.

Wu, Y., Borde, M., Heissmeyer, V., Feuerer, M., Lapan, A.D., Stroud, J.C., Bates, D.L., Guo, L., Han, A., Ziegler, S.F., et al. (2006). FOXP3 Controls Regulatory T Cell Function through Cooperation with NFAT. Cell *126*, 375–387.

Zhang, W., Sloan-Lancaster, J., Kitchen, J., Trible, R.P., and Samelson, L.E. (1998). LAT. Cell *92*, 83–92.

Zhou, X., Jeker, L.T., Fife, B.T., Zhu, S., Anderson, M.S., McManus, M.T., and Bluestone, J.A. (2008). Selective miRNA disruption in T reg cells leads to uncontrolled autoimmunity. Journal of Experimental Medicine *205*, 1983–1991.

Zhu, J., Yamane, H., and Paul, W.E. (2010). Differentiation of effector CD4 T cell populations. Annu. Rev. Immunol. *28*, 445–489.